学位論文

Slave Boson Analysis on Multi-Orbital Periodic Anderson Model
(スレーブボソン法を用いた多軌道アンダーソンモデルの解析)

平成 28 年 11 月博士（理学）申請

東京大学大学院理学系研究科

物理学専攻

檜原　太一

Abstract

In this thesis, heavy electrons on f^2-configuration systems with singlet ground states are theoretically investigated. Here, the "f^2-configuration system" denotes the heavy electron system containing two electrons in each site of the f-orbital. Some uranium and praseodymium compounds belong to this system. While basic properties of heavy electron systems for cerium and ytterbium compounds (f^1-configuration system) are well explained by Doniach's phase diagram, several f^2-configuration systems exhibit unconventional behaviors that cannot be explained by this diagram. In contrast to the f^1-configuration systems, the f^2-configuration systems need to consider multi-orbital system. Moreover, these systems realize non-magnetic localized states because the Kramers theorem doese not hold in these systems.

Since the unconventional behaviors are expected to be caused by the non-magnetic localized ground state, intensive studies based on a Kondo lattice model or a multi-orbital impurity Anderson model have been carried out to reveal the origin of these behaviors. However, using these models cannot evaluate an itinerant nature of f-electrons in a lattice system such as a heavy Fermi liquid and a superconductivity owing to heavy electrons. In order to reveal the relation between the non-magnetic ground state and the itinerant nature, theoretical studies based on a multi-orbital periodic Anderson model is inevitable.

Thus far, several theoretical methods that can be applied to this model in some special cases have been presented. In contrast to these methods, a rotaionally-invariant slave-boson formalism, which we use in this thesis, can be used in general multi-orbital systems. Therefore, this method can shed new light on the f^2-configuration systems that are difficult to evaluate in the other methods, especially non-magnetic singlet ground state systems.

In this thesis, we perform a saddle point approximation of the slave-boson formalism to two kinds of multi-orbital periodic Anderson models: one is cubic symmetry system with Γ_1 singlet ground state of the f^2-configuraion, and the other is hexagonal symmetry system with Γ_4 singlet ground state of the f^2-configuration. Each system is a candidate of energy schemes of UBe_{13} and of UPt_3, respectively.

As a result, we reveal that these two systems exhibit different behaviors. In the case of the Γ_1 singlet ground state, there are three possible phases at the f^2-configuration: a CEF singlet state, and two itinerant states. All the phase transitions between two of these states are first-order transitions. These transitions originate from either charge-transfer transition of f-orbitals or effective energy level crossing.

On the other hand, in the case of the Γ_4 singlet ground state, the system exhibits a first-order Brinkmann-Rice transition at the f^2-configuration. This behavior is totally different from the case of the Γ_1 singlet ground state. It is comfirmed that these behaviors result in different configurations of the singlet ground states.

We also discuss the heavy electron systems in an intermediate-valence state between the f^2-

and f^3-configurations. It is found that an anisotropy of hybridizations realizes heavy electrons related to the ground state of the f^2-configuration.

Contents

Chapter 1

Introduction for f^2-configuration systems

1.1 Review for Heavy Electron Systems

"Heavy electron system" is a name given to a system in which relatively localized electrons play a significant role. Heavy electron systems have mainly been identified in f-electron systems such as cerium, ytterbium, praseodymium, and uranium compounds. One of the characteristics of these systems is that an effective mass estimated from the electronic specific heat is 100-1000 times larger than that of conventional metals. This mass enhancement arises from the duality of the f-electrons' behavior: the localized characteristics, such as electron-electron interactions, and the itinerant characteristics, such as hybridizations with surrounding conduction electrons. We call the metalic state without mass enhancement a Fermi liquid (FL), while we call the enhanced mass state a heavy Fermi liquid (HFL). In addition, the systems exhibit other kinds of electronic states, such as a non-Fermi liquid (NFL), a magnetically ordered state (MO), an unconventional superconductivity (SC) and so on. Phase transitions or crossovers between these electronic states can be observed by lowering the temperature, applying pressure, applying a magnetic field, and so on. Such rich phenomena have attracted much attention and intensive studies have been carried out, both in theoretical and experimental research over a quarter of a century [1].

It is well accepted that the physical properties of heavy electron systems strongly depend on the f^n-configuration, where n is the number of electrons in each f-orbital. Roughly speaking, cerium and ytterbium (in the hole picture) ions tend to have an f^1-configuration, while uranium and praseodymium ions tend to have f^2 or f^3-configurations. Intensive studies have revealed that the basic properties of f^1-configuration systems can be well explained with Doniach's phase diagram (see Fig. 1.1) [2]. On the contrary, it is also reported that some compounds belonging to the f^2-configuration systems show unconventional behaviors that cannot be explained by Doniach's phase diagram.

1.1.1 Basic properties on f^1-configuration systems

In this thesis, we mainly focus on f^2-configuration systems. However, before discussing the unconventional behaviors of f^2-configuration systems, let us first review the basic properties of

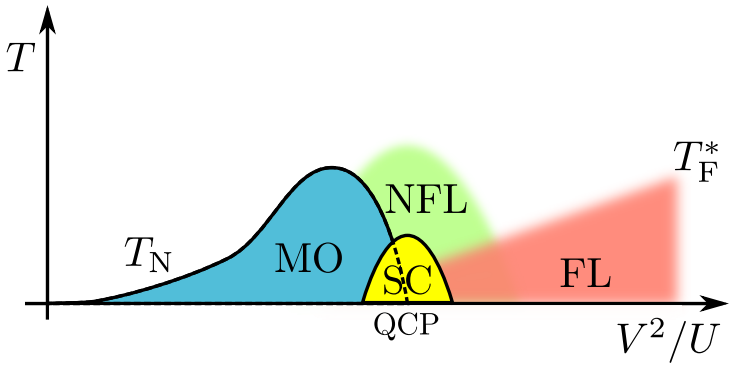

Figure 1.1: A schematic phase diagram for f^1-configuration systems, called Doniach's phase diagram. FL, NFL, SC and MO denote a Fermi liquid, non-Fermi liquid, superconductivity, and magnetically ordered state, respectively. $T_{\rm N}$ and $T_{\rm F}^*$ represent the transition temperature and typical energy scale for FL, respectively. The QCP is the point at $T_N = 0$. HFL is realized in the vicinity of the QCP inside the FL.

f^1-configuration systems by using the single-orbital periodic Anderson model given by:

$$\mathcal{H} = \sum_{\boldsymbol{k}\sigma} \xi_{\boldsymbol{k}} c^\dagger_{\boldsymbol{k}\sigma} c_{\boldsymbol{k}\sigma} + \sum_{i\sigma} (E_f - \mu) f^{\rm phys\dagger}_{\boldsymbol{k}\sigma} f^{\rm phys}_{\boldsymbol{k}\sigma} + \sum_{\boldsymbol{k}\sigma} \left(V f^{\rm phys\dagger}_{\boldsymbol{k}\sigma} c_{\boldsymbol{k}\sigma} + \text{h.c.} \right) + \sum_i U f^{\rm phys\dagger}_{i\uparrow} f^{\rm phys\dagger}_{i\downarrow} f^{\rm phys}_{i\downarrow} f^{\rm phys}_{i\uparrow}, \tag{1.1}$$

where $\xi_{\boldsymbol{k}}$ represent the energy dispersion of conduction electrons measured from the chemical potential μ, E_f is the f-electron energy level, V is the hybridization between the conduction electrons and the f-electrons, U is the intra-orbital Coulomb interaction, $f^{\rm phys}_{\boldsymbol{k}\sigma}$ ($f^{\rm phys\dagger}_{\boldsymbol{k}\sigma}$) and $c_{\boldsymbol{k}\sigma}$ ($c^\dagger_{\boldsymbol{k}\sigma}$) denote the annihilation (creation) operators of the localized f-electron and those of the conduction electron, respectively. In order to distinguish these from the pseudo fermion operators $f_{\boldsymbol{k}\sigma}$ introduced later, we denote the original (physical) f-electrons as $f^{\rm phys}_{\boldsymbol{k}\sigma}$. This Hamiltonian is the simplest model for describing the rich phenomena in a Doniach's phase diagram as shown in Fig. 1.1.

In the case of $V \ll U$, the f-electrons behave as localized electrons, which have spin degrees of freedom. These localized spins interact with each other indirectly through the conduction electrons (RKKY interaction). Namely, a paramagnetic state is realized in the high temperature region with the constant entropy $k_{\rm B} \ln 2$ for the f-electrons. Meanwhile, MO state arises below the transition temperature $T_{\rm N}$ owing to the RKKY interactions.

In contrast, in the $V \gg U$ region, the f-electrons behave as renormalized itinerant electrons below $T_{\rm F}^*$, where $T_{\rm F}^*$ represents a typical energy scale connected to the Fermi temperature $T_{\rm F}$ at $U = 0$. Below $T_{\rm F}^*$, the electronic states can be understood by means of Landau's Fermi liquid theory. Namely, the f-electrons are renormalized by Coulomb interactions and are described as quasiparticles (QPs) characterized by a finite lifetime and enhanced effective mass.

In order to connect the above two limits, it is natural to expect the existence of a quantum critical point (QCP) at which $T_{\rm N}$ approaches zero (see Fig.1.1). In the vicinity of the QCP, Landau's QP picture is no longer valid because of the strong spin fluctuations. Such a region is called a NFL state whose physical quantities show anomalous power-law behaviors against temperature. Moreover, unconventional SC arises around the QCP by using the spin fluctuation

as a "glue" of Cooper pairs.

In this thesis, we mainly focus on FL and HFL. For that reason, let us briefly explain how to describe the QP theoretically by means of Green's functions [3]. The Green's function of the Hamiltonian in eq. (1.1) for each of the momentum k, the frequency ω, and the spin σ is written in a 2×2 matrix form as,

$$-\hat{G}_\sigma\left(\boldsymbol{k},\omega\right)^{-1} = \begin{pmatrix} -\omega + \xi_{\boldsymbol{k}} & V \\ V & -\omega + E_f - \mu + \Sigma_\sigma\left(\boldsymbol{k},\omega\right) \end{pmatrix} \tag{1.2}$$

where $\Sigma_\sigma\left(\boldsymbol{k},\omega\right)$ is the self-energy for the f-electrons, including the effect of the intra-orbital interaction U. At zero temperature, the self-energy can be expanded with respect to ω around 0 at the Fermi surface $\boldsymbol{k}_{\mathrm{F}}$ as follows:

$$\Sigma_\sigma\left(\boldsymbol{k},\omega\right) \sim \mathrm{Re}\Sigma_\sigma\left(\boldsymbol{k}_{\mathrm{F}},0\right) + \left.\frac{\partial \mathrm{Re}\Sigma_\sigma\left(\boldsymbol{k}_{\mathrm{F}},\omega\right)}{\partial\omega}\right|_{\omega=0} \omega + \frac{1}{2}\left.\frac{\partial^2 \mathrm{Im}\Sigma_\sigma\left(\boldsymbol{k}_{\mathrm{F}},\omega\right)}{\partial\omega^2}\right|_{\omega=0} i\omega^2, \tag{1.3}$$

where we omit the higher order of ω, that is, the second and higher orders for the real part and the third and higher orders for the imaginary part. In a FL state, the constant term and the first-order term for the imaginary part are zero since the QPs at the Fermi energy have infinite lifetime in the zero temperature. In the general Fermi liquid theory, expansion with respect to k is also considered. However, we neglect this component in order to be consistent with the saddle-point approximation of the slave boson formalism discussed in this thesis, which does not include the momentum dependence of the self-energy.

Substituting eq. (1.3) into eq. (1.2), we obtain:

$$-\hat{G}_\sigma\left(\boldsymbol{k},\omega\right)^{-1} \sim -\hat{G}^{\mathrm{coh}}_\sigma\left(\boldsymbol{k},\omega\right)^{-1} = \begin{pmatrix} -\omega + \xi_{\boldsymbol{k}} & V \\ V & z^{-1}\left(-\omega + \tilde{E}_f - i\gamma_{\boldsymbol{k}\omega}\right) \end{pmatrix}, \tag{1.4}$$

where the renormalization factor z, the renormalized QP energy level $\tilde{E}_f$, and the inverse of the QP lifetime $\gamma_{\boldsymbol{k}\omega}$ are given by,

$$z = \left(1 - \left.\frac{\partial \mathrm{Re}\Sigma_\sigma\left(\boldsymbol{k}_{\mathrm{F}},\omega\right)}{\partial\omega}\right|_{\omega=0}\right)^{-1}, \tag{1.5}$$

$$\tilde{E}_f = z\left(E_f - \mu + \mathrm{Re}\Sigma_\sigma\left(\boldsymbol{k}_{\mathrm{F}},0\right)\right), \tag{1.6}$$

$$\gamma_{\boldsymbol{k}\omega} = -z\left.\frac{\partial^2 \mathrm{Im}\Sigma_\sigma\left(\boldsymbol{k}_{\mathrm{F}},\omega\right)}{\partial\omega^2}\right|_{\omega=0} \omega^2. \tag{1.7}$$

Here, the coherent Green's function $G^{\mathrm{coh}}_\sigma\left(\boldsymbol{k},\omega\right)$ is written as,

$$G^{\mathrm{coh}}_\sigma\left(\boldsymbol{k},\omega\right) = \begin{pmatrix} G^{cc}_\sigma\left(\boldsymbol{k},\omega\right) & G^{cf}_\sigma\left(\boldsymbol{k},\omega\right) \\ G^{fc}_\sigma\left(\boldsymbol{k},\omega\right) & G^{ff}_\sigma\left(\boldsymbol{k},\omega\right) \end{pmatrix}, \tag{1.8}$$

where,

$$G_\sigma^{cc}(\boldsymbol{k},\omega) = \frac{1}{\omega - \xi_{\boldsymbol{k}} + \frac{zV^2}{\omega - \tilde{E}_f + i\gamma_{\boldsymbol{k}\omega}}}, \tag{1.9}$$

$$G_\sigma^{ff}(\boldsymbol{k},\omega) = \frac{z}{\omega - \tilde{E}_f + i\gamma_{\boldsymbol{k}\omega} + \frac{zV^2}{\omega - \xi_{\boldsymbol{k}}}}, \tag{1.10}$$

$$G_\sigma^{cf}(\boldsymbol{k},\omega) = G_\sigma^{fc*}(\boldsymbol{k},\omega) = \frac{zV}{\left(\omega - \tilde{E}_f + i\gamma_{\boldsymbol{k}\omega}\right)(\omega - \xi_{\boldsymbol{k}}) - zV^2}. \tag{1.11}$$

Let us discuss G^{ff} in the situation where the number of f-electrons n_f is larger than 1 at $U = 0$: for example, the number of conduction electrons is $n_c = 0.5$ and the total number of electrons is $N = n_c + n_f = 1.75$ ($n_f = 1.25$), for example. As U increases from zero, n_f approaches 1 because the localized effect U favors an integer filling state than a mixed valence state. Simultaneously, z is suppressed to zero and $\tilde{E}_f$ approaches the Fermi energy for the system to be close to the half-filled. On this occasion, according to eq. (1.11), a flat band dispersion, which indicates an enhanced effective mass, is realized around the Fermi energy. In f-electron systems, the HFL is realized not only because of large U but also because of small V.

It is to be noted that the above argument breaks when the renormalization factor becomes zero; i.e., no QPs exist at the Fermi surface. In this region, the incoherent part of the Green's function, which we omitted in the above discussion, plays an significant role in describing the NFL and MO state.

In summary of this subsection, we mention that the rich phenomena in the Doniach's phase diagram can be understood from the competition between the two means of resolving the f-electrons entropy $k_{\mathrm{B}} \ln 2$ arising from the spin degeneracy: one is phase transition to an MO state due to the RKKY interaction, and the other is the formation of the QPs. This competition indicates that the spin degeneracy of f-electrons play an important role in heavy electron systems in the case of f^1-configuration systems.

1.1.2 Basic properties of f^2-configuration systems

In the case of f^2-configuration systems, on the other hand, there are two essential differences from f^1-configuration systems: one is that the multi f-orbitals should be taken into account when modeling the Hamiltonian, and the other is that not only magnetic multiplets but also non-magnetic multiplets or singlets can be realized in the localized f-electron state. The former is obvious since the fully-occupied f-orbital does nothing to the conduction electrons, while the latter is more important. In the f^1-configuration systems, all the localized states are magnetic multiplet owing to Kramer's theorem. Kramer's theorem remarks that every localized state with a half-integer total angular momentum should be an even-number multiplets, owing to the time-reversal symmetry. This theorem is valid for all odd-number f-electron configurations. In other words, f^2-configuration systems realize various kinds of localized states such as non-magnetic singlet and multiplet states. When one of these non-magnetic states becomes a ground state, different phenomena from those of the f^1-configuration systems are expected.

Let us explain the localized f-electron states in the case of the f^1 and f^2-configurations. The energy levels of the f-orbital, which has fourteen-fold degeneracy from the orbital angular momentum $l = 3$ and spin angular momentum $s = 1/2$, are split by the three effects in the

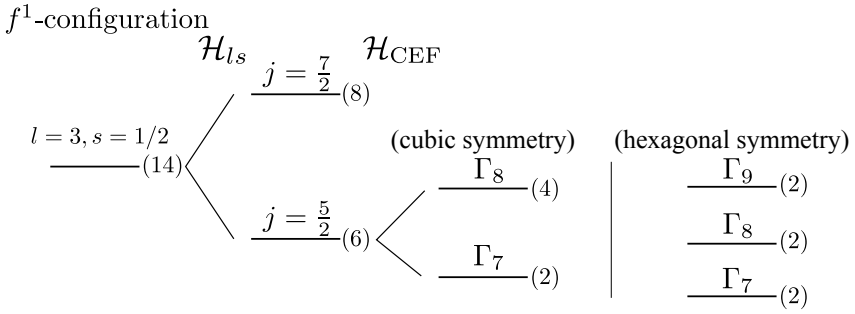

Figure 1.2: The energy scheme for the f^1-configuration in the case of cubic and hexagonal symmetry. The number in parentheses indicates the degeneracy of the state.

atomic limit, the spin-orbit coupling $\mathcal{H}_{ls}$ scaled by λ_{ls}, the electron-electron interactions $\mathcal{H}_U$ scaled by U, and the crystalline electric field (CEF) effect $\mathcal{H}_{\rm CEF}$ scaled by $\Delta_{\rm CEF}$. In typical heavy electron systems, λ_{ls} is on the order of thousands of kelvin in the atomic level [4], U is on the order of tens of thousands kelvin, and $\Delta_{\rm CEF}$ is on the order of tens or hundreds of kelvin, where $\Delta_{\rm CEF}$ strongly depends on the crystal structure of the systems.

Let us first discuss the f^1-configuration, where $\mathcal{H}_U$ does not affect the energy splitting. In this case, large spin-orbit coupling splits the fourteen-fold degeneracy into a sextet ground state with $j = 3-1/2 = 5/2$ and an octet excited state with $j = 7/2 = (3 + 1/2)$. Since $\lambda_{ls} \gg \Delta_{\rm CEF}$, $j = 7/2$ can be ignored. Then, in the case of cubic symmetry, the $j = 5/2$ sextet is raised by $\Delta_{\rm CEF}$ into a Γ_7 doublet and a Γ_8 quartet. Likewise, in the case of hexagonal symmetry, the $j = 5/2$ splits to three doublets a Γ_7, Γ_8, and Γ_9. Here, all these eigenstates are Kramer's doublet states. Figure 1.2 summarizes the energy scheme for the f^1-configuration.

In the case of the f^2-configuration systems, ninety-one-fold degeneracy ($_{14}\mathrm{C}_2 = 91$) is raised by the three effects. In order to reduce the degeneracy and to extract several significant energy levels (a ground state and low-energy excited states), two coupling schemes, namely the LS and jj coupling schemes, are frequently used.

The LS coupling scheme first performs $\mathcal{H}_U$ and extracts $L = 3+2 = 5$ and $S = 1/2+1/2 = 1$ as the ground state according to Hund's rule. Then, the thirty-three-fold degeneracy is split into $J = 5-1 = 4$ (ground state), $J = 5+0 = 5$, and $J = 5+1 = 6$ by spin-orbit coupling. On the other hand, the jj coupling scheme first performs spin-orbit coupling and considers the two electrons in the $j = 5/2$ sextet. Then, $\mathcal{H}_U$ splits the fifteen-fold degeneracy ($_6\mathrm{C}_2$) into $J = 4$ (ground state) ,$J = 2$, and $J = 0$.

Both coupling schemes produce the same total angular momentum $J = 4$ as a ground state. However, the eigenstates of both states are different: all the eigenstates in the jj coupling scheme are constructed from the $j = 5/2$ states, while those in the LS coupling scheme contain the contribution from the $j = 7/2$ state.

Finally, the $J = 4$ state of both coupling schemes is split by the CEF effect $\Delta_{\rm CEF}$. For example, in cubic symmetry, the CEF effect raises the nine-fold degeneracy of $J = 4$ into four multiplet states: Γ_1, a non-magnetic singlet; Γ_3, a non-magnetic doublet; and Γ_4 and Γ_5 triplets. Likewise, in hexagonal symmetry, the irreducible representations of CEF multiplets are Γ_1 singlet, Γ_3 singlet, Γ_4 singlet, Γ_5 doublet, and Γ_6 doublet.

Note that the Γ_1 and Γ_3 in cubic symmetry and the Γ_1, Γ_3, and Γ_4 in hexagonal symmetry are nonmagnetic multiplets that cannot be realized in the f^1-configuration. In this thesis, we

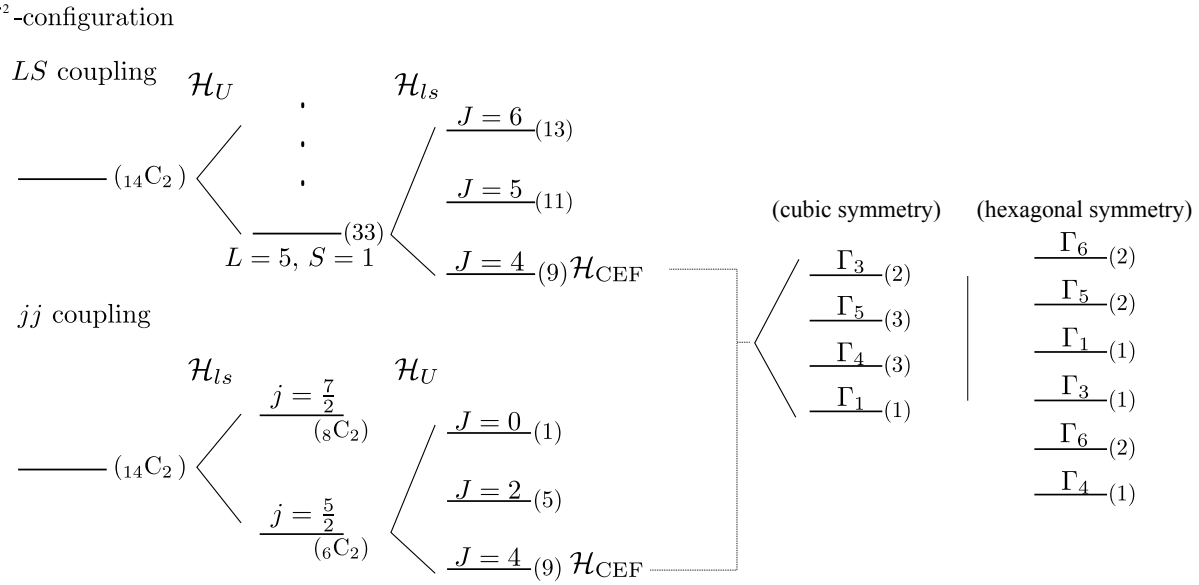

Figure 1.3: Two energy schemes, LS and jj coupling, for the f^2-configuration in the cases of cubic and hexagonal symmetry. The irreducible representations for the CEF effect are the same in both coupling schemes. Note that the CEF eigenstates of the two coupling schemes are different. The number in parentheses indicates the degeneracy of the state.

focus on two cases: the Γ_1 singlet ground state in cubic symmetry and the Γ_4 singlet ground state in hexagonal symmetry. Each ground state is a candidate for the localized energy scheme identified in UBe_{13} and UPt_3, respectively. We will introduce these two compounds in the next section.

1.2 Experimental Review of f^2-configuration systems

In this section, we review physical properties of UBe_{13} and UPt_3. Both compounds are the candidates of the f^2-configuration systems with the non-magnetic singlet ground states and show unconventional behaviors that cannot be explained by the f^1-configuration systems.

1.2.1 UBe_{13}

The crystal structure of UBe_{13} has an Fm3c cubic symmetry. Its electronic specific heat coefficient is 1.1 J/molK^2, which indicates that UBe_{13} is a heavy electron system [5, 6]. This compound is well known for its NFL behavior and its unconventional SC below $T_c \approx 0.85$K [7, 8, 9].

Interesting experimental results for the series of $U_{0.9}M_{0.1}Be_{13}$ (M = Y, Sc, La, and so on) were reported by Kim et. al. [10]. They focused on the relationship between the physical properties and lattice constant a of various systems. When lattice constant becomes smaller than that of UBe_{13}, the resistivity exhibits $-\log T$ dependence as a result of a Kondo effect. On the other hand, when the lattice constant is greater than that of UBe_{13}, metallic behavior is observed instead of the upturn of resistivity. Moreover, the electronic specific heat coefficient

achieves a maximum value at UBe_{13}. These phenomena are inconsistent with conventional heavy heavy electron systems. Namely, small hybridization due to the large lattice constant should enhance the Kondo effect and effective mass.

In order to explain the NFL behavior, Cox proposed a two-channel Kondo model using the Γ_3 non-magnetic doublet ground state with an f^2-configuration [11, 12]. Although this theory succeeds in explaining the anomalous power-law behavior, the energy scheme fails to explain the behaviors in the series of $U_{0.9}M_{0.1}Be_{13}$. To address this problem, Nishiyama and Miyake proposed another scenario using the Γ_1 singlet ground state [13, 14, 15]. They proposed that the NFL behavior originates in the competition between the CEF singlet and CEF triplet states. They also pointed out that similar behaviors in the series of $U_{0.9}M_{0.1}Be_{13}$ can be understood through this energy scheme. Another scenario for the origin of the NFL involves the presence of a field-induced antiferromagnetic quantum critical point [7, 16]. Further studies, especially a microscopic theory of the lattice system, are needed for identifying the origin of the NFL and SC of UBe_{13}.

1.2.2 UPt_3

The crystal structure of UPt_3 is a P63/mmc hexagonal structure. The electronic specific heat coefficient is 420 $mJ/molK^2$, which is twenty times larger than that of the free electrons [1, 17]. In addition to this contribution, the specific heat exhibits $T^3 \ln T$ behavior, which indicates the existence of strong spin fluctuations in this system. In fact, neutron scattering measurements suggest antiferromagnetic ordering with a wave number of (0.5, 0, 0) below $T_N = 5K$ with a small magnetic moment of $0.02\mu_B$ [18]. However, other experimental data, such as nuclear magnetic resonance (NMR) and the specific heat, do not support the ordered state. Hence, it has been interpreted that the magnetic moments fluctuate at higher frequencies than the NMR can detect.

The CEF energy levels of UPt_3 have not been determined directly because the $5f$-electrons of this compound tend to be itinerant. Thus far, the CEF ground state of UPt_3 has been assumed to be a Γ_4 non-Kramers singlet ground state in analogy to UPd_2Al_3 [19, 20], which has two well-localized f-electrons and one itinerant f-electron at each uranium ion with a similar crystal structure to UPt_3. Because of the two localized f-electrons, the CEF energy levels of UPd_2Al_3 have been determined experimentally. According to the magnetic susceptibility and the results of a neutron scattering experiment [19, 21], UPd_2Al_3 is determined to be a Γ_4 singlet ground state. Since the magnetic susceptibility of UPt_3 exhibits a similar behavior to UPd_2Al_3, it is assumed that the CEF ground state of UPt_3 is also a Γ_4 singlet state [20]. However, the relation between the non-magnetic singlet ground state and the HFL has not yet been made clear.

UPt_3 also exhibits multi-phase spin-triplet superconductivity in the field-temperature phase diagram[22]. Especially, two phase transitions are observed at $T_{c1} = 540mK$ and $T_{c2} = 490mK$ in zero magnetic field [17, 23, 24]. The gap symmetry of the superconductivity has attracted much attention.

It has been expected that the d-vector for the spin-triplet superconductivity should be confined to some crystal axis, owing to the strong spin-orbit coupling. Based on this assumption, group theory argues that the gap symmetry cannot have a line-node in the two-dimension irreducible representations, which is able to produce multi-phase superconductivity, when we classify the gap symmetry in terms of total angular momentum $\boldsymbol{J} = \boldsymbol{L} + \boldsymbol{S}$ [25].

However, many experimental results support the existence of the line-node [26, 27, 28, 29, 30]. Moreover, Tou *et al.* studied the Knight shift measurement and confirmed that the SC is non-unitary spin-triplet state whose d-vector is weakly confined [31, 32, 33]. Namely, the d-vector is weakly confined in b-c plane and rotates to a-b plane when a field larger than than $H_{\rm rot} \sim 2.2$kOe is applied along the c-axis.

These results suggest that the spin-orbit coupling that affects a Cooper pair is small. However ,the contradiction between these experimental results and the theoretical assumption has been a great issue for this system. Miyake argued that almost all the spin-orbit coupling is exhausted to form the Kramers spin before forming the Cooper pair and that the gap symmetries with the line node are allowed, owing to the small "spin-orbit coupling" that affects the Cooper pair [34]. In the case of Sr_2RuO_4, which is one of the other candidates for spin-triplet superconductivity with strong spin-orbit coupling [35] but is not a heavy electron system, Yanase *et al* evaluated a microscopic model and pointed out that the effect of spin-orbit coupling λ_{ls} on the Cooper pair is scaled by the Fermi energy $T_{\rm F}$ as $\lambda_{ls}/T_{\rm F}$ under the condition $T_c \ll \lambda_{ls} \ll T_{\rm F}$ [36, 37]. Their result indicates that the effect of spin-orbit coupling that confines the d-vector can be estimated to be small compared with the conclusions of the phenomenological discussion [38]. Meanwhile, in the case of UPt_3, the typical energy scale for QPs is smaller than the spin-orbit coupling $\lambda_{ls} \gg T_{\rm F}^*$. Hence, it is questionable whether the conclusion from Sr_2RuO_4 can be applied to UPt_3 straightforwardly[38]. Further research is needed to explain the contradiction.

Meanwhile, Tou *et al.* also suggested that the decrease in the Knight shift below $H_{\rm rot}$ is too small, being on the order of 0.1%, while a 2.6% decrease is estimated from the conventional heavy electron theory[39]. Because the Knight shift is proportional to the spin susceptibility, the small Knight shift indicates that the heavy QPs in UPt_3 do not enhance spin susceptibility. Ikeda and Miyake suggested that the anomalous Fermi liquid can be explained with the Γ_4 non-Kramers singlet ground state by using Kotliar-Ruckenstein slave boson formalism [40, 41]. Namely, the QP with a non-magnetic singlet ground state does not enhance spin susceptibility. Such behavior also verified in the impurity model by calculation of the numerical renormalization group (NRG) [42].

1.3 Theoretical Review of f^2-configuration systems

In this section, we briefly review previous theoretical studies on f^2-configuaration systems and point out current problems. We also introduce the Rotationally invariant slave boson (RISB) formalism using in this thesis.

First, let us ignore CEF effects and consider degenerated multi-orbital system including Hund's coupling. Several studies have reported that Hund's coupling decreases the typical energy scale [43, 44, 45, 46]. Yotsuhashi *et al.* applied Wilson's NRG method to a two-orbital Kondo model with Hund's coupling [47] and calculated the orbital-dependent energy-scale $T_{\rm K1}$ and $T_{\rm K2}$. In the case of $T_{\rm K1} > T_{\rm K2}$, They pointed out that $T_{\rm K2}$ is suppressed drastically as Hund's coupling increased. Their studies shed light on the role of Hund's coupling in multi-orbital systems.

When a CEF effect is taken into account, a variety of interesting physical properties arises. In particular, we focus on two kinds of the singlet-ground-state systems in this thesis: one is the Γ_1 singlet ground state in cubic symmetry; the other is the Γ_4 singlet ground state in hexagonal and tetragonal symmetry. These states provide unconventional physical properties owing to a

cooperation with several low-energy excited states. Note that these two ground states exhibit different behaviors as follows.

In the case of the Γ_1 singlet ground state, theoretical models extracting two energy states at the f^2-configuration, $\Gamma_1(1) - \Gamma_4(3)$, have been mainly calculated in previous research. The eigenstates at the f^1-configuration in cubic symmetry are the Γ_7 doublet and Γ_8 quartet state. The impurity system has been investigated by means of NRG [48, 49, 13]. These studies revealed the three states existing in this system at the f^2-configuration: a CEF singlet state, Kondo-Yosida singlet state, and NFL. While the CEF singlet and KY singlet cross over smoothly and do not display any suppression of the energy scale T_{F^*}, the CEF triplet state and the other states exhibits a phase transition. The typical energy scale T_{F}^* suppresses drastically in the vicinity of this phase transition. A NFL is also reported at the CEF triplet state with a residual entropy $\sim 0.75 k_{\mathrm{B}} \ln 2$. The origin of the NFL is not yet clear, however, Koga and Matsumoto suggested that the NFL relates to the Γ_1 hexadecapolar moment [50].

In the case of the Γ_4 singlet ground state, theoretical models extracting three energy states at the f^2-configuration, $\Gamma_4(1) - \Gamma_5(2) - \Gamma_3(1)$, have been mainly calculated in previous research. Several studies have been carried out based on the impurity Anderson model by NRG [51, 14, 15]. It was reported that two stable states, a CEF singlet and Kondo-Yosida (KY) singlet state, exist in the vicinity of the f^2-configuration. In addition, the typical energy scale T_{F}^* suppresses in the vicinity of the phase boundary of these two states unlike the case of the Γ_1 singlet ground state. This suppression indicates that the CEF and KY singlet states compete each other and that HFL or NFL arise around the phase boundary. They also pointed out that the NFL is magnetically robust comparing with the NFL in the f^1-configuration systems induced by spin fluctuations.

Thus far, intensive studies based on impurity Anderson model, Kondo model, or Kondo lattice model have been performed in order to discuss f^2-configuration systems[52, 53]. These models are efficient for some typical situations: Kondo lattice model is efficient for the situation in which f-electrons are completely localized and an impurity Anderson model is efficient for the dilute system. In this regard, these models cannot capture the itinerant nature of f-electrons in lattice systems such as a HFL and SC. In order to discuss the HFL and SC, it is inevitable to investigate a multi-orbital periodic Anderson model.

There are several methods which can tackle this model: dynamical mean field theory (DMFT) [54], a 1/N expansion [55], and slave boson mean field theory [56]. DMFT is frequently employed to analyze correlated systems because it enables us to obtain highly accurate results at finite temperature [57, 58]. However, the DMFT calculation contains a technical problem: a negative sign problem. This problem emerges when a Hund's coupling and Pair hopping interaction play an crucial role. Namely, the negative sign problem is a fatal problem to analyze the f^2-configuration system. More efficient methods are preferred to capture the physical properties in the f^2-configuration systems.

On the other hand, the $1/N$ expansion was successfully used to discuss the NFL and SC in a non-Kramers doublet system [55]. However, this formalism has a strong limitation on the f^2-configuration systems. The $1/N$ expansion is efficient for an f^0-f^1 system because the number of perturbation channels is always consistent with the concept of this method. Namely, in an N-orbital system, there are $2N$ hopping processes (including the spin channel) from the f^0 state to a f^1 state, while there is only one hopping process from a f^1 state to the f^0 state. The $1/N$ expansion ignores hopping processes on the order of $1/N$. In the case of f^2-configuration systems, however, we cannot always construct an ideal energy scheme for the $1/N$ expansion

unlike the f^0-f^1 system.

In comparison with above two methods, slave boson formalism is simpler and widely applicable method. This formalism enables us to evaluate the renormalization factor z and the QP energy shift $\tilde{E}_f$ by means of saddle point approximation. It is verified that these quantities correspond to the results of the Gutzwiller approximation [59]. In the 1990s, The Kotliar-Ruckenstein slave boson (KRSB) formalism attracted much interest for its simple derivation and for the expectation that this formalism can be extended beyond the saddle point level by introducing Gaussian fluctuations [60, 61, 62]. Since estimation of the renormalization factor z is the first step of analyzing heavy electron systems. It is expected that this formalism will shed light on the complicated heavy electron systems such as uranium compounds. In fact, several studies on the f^2-configuration systems have been carried out by means of KRSB saddle point approximation [63, 64, 40, 41].

However, it has been pointed out that the KRSB formalism contains two severe problems: (i) There is no established procedure for introducing Gaussian fluctuations from the saddle point [65, 66, 67, 68] and (ii) the KRSB formalism can not be applied to multi-orbital systems that include non-density-density-type interactions such as Hund's coupling [56]. In particular, latter is a crucial to analyze f^2-configuration systems because they are essentially multi-orbital systems. Lechermann *et al.* pointed out problem (ii) and overcame it by proposing an extended KRSB formalism called rotationally invariant slave boson (RISB) formalism [56]. While this formalism mainly used in multi-orbital Hubbard model, few studies have carried out on f^2-configuration systems. Although other slave boson procedures have been proposed [69], these procedures give essentially the same results as the RISB formalism in the saddle point approximation. Therefore, we focus on the RISB formalism in this thesis.

Due to problem (i), considering the Gaussian fluctuation on the RISB formalism is rather difficult problem. Thus far, there are no previous studies who consider this approximation. However, we expect that it is possible to consider the Gaussian fluctuation even in the RISB formalism since many previous studies have been addressed to introduce Gaussian fluctuations into the KRSB formalism. In this sense, RISB formalism will be a strong method to investigate complicated heavy electron systems. Therefore, as a first step, it is significant to discuss the f^2-configuration systems by means of the RISB saddle point approximation.

1.4 Purpose of this thesis

The purpose of this thesis is to investigate how non-Kramers singlet ground states affect the itinerant nature of f-electrons by using the RISB saddle point approximation. In particular, we discuss two types of singlet ground state: one is the Γ_1 singlet ground state in cubic symmetry, and the other is the Γ_4 singlet ground state in hexagonal symmetry. This thesis is organized as follows. First, in chapter 2, we construct the effective three-orbital Hamiltonian that can obtain these ground states with realistic parameters. In chapter 3, we review the RISB formalism. We first discuss the KRSB formalism in a single orbital system and point out why it cannot apply to general multi-orbital systems. Then, the RISB formalism and its saddle point approximation is introduced. In chapter 4, we show the results of the Γ_1 and Γ_4 singlet ground state systems. Discussion and summary of this thesis are presented in chapter 5.

Chapter 2

Model Hamiltonian for multi-orbital f-electron systems

In this chapter, we derive two kinds of effective Hamiltonians: the three-orbital periodic Anderson model with different CEF splittings. One of the Hamiltonian considers cubic symmetry which can treat a Γ_1 CEF eigenstate as a ground state at the f^2-configuration. The three orbitals consist of $j = 5/2$ states where we assume the infinitely large spin-orbit coupling on the f-orbital. The other Hamiltonian considers hexagonal symmetry which can treat a Γ_4 CEF eigenstate as a ground state at the f^2-configuration. Since the Γ_4 CEF eigenstate degenerate with a Γ_3 CEF eigenstate in the case of jj-coupling scheme, the contribution of $j = 7/2$ states is necessary to obtain the ground state. Hence, we derive the effective three orbitals that consist of both the $j = 5/2$ and $j = 7/2$ states.

This chapter is organized as follows. In section 2.1, we introduce the multi-orbital periodic Anderson model and define the form of the itinerant part of this model, i.e., density of states of conduction electrons and hybridizations between the conduction and f-electrons. In section 2.2, a Hamiltonian for the f-electrons in the atomic limit is introduced without any approximations. The localized part of the multi-orbital periodic Anderson models are derived in section 2.3 (cubic symmetry) and 2.4 (hexagonal symmetry) from the Hamiltonian in section 2.2.

2.1 Construction of Effective Model Hamiltonian

In this thesis, we discuss the f^2-configuration systems with the following multi-orbital periodic Anderson model,

$$\mathcal{H}_{\rm AM} = \sum_{ij}\sum_{\nu\in\mathcal{N}} \left(t_{ij} - \mu\right) c^\dagger_{i\nu} c_{j\nu} + \mathcal{H}_{\rm loc} + \sum_{i}\sum_{\nu\in\mathcal{N}} \left(V_\nu c^\dagger_{i\nu} f^{\rm phys}_{i\nu} + {\rm h.c.} \right), \tag{2.1}$$

$$\tag{2.2}$$

where $\mathcal{N}$ represents the set of the f-orbitals ν (including the spin degrees-of-freedom); $c^\dagger_{i\nu}$ ($c_{i\nu}$) and $f^{\rm phys\dagger}_{i\nu}$ ($f^{\rm phys}_{i\nu}$) denote the creation (annihilation) operator for the conduction electron and a f-electron at site i and state ν, respectively; t_{ij} represents the hopping term of the conduction electrons; μ describes a chemical potential; V_ν represents the hybridization between the conduction and the f-electrons; and the localized Hamiltonian $\mathcal{H}_{\rm loc}$ contains the effect of the localized f-electrons.

For simplicity, we introduce multi conduction bands labeled by $\nu \in \mathcal{N}$ and assume that the f-electrons hybridize with the same representation of the conduction electrons. In addition, we also assume that the density of state (DOS) $\rho_\nu(\varepsilon)$ for the conduction electrons is given by,

$$\rho_\nu(\varepsilon) = \begin{cases} 1/2D & (-D < \varepsilon < D) \\ 0 & \text{otherwise} \end{cases}, \tag{2.3}$$

where D represents half of the band width and is used as an unit of energy in the following.

The local Hamiltonian $\mathcal{H}_{\rm loc}$ is written as,

$$\mathcal{H}_{\rm loc} = \sum_i \sum_{\nu\in\mathcal{N}} (E_\nu - \mu) f^{\rm phys\dagger}_{i\nu} f^{\rm phys}_{i\nu} + \sum_i \sum_{\nu_1\nu_2\nu_3\nu_4\in\mathcal{N}} I^{\nu_3\nu_4}_{\nu_1\nu_2} f^{\rm phys\dagger}_{i\nu_4} f^{\rm phys\dagger}_{i\nu_3} f^{\rm phys}_{i\nu_2} f^{\rm phys}_{i\nu_1}, \tag{2.4}$$

where E_ν and $I^{\nu_3\nu_4}_{\nu_1\nu_2}$ represent the energy level of the ν orbital and the interaction among the f-electrons, respectively. The purpose of this thesis is to evaluate the f^2-configuration systems with the Γ_1 ground state in cubic symmetry and the Γ_4 ground state in hexagonal symmetry. Hence, it is necessary to realize these ground states from $\mathcal{H}_{\rm loc}$. In the following sections, we address to construct $\mathcal{H}_{\rm loc}$ that realizes the Γ_1 ground state in cubic symmetry or the Γ_4 ground state in hexagonal symmetry.

2.2 f-electron Systems in Atomic Limit

In order to construct $\mathcal{H}_{\rm loc}$, it is significant to review the general relations on the f-orbitals. In this section, we introduce the explicit forms of $\mathcal{H}_{ls}$, $\mathcal{H}_{\rm CEF}$, and $\mathcal{H}_U$ on the f-orbitals in the atomic limit. For simplicity, we omit the site index i in the following discussion.

The f-orbital contains fourteen-fold degeneracy owing to the orbital angular momentum $l = 3$ and the spin $s = 1/2$; each state is distinguished by the z-component of the orbital angular momentum $m_z \in \{-3, -2, \cdots, 3\}$ and that of the spin $s_z \in \{\downarrow = -\frac{1}{2}, \uparrow = \frac{1}{2}\}$. we can describe the explicit form of the $\mathcal{H}_{ls}$, $\mathcal{H}_{\rm CEF}$, and $\mathcal{H}_U$ by using the creation (annihilation) operator for the m_z and s_z state as $f^{\rm phys\dagger}_{m_z s_z}$ ($f^{\rm phys}_{m_z s_z}$).

First, $\mathcal{H}_{ls}$ is given by,

$$\begin{aligned}
\mathcal{H}_{ls} &= \lambda_{ls} \boldsymbol{l}\cdot\boldsymbol{s}, \\
&= \lambda_{ls} \sum_{m_z s_z} m_z s_z f^{\rm phys\dagger}_{m_z s_z} f^{\rm phys}_{m_z s_z} \\
&+ \frac{1}{2}\lambda_{ls} \sum_{m_z s_z} \sqrt{(l-m_z)(l+m_z+1)}\sqrt{(s+s_z)(s-s_z+1)} f^{\rm phys\dagger}_{m_z+1 s_z-1} f^{\rm phys}_{m_z s_z} \\
&+ \frac{1}{2}\lambda_{ls} \sum_{m_z s_z} \sqrt{(l+m_z)(l-m_z+1)}\sqrt{(s-s_z)(s+s_z+1)} f^{\rm phys\dagger}_{m_z-1 s_z+1} f^{\rm phys}_{m_z s_z}
\end{aligned} \tag{2.5}$$

where λ_{ls} represents the spin-orbit coupling.

Second, $\mathcal{H}_{\rm CEF}$ depends on the crystal structure and the angular momentum of the f-electrons. In the case of cubic (O_h or T_d) symmetry, the CEF Hamiltonian $\mathcal{H}_{\rm cubic}$ is given by,

$$\mathcal{H}_{\rm cubic} = B_{40}\left(\hat{O}_{40} + 5\hat{O}_{44}\right) + B_{60}\left(\hat{O}_{60} - 21\hat{O}_{64}\right), \tag{2.6}$$

where $B_{\alpha\beta}$ and $\hat{O}_{\alpha\beta}$ denote the CEF parameters and Steven's operators, respectively. Steven's operators for f-electrons ($J = l = 3$) are listed in Table 2.2 [70]. Using this table, eq. (2.6) can be written as,

$$\begin{aligned}\mathcal{H}_{\text{cubic}} = &\sum_{m_z s_z} \left(B_{40}O_{40(m_z,m_z)} + B_{60}O_{60(m_z,m_z)}\right) f^{\text{phys}\dagger}_{m_z s_z} f^{\text{phys}}_{m_z s_z} \\ &+ \sum_{m_z s_z} \left(5B_{40}O_{44(m_z+4,m_z)} - 21B_{60}O_{64(m_z+4,m_z)}\right) f^{\text{phys}\dagger}_{m_z+4 s_z} f^{\text{phys}}_{m_z s_z} \\ &+ \sum_{m_z s_z} \left(5B_{40}O_{44(m_z-4,m_z)} - 21B_{60}O_{64(m_z-4,m_z)}\right) f^{\text{phys}\dagger}_{m_z-4 s_z} f^{\text{phys}}_{m_z s_z}, \end{aligned} \tag{2.7}$$

where $O_{nm(m_z,m'_z)}$ denotes (m_z, m'_z) component of the matrix elements of Steven's operator $\hat{O}_{nm}$. For instance, $O_{64(+2,-2)}$ is equal to 60 in accordance with Table 2.2. Likewise, in the case of hexagonal (D_{6h}) symmetry, The CEF Hamiltonian $\mathcal{H}_{\text{hex}}$ is given by,

$$\begin{aligned}\mathcal{H}_{\text{hex}} &= B_{20}\hat{O}_{20} + B_{20}\hat{O}_{40} + B_{60}\hat{O}_{60} + B_{66}\hat{O}_{66} \\ &= \sum_{m_z s_z} \left(B_{20}O_{20(m_z,m_z)} + B_{40}O_{40(m_z,m_z)} + B_{60}O_{60(m_z,m_z)}\right) f^{\text{phys}\dagger}_{m_z s_z} f^{\text{phys}}_{m_z s_z} \\ &+ \sum_{m_z s_z} B_{66}O_{66(m_z+6,m_z)} f^{\text{phys}\dagger}_{m_z+6 s_z} f^{\text{phys}}_{m_z s_z} \\ &+ \sum_{m_z s_z} B_{66}O_{66(m_z-6,m_z)} f^{\text{phys}\dagger}_{m_z-6 s_z} f^{\text{phys}}_{m_z s_z}. \end{aligned} \tag{2.8}$$

Finally, the electron-electron interactions $\mathcal{H}_U$ can be derived in accordance with group theory by using Slater-Condon parameters F^k and Gaunt coefficient $c_k(m_z, m'_z)$. $\mathcal{H}_U$ is given by,

$$\begin{aligned}\mathcal{H}_U = &\sum_{m_{z1}\ldots m_{z4}} \sum_{s_z} I^{m_{z3}m_{z4}}_{m_{z1}m_{z2}} f^{\text{phys}\dagger}_{m_{z4}s_z} f^{\text{phys}\dagger}_{m_{z3}s_z} f^{\text{phys}}_{m_{z2}s_z} f^{\text{phys}}_{m_{z1}s_z} \\ &+ I^{m_{z3}m_{z4}}_{m_{z1}m_{z2}} f^{\text{phys}\dagger}_{m_{z4}s_z} f^{\text{phys}\dagger}_{m_{z3}\bar{s}_z} f^{\text{phys}}_{m_{z2}\bar{s}_z} f^{\text{phys}}_{m_{z1}s_z} \end{aligned} \tag{2.9}$$

$$I^{m_{z3}m_{z4}}_{m_{z1}m_{z2}} = \sum_{k=0}^{6} F^k c_k(m_{z1}, m_{z4})\, c_k(m_{z2}, m_{z3})\, \delta_{m_{z1}+m_{z2},m_{z3}+m_{z4}}. \tag{2.10}$$

$c_k(m_z, m'_z)$ is listed in table 2.1 for the case of interactions among the f-electrons (f-f interaction), and has the relation: $c_k(m_z, m'_z) = (-1)^{(m_z - m'_z)} c_k(m'_z, m_z)$ [71, 72, 73]. According to the Wigner-Eckart theorem, $c_k(m_z, m'_z)$ with odd number k are 0 in the f-f interactions. Note that the representation of $\mathcal{H}_U$ is a general form derived from the group theory. All the typical Coulomb interactions such as an intra-orbital interaction, an inter-orbital interaction, and Hund's coupling can be obtained by a linear combination of Slater-Condon parameters F^k. In this thesis, in order to reduce the number of parameters, we fix the ratio of Slater-Condon parameters as,

$$F^0 = U, F^2 = 0.5U, F^4 = 0.3U, F^6 = 0.1U, \tag{2.11}$$

where U is a scaling parameter controlling the strength of interactions.

Although $\mathcal{H}_{\text{loc}}$ can be described by $\mathcal{H}_{ls} + \mathcal{H}_{\text{CEF}} + \mathcal{H}_U$, the system contains enormous degree of freedoms: 14 states in the f^1-configuration system, ${}_{14}\text{C}_2 = 91$ states in the f^2-configuration

systems, ${}_{14}\mathrm{C}_3 = 364$ states in the f^3-configuration systems and so on. Because we expect that most of the excited states do not affect the physical properties, it is important for efficient calculations to omit some excited states with appropriate approximations.

As we discussed in chapter 1, both jj and LS coupling schemes are frequently used for this purpose. Although these coupling schemes are efficient for describing localized energy states on each f^n-configuration, the relation among the f^n-configurations are unclear. Namely, these coupling schemes employ different CEF parameters in each f^n-configuration. Since the CEF parameters are nothing but one-body terms, these coupling schemes ignore the relation among different configurations.

In order to discuss the itinerant character of the f-electrons, the transition processes from the f^n-configuration to the f^{n-1}-configuration or the f^{n+1}-configuration should be taken into consideration. Then, the above inconsistency is a fatal problem.

Meanwhile, we expect that it is enough to consider three-orbitals mainly based on $j = 5/2$ states to evaluate the uranium compounds due to the large spin orbit coupling. In the following sections, we discuss how to construct the effective three-orbital Hamiltonian $\mathcal{H}_{\mathrm{loc}}$ from $\mathcal{H}_{ls} + \mathcal{H}_{\mathrm{CEF}} + \mathcal{H}_U$. Section 2.3 (Section 2.4) focuses on the case of cubic symmetry with realizing Γ_1 ground state (hexagonal symmetry with realizing Γ_4 ground state) at the f^2-configuration.

(m, m')	c_0	c_2	c_4	c_6
$(\pm3, \pm3)$	1	$-5/15$	$3/33$	$-5/429$
$(\pm3, \pm2)$	0	$5/15$	$-\sqrt{30}/33$	$5\sqrt{7}/429$
$(\pm3, \pm1)$	0	$-\sqrt{10}/15$	$3\sqrt{6}/33$	$-10\sqrt{7}/429$
$(\pm3, 0)$	0	0	$-3\sqrt{7}/33$	$10\sqrt{21}/429$
$(\pm3, \mp1)$	0	0	$\sqrt{42}/33$	$-5\sqrt{210}/429$
$(\pm3, \mp2)$	0	0	0	$5\sqrt{462}/429$
$(\pm3, \mp3)$	0	0	0	$-10\sqrt{231}/429$
$(\pm2, \pm2)$	1	0	$-7/33$	$30/429$
$(\pm2, \pm1)$	0	$\sqrt{15}/15$	$4\sqrt{2}/33$	$-5\sqrt{105}/429$
$(\pm2, 0)$	0	$-2\sqrt{5}/15$	$-\sqrt{3}/33$	$20\sqrt{14}/429$
$(\pm2, \mp1)$	0	0	$-\sqrt{14}/33$	$-15\sqrt{42}/429$
$(\pm2, \mp2)$	0	0	$\sqrt{70}/33$	$30\sqrt{14}/429$
$(\pm1, \pm1)$	1	$3/15$	$1/33$	$-75/429$
$(\pm1, 0)$	0	$\sqrt{2}/15$	$\sqrt{15}/33$	$25\sqrt{14}/429$
$(\pm1, \mp1)$	0	$-2\sqrt{6}/15$	$-2\sqrt{10}/33$	$-10\sqrt{105}/429$
$(0, 0)$	1	$4/15$	$6/33$	$100/429$

Table 2.1: List of Gaunt coefficients in the case of f-f interactions.

2.3 Effective Hamiltonian for Cubic Systems

In this section, we construct the effective local Hamiltonian $\mathcal{H}_{\mathrm{loc}}$ that enables us to discuss the Γ_1 ground state in cubic symmetry. In order to reduce the number of orbitals, we assume $\lambda_{ls} \to \infty$ and ignore $j = 7/2$ states. Namely, we consider the effective three-orbital model composed of $j = 5/2$ for the case of cubic symmetry. Table 2.3 lists the eigenstates of $j = 5/2$ in terms of an orbital and a spin angular momentum $|m_z, s_z\rangle$.

$$\hat{O}_{20}^{J} = 3J_z^2 - J\left(J+1\right)$$

$\hat{O}_{20}^{J}$	$(0,0)$	$(\pm1,\pm1)$	$(\pm2,\pm2)$	$(\pm3,\pm3)$	$(\pm4,\pm4)$
$J=3$	-12	-9	0	15	-
$J=4$	-20	-17	-8	7	28
	$\left(\pm\frac{1}{2},\pm\frac{1}{2}\right)$	$\left(\pm\frac{3}{2},\pm\frac{3}{2}\right)$	$\left(\pm\frac{5}{2},\pm\frac{5}{2}\right)$	-	-
$J=\frac{5}{2}$	-8	-2	10	-	-

$$\hat{O}_{40}^{J} = 35J_z^4 - 30J\left(J+1\right)J_z^2 + 25J_z^2 - 6J\left(J+1\right) + 3J^2\left(J+1\right)^2$$

$\hat{O}_{40}^{J}$	$(0,0)$	$(\pm1,\pm1)$	$(\pm2,\pm2)$	$(\pm3,\pm3)$	$(\pm4,\pm4)$
$J=3$	360	60	-420	180	-
$J=4$	1080	540	-660	-1260	840
	$\left(\pm\frac{1}{2},\pm\frac{1}{2}\right)$	$\left(\pm\frac{3}{2},\pm\frac{3}{2}\right)$	$\left(\pm\frac{5}{2},\pm\frac{5}{2}\right)$	-	-
$J=\frac{5}{2}$	120	-180	60	-	-

$$\hat{O}_{60}^{J} = 231J_z^6 - 315J\left(J+1\right)J_z^4 + 735J_z^4 + 105J^2\left(J+1\right)^2J_z^2 - 525J\left(J+1\right)J_z^2 + 294J_z^2 - 5J^3\left(J+1\right)^3 + 40J^2\left(J+1\right)^2 - 60J\left(J+1\right)$$

$\hat{O}_{60}^{J}$	$(0,0)$	$(\pm1,\pm1)$	$(\pm2,\pm2)$	$(\pm3,\pm3)$	$(\pm4,\pm4)$
$J=3$	-3600	2700	-1080	180	-
$J=4$	-25200	1260	27720	-21420	5040
	$\left(\pm\frac{1}{2},\pm\frac{1}{2}\right)$	$\left(\pm\frac{3}{2},\pm\frac{3}{2}\right)$	$\left(\pm\frac{5}{2},\pm\frac{5}{2}\right)$	-	-
$J=\frac{5}{2}$	0	0	0	-	-

$$\hat{O}_{44}^{J} = \frac{1}{2}\left(J_+^4 + J_-^4\right)$$

$\hat{O}_{44}^{J}$	$(\pm2,\mp2)$	$(\pm3,\mp1)$	$(\pm4,0)$
$J=3$	60	$12\sqrt{15}$	-
$J=4$	180	$60\sqrt{7}$	$12\sqrt{70}$
	$\left(\pm\frac{5}{2},\mp\frac{3}{2}\right)$	-	-
$J=\frac{5}{2}$	$12\sqrt{5}$	-	-

$$\hat{O}_{64}^{J} = \frac{1}{4}\left[\left(11J_z^2 - J\left(J+1\right) - 38\right)\left(J_+^4 + J_-^4\right) + \left(J_+^4 + J_-^4\right)\left(11J_z^2 - J\left(J+1\right) - 38\right)\right]$$

$\hat{O}_{64}^{J}$	$(\pm2,\mp2)$	$(\pm3,\mp1)$	$(\pm4,0)$
$J=3$	-360	$60\sqrt{15}$	-
$J=4$	-2520	$-180\sqrt{7}$	$360\sqrt{70}$
	$\left(\pm\frac{5}{2},\mp\frac{3}{2}\right)$	-	-
$J=\frac{5}{2}$	0	-	-

$$\hat{O}_{66}^{J} = \frac{1}{2}\left(J_+^6 + J_-^6\right)$$

$\hat{O}_{66}^{J}$	$(\pm3,\mp3)$	$(\pm4,\mp2)$
$J=3$	360	-
$J=4$	2520	$720\sqrt{7}$
	-	-
$J=\frac{5}{2}$	-	-

Table 2.2: Matrix elements of Steven's operators in the case of $J=3$, $J=4$, and $J=5/2$. Numbers in parenthesis and under the parenthesis denote the non-zero matrix component and its value.

$j = 5/2$ state	
$\|j_z\rangle$	$\|m_z, s_z\rangle$
$\|\pm 5/2\rangle$	$\pm\sqrt{\frac{1}{7}}\|\pm 2,\uparrow\rangle \mp \sqrt{\frac{6}{7}}\|\pm 3,\downarrow\rangle$
$\|\pm 3/2\rangle$	$\pm\sqrt{\frac{2}{7}}\|\pm 1,\uparrow\rangle \mp \sqrt{\frac{5}{7}}\|\pm 2,\downarrow\rangle$
$\|\pm 1/2\rangle$	$\pm\sqrt{\frac{3}{7}}\|0,\uparrow\rangle \mp \sqrt{\frac{4}{7}}\|\pm 1,\downarrow\rangle$

Table 2.3: $j = 5/2$ states written in terms $|m_z, s_z\rangle$.

The CEF Hamiltonian for the $j = 5/2$ states $\mathcal{H}^{5/2}_{\rm cubic}$ can be written as,

$$\begin{aligned}\mathcal{H}^{5/2}_{\rm cubic} = &\sum_{j_z} B^{5/2}_{40} O_{40(j_z,j_z)} f^{\rm phys\dagger}_{j_z} f^{\rm phys}_{j_z} \\ &+ \sum_{j_z} 5B^{5/2}_{40} O_{44(j_z+4,j_z)} f^{\rm phys\dagger}_{j_z+4} f^{\rm phys}_{j_z} \\ &+ \sum_{j_z} 5B^{5/2}_{40} O_{44(j_z-4,j_z)} f^{\rm phys\dagger}_{j_z-4} f^{\rm phys}_{j_z},\end{aligned} \tag{2.12}$$

where $j_z \in \{-\frac{5}{2}, -\frac{3}{2}, \cdots, \frac{5}{2}\}$, $B^{5/2}_{40}$ represents a CEF parameter for $j = 5/2$. The elements of Steven's operators $O_{nm(j_z,j'_z)}$ for $j = 5/2$ are listed in table 2.2. Note that the sixth-order of Steven's operators do not act on the $j = 5/2$ state (see table 2.2). By transforming the basis of eq.(2.7) from $|m_z, s_z\rangle$ states into the eigenstates of $\mathcal{H}_{\rm ls}$, the following relations can be derived: $B^{5/2}_{40} = 11/7B_{40}$ and $B^{5/2}_{60} = 0$.

We obtain the f-electron orbitals for effective localized Hamiltonian $\mathcal{H}_{\rm loc}$ by diagonalizing eq. (2.12). The eigenvalues Δ_ν and eigenstates $|\nu\rangle$ of $\mathcal{H}^{5/2}_{\rm cubic}$ are given by,

$$\Delta_{\pm\Gamma_7} = \Delta_{\Gamma_7} = -240B^{5/2}_{40}, \tag{2.13}$$

$$|\Gamma_{\pm 7}\rangle = \sqrt{\frac{1}{6}}|\pm\frac{5}{2}\rangle - \sqrt{\frac{5}{6}}|\mp\frac{3}{2}\rangle, \tag{2.14}$$

$$\Delta_{\pm\Gamma_{81}} = \Delta_{\pm\Gamma_{82}} = \Delta_{\Gamma_8} = 120B^{5/2}_{40}, \tag{2.15}$$

$$|\Gamma_{\pm 81}\rangle = \sqrt{\frac{5}{6}}|\pm\frac{5}{2}\rangle + \sqrt{\frac{1}{6}}|\mp\frac{3}{2}\rangle, \tag{2.16}$$

$$|\Gamma_{\pm 82}\rangle = |\pm\frac{1}{2}\rangle, \tag{2.17}$$

where Γ_7 doublet and Γ_8 quartet are the irreducible representations of symmetry point group in cubic symmetry. Hereafter, we assume elements of the set $\mathcal{N}$ in eq. (2.1) as:

$$\mathcal{N} = \{\Gamma_{+7}, \Gamma_{-7}, \Gamma_{+81}, \Gamma_{-81}, \Gamma_{+82}, \Gamma_{-82}\}. \tag{2.18}$$

Then, the one-body term of the effective local Hamiltonian E_ν is the sum of Δ_ν and the f-electron energy level E_f.

The two-body terms of the effective local Hamiltonian $I^{\nu_3\nu_4}_{\nu_1\nu_2}$ can be written as,

$$I^{\nu_3\nu_4}_{\nu_1\nu_2} = \sum_{m_{1\cdots4}\in\{-3\cdots3\}} \sum_{\sigma_{1\cdots4}\in\{-1/2,1/2\}} \delta_{\sigma_1\sigma_4}\delta_{\sigma_2\sigma_3} \prod_{i=1}^{4} A^{m_i\sigma_i}_{\nu_i} \sum_{k=0}^{6} F^k c_k(m_1, m_4)\, c_k(m_2, m_3). \tag{2.19}$$

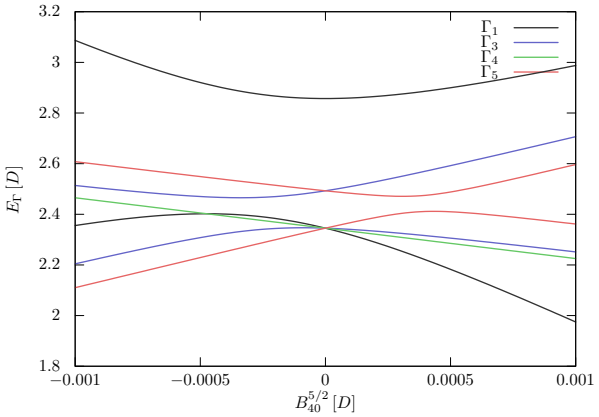

Figure 2.1: Figure shows the eigenvalues of the f^2-configuration in cubic symmetry with $U = 2.5D$.

Here, $A_{\nu_i}^{m_i\sigma_i}$ represents the coefficient of the $|m_i\sigma_i\rangle$ state in the $|\nu\rangle$ state. $A_{\nu_i}^{m_i\sigma_i}$ is derived from eq. (2.17) and table 2.12.

At the end of this section, we mention that $\mathcal{H}_{\rm loc}$ can realize the Γ_1 singlet state as a ground state of the f^2-configuration. Figure 2.1 shows the energy scheme of the f^2-configuration as a function of $B_{40}^{5/2}$ with $U = 2.5D$ and $E_f = 0$. In the case of $B_{40}^{5/2} > 0$, the Γ_1 singlet ground state is realized, while the Γ_5 triplet ground state is realized in the opposite region $B_{40}^{5/2} < 0$. It is to be noted that the non-magnetic doublet state Γ_3, which is one of the other scenarios for the non-Fermi liquid behavior on UBe_{13}, cannot be a ground state in any parameter set. We will discuss the $B_{40}^{5/2} = 0.0001D$ case in chapter 4.

2.4 Effective Hamiltonian for hexagonal Systems

Let us construct the another effective local Hamiltonian $\mathcal{H}_{\rm loc}$: hexagonal symmetry case with the Γ_4 singlet ground state at the f^2-configuration. In contrast to the Γ_1 singlet ground state in cubic symmetry, there is a serious problem that the effective local Hamiltonian in the case of $\lambda_{ls} \to \infty$ cannot realize Γ_4 singlet ground state. Namely, the Γ_4 state degenerates to the Γ_3 state in this case. Hereafter, we call the degeneracy of different irreducible representations as "accidental degeneracy".

The accidental degeneracy can be understood from the jj coupling scheme. As we mentioned in chapter 1, the $J = 4$ state is a ground state in this energy scheme at the f^2-configuration. The explicit form of the CEF Hamiltonian for $J = 4$ is written as,

$$\mathcal{H}_{\rm hex}^4 = B_{20}^4\hat{O}_{20} + B_{20}^4\hat{O}_{40} + B_{60}^4\hat{O}_{60} + B_{66}^4\hat{O}_{66}, \tag{2.20}$$

where B_{nm}^4 denotes CEF parameters of Steven's operator $\hat{O_{nm}}$ for $J = 4$ listed in table 2.2. The Γ_3 and Γ_4 states are derived by the diagonalization of $\mathcal{H}_{\rm hex}^4$. The eigenvalues E_Γ and eigenstates

$|\Gamma\rangle$ are given by,

$$E_{\Gamma_3} = 7B_{20}^4 - 1260B_{40}^4 - 21420B_{60}^4 + 2520B_{66}^4, \tag{2.21}$$

$$|\Gamma_3\rangle = \frac{1}{\sqrt{2}}\left(|+3\rangle + |-3\rangle\right), \tag{2.22}$$

$$E_{\Gamma_4} = 7B_{20}^4 - 1260B_{40}^4 - 21420B_{60}^4 - 2520B_{66}^4, \tag{2.23}$$

$$|\Gamma_4\rangle = \frac{1}{\sqrt{2}}\left(|+3\rangle - |-3\rangle\right). \tag{2.24}$$

By using Clebsch-Gordon coefficients, the Γ_3 and Γ_4 states can be rewritten in terms of two $j = 5/2$ states $|j_{1z}, j_{2z}\rangle$ as follows:

$$|\Gamma_3\rangle = \frac{1}{\sqrt{2}}\left(\left\{+\frac{5}{2}, +\frac{1}{2}\right\} + \left\{-\frac{5}{2}, -\frac{1}{2}\right\}\right), \tag{2.25}$$

$$|\Gamma_4\rangle = \frac{1}{\sqrt{2}}\left(\left\{+\frac{5}{2}, +\frac{1}{2}\right\} - \left\{-\frac{5}{2}, -\frac{1}{2}\right\}\right), \tag{2.26}$$

where $\{\alpha, \beta\}$ denotes the anti-commutation rule of fermions with normalization factor,

$$\frac{1}{\sqrt{2}}\left(|\alpha, \beta\rangle - |\beta, \alpha\rangle\right). \tag{2.27}$$

These two energy levels seem to split in the case of finite B_{66}^4. However, we can derive that all the sixth-order of Steven's operators for $J = 4$ have to be zero in the case of the jj coupling scheme as follows.

In the jj coupling scheme, all the eigenstates have to be composed of several $j = 5/2$ states. The matrix components of the sixth-order of Steven's operators for $j = 5/2$ are zero as we mentioned in section 2.3. Performing the CEF Hamiltonian for $j = 5/2$ to the eigenstates eqs. (2.25) and (2.26), we can verify the accidental degeneracy of the two states.

An accidental degeneracy often occurs in the jj coupling scheme due to the absence of sixth-order Steven's operators. In order to split the degeneracy, it is significant to consider a contribution from the $j = 7/2$ states. Hotta and Harima proposed an extended jj coupling scheme that takes into account the $j = 7/2$ state as a second perturbation expansion in terms of $1/\lambda_{ls}$ [74]. Their formalism only focuses on energy shifts and does not modify eigenstates from the $j = 5/2$ states. In this chapter, we propose the other scheme to split the accidental degeneracy. In contrast to the extended jj coupling scheme, our scheme modifies both the eigenvalues and eigenstates from the $j = 5/2$ states.

The procedure of present scheme is as follows. First, we consider finite but large λ_{ls} and diagonalize $\mathcal{H}_{ls} + \mathcal{H}_{\rm CEF}$. Here, the explicit form of $\mathcal{H}_{\rm CEF}$ is eq. 2.8. Next, we ignore the upper four excited states where these states correspond to $j = 7/2$ in the case of $\lambda_{ls} \to \infty$. Finally, the two-body terms of the effective local Hamiltonian $I_{\nu_1\nu_2}^{\nu_3\nu_4}$ are calculated by using the eigenstates of the lower three-orbitals.

Hereafter, we set the following parameters as $\lambda_{ls} = 0.5D$, $B_2^0 = 0.003D$, $B_4^0 = -0.0002D$, and $B_6^0 = 0.00005D$. Figure 2.2 shows the eigenenergies of $\mathcal{H}_{ls} + \mathcal{H}_{\rm CEF}$ at the f^1-configuration as a function of B_{66}. There are large energy gap between the lower six-states and the upper eight-states E_g due to the spin-orbit coupling. Note that the sixth-order of Steven's operators, O_{60} and O_{66}, affect the eigenstates through the $j = 7/2$ states in this scheme. The six-states

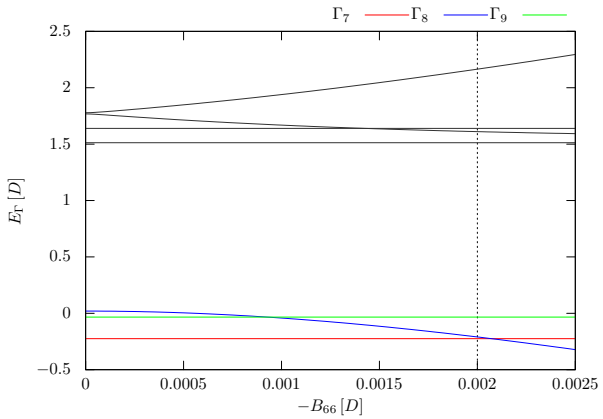

Figure 2.2: Energy scheme in the f^1-configuration systems in the case of $\lambda_{ls} = 0.5D$, $B_{20} = 0.003D$, $B_{40} = -0.0002D$, and $B_{60} = 0.00005D$ in hexagonal symmetry. Red, green, and blue lines represent Γ_7, Γ_8, and Γ_9 state. Black lines are the other energy levels.

can be labeled by the irreducible representations of the symmetry point group in hexagonal symmetry: Γ_7, Γ_8, and Γ_9. These eigenstates can be written in terms of both the $j = 5/2$ states $|j_z\rangle_{\frac{5}{2}}$ and the $j = 7/2$ states $|j_z\rangle_{\frac{7}{2}}$ as follows:

$$\begin{aligned}
|\Gamma_{\pm 7}\rangle &= \alpha_{\Gamma_7}|\pm 1/2\rangle_{\frac{5}{2}} + \beta_{\Gamma_7}|\pm 1/2\rangle_{\frac{7}{2}}, \\
|\Gamma_{\pm 8}\rangle &= \alpha_{\Gamma_8}|\pm 5/2\rangle_{\frac{5}{2}} + \beta_{\Gamma_8}|\pm 5/2\rangle_{\frac{7}{2}} + \gamma_{\Gamma_8}|\mp 7/2\rangle_{\frac{7}{2}}, \\
|\Gamma_{\pm 9}\rangle &= \alpha_{\Gamma_9}|\pm 3/2\rangle_{\frac{5}{2}} + \beta_{\Gamma_9}|\pm 3/2\rangle_{\frac{7}{2}},
\end{aligned} \tag{2.28}$$

where α_ν, β_ν, and γ_ν represent the coefficient of the $|j_z\rangle_{\frac{5}{2}}$ and $|j_z\rangle_{\frac{7}{2}}$ states.

Figure 2.3 shows α_ν, β_ν, and γ_ν as a function of B_{66}. In spite of the large energy gap $E_g \sim 1.5D$ (see Fig. 2.2), $|\Gamma_{\pm 8}\rangle$ states are clearly modified by the contribution of $|\pm\frac{7}{2}\rangle_{\frac{7}{2}}$. This result indicates that the accidental degeneracy at the f^2-configuration will split by using the present scheme.

Hereafter, we take the lower six-states as elements of the set $\mathcal{N}$:

$$\mathcal{N} = \{\Gamma_{+7}, \Gamma_{-7}, \Gamma_{+8}, \Gamma_{-8}, \Gamma_{+9}, \Gamma_{-9}\}\,. \tag{2.29}$$

Then, the one-body term of the effective local Hamiltonian E_ν is derived from the sum of the eigenenergy of ν state and the f-electron energy level E_f. We note that Fig. 2.2 assumes $E_f = 0$.

Although the two-body terms of the effective local Hamiltonian $I^{\nu_3\nu_4}_{\nu_1\nu_2}$ are also written as eq. (2.10), the contents of $A^{m_i\sigma_i}_{\nu_i}$ and $\mathcal{N}$ are different from section 2.3: $A^{m_i\sigma_i}_{\nu_i}$ is derived from eq. (2.28), table 2.12, and the eigenstates of $j = 7/2$.

Figure 2.4 shows the B_{66} dependence of the energy scheme of the f^2-configurations in the case of $U = 2.5D$ and $E_f = 0$. In the range of $-0.0025D < B_{66} < -0.00125D$, the Γ_4 ground state is realized. It is to be noted that the ground state becomes Γ_1 singlet by further decreasing B_{66}. We will discuss the $B_{66} = -0.02D$ case in chapter 5.

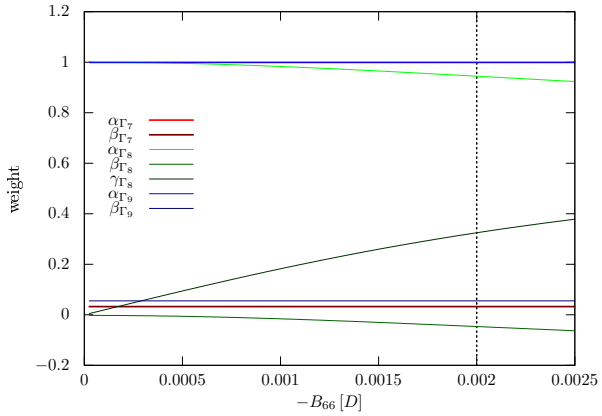

Figure 2.3: Coefficients of eigenstates defined in eq. (2.28).

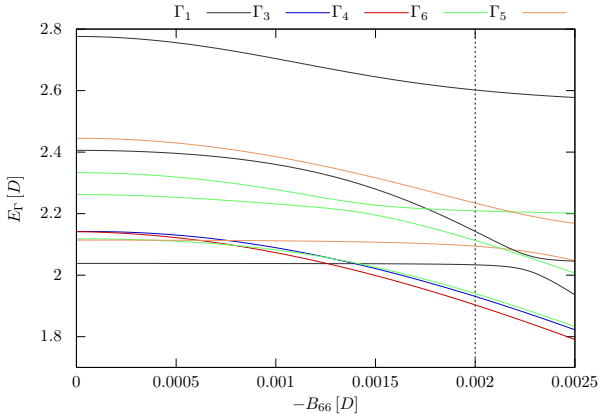

Figure 2.4: Energy scheme in the f^2-configuration systems in the case of $\lambda_{ls} = 0.5D$, $B_2^0 = 0.003D$, $B_4^0 = -0.0002D$, and $B_6^0 = 0.00005D$ in hexagonal symmetry.

Before closing this section, let us discuss an applicable range of the present scheme. The present scheme seems to be valid for the case of $U \ll \lambda_{ls}$ since we ignore the upper eight-states mainly composed of the $j = 7/2$ state. However, Figs. 2.2 and 2.4 result that present scheme is valid even for the case of $U = 2.5D$ and $\lambda_{ls} = 0.5D$.

In the f^2-configuration, eigenstates relating to the upper eight-states (the present scheme ignores these states) should be higher than at least E_g from the lowest eigenenergy shown in Fig. 2.4. These eigenstates can be negligible, because the energy gap between the lowest and the highest eigenenergies in Fig. 2.4 is approximately $0.8D$.

A wide applicable range was also pointed out in the extended jj coupling scheme by Hotta and Harima. They proposed that the extended jj coupling scheme is valid for $0.1U \ll \lambda_{ls}$ when the CEF splitting is of the order of 10^{-4}eV. The applicable range of the present scheme is similar as that of the extended jj coupling scheme since both schemes contain the effect of $j = 7/2$ states.

Chapter 3

Slave Boson Formalism

In the previous chapter, we introduced effective model Hamiltonians for the f^2-configuration systems. Because we cannot solve these Hamiltonians exactly, some approximations that enable us to discuss the itinerant character of f-electrons are needed. In this chapter, we review one of the slave boson formalisms called rotationally invariant slave boson (RISB) formalism. This formalism can be applied to the general multi-orbital periodic Anderson model and enables us to calculate the quasiparticle renormalization factor and the energy level. This formalism is an extension of Kotliar-Ruckenstein slave boson (KRSB) formalism. Hence, we first review the KRSB formalism based on the single-orbital periodic Anderson model in section 3.1. In section 3.2, we point out the reason why the KRSB formalism cannot be applied to the general multi-orbital systems. After the discussion, the RISB is reviewed in section 3.3. In section 3.4, we derive the saddle point approximation of the RISB.

3.1 Single-Orbital System in Kotliar-Ruckenstein Slave Boson Formalism

In this section, we review the KRSB formalism applied to the single-orbital periodic Anderson model of eq. (1.1). Because of the duality of itinerant and localized character of the f-electrons, Hamiltonian in eq. (1.1) cannot be solved exactly. Hence, it is inevitable to perform proper approximation in order to extract the physical quantities in which we are interested. In this sense, KRSB formalism is one of the simplest methods to evaluate the QP properties of the system.

In the slave boson formalism, all the localized terms in eq. (1.1) are transformed into quadratic forms by converting the original f-electron operator into a combination of slave boson and pseudo fermion operators. This conversion enables us to treat two-body interactions as one-body terms. In exchange, the hybridization or the hopping terms are transformed into complicated forms that consist of coupling of several slave bosons and pseudo fermions. Because the slave boson operators produce many unphysical states, the slave boson Hamiltonian is defined in an enlarged Hilbert space compared with that used in eq. (1.1) and thus some constraint conditions are required to exclude these unphysical states.

Let us discuss how to convert the original Hamiltonian eq. (1.1) into a slave boson Hamiltonian. In the single orbital system, there are 4 localized states: empty state $|0\rangle$, single occupied state with up spin$|\uparrow\rangle$ and with down spin $|\downarrow\rangle$, and double occupied state $|\uparrow\downarrow\rangle$. In the KRSB

formalism, these states are transformed as,

$$\begin{aligned}
|0\rangle \to |\underline{0}\rangle &= \phi_0^\dagger |\mathrm{vac}\rangle_b \otimes |\mathrm{vac}\rangle_f, \\
|\uparrow\rangle \to |\underline{\uparrow}\rangle &= \phi_\uparrow^\dagger |\mathrm{vac}\rangle_b \otimes f_\uparrow^\dagger |\mathrm{vac}\rangle_f, \\
|\downarrow\rangle \to |\underline{\downarrow}\rangle &= \phi_\downarrow^\dagger |\mathrm{vac}\rangle_b \otimes f_\downarrow^\dagger |\mathrm{vac}\rangle_f, \\
|\uparrow\downarrow\rangle \to |\underline{\uparrow\downarrow}\rangle &= \phi_{\uparrow\downarrow}^\dagger |\mathrm{vac}\rangle_b \otimes f_\uparrow^\dagger f_\downarrow^\dagger |\mathrm{vac}\rangle_f,
\end{aligned} \tag{3.1}$$

where the site index i is omitted for simplicity. $f_\sigma^\dagger$ describes a creation operator for the pseudo fermion with the spin σ and $\phi_n^\dagger$ is a boson creation operator corresponding to the original f-electron localized state $n \in \mathfrak{G} = \{0, \uparrow, \downarrow, \uparrow\downarrow\}$. In this slave boson formalism, the original Hilbert space $|n\rangle$ is extended to $|\underline{n}\rangle = |n\rangle_b \otimes |n\rangle_f$ where $|n\rangle_b$ is Hilbert space for the slave bosons and $|n\rangle_f$ is Fock space for the pseudo fermions. Note that this extended Hilbert space contains not only the physical states but also other unphysical states such as $\phi_0^\dagger \phi_0^\dagger |\mathrm{vac}\rangle_b \otimes f_\uparrow^\dagger |\mathrm{vac}\rangle_f$. Hence, it is necessary to impose the following constraint conditions in order to exclude all the unphysical states at each site i:

$$1 = \sum_{n\in\mathfrak{G}} \phi_{in}^\dagger \phi_{in} = \phi_{i0}^\dagger \phi_{i0} + \phi_{i\uparrow}^\dagger \phi_{i\uparrow} + \phi_{i\downarrow}^\dagger \phi_{i\downarrow} + \phi_{i\uparrow\downarrow}^\dagger \phi_{i\uparrow\downarrow}, \tag{3.2}$$

$$f_{i\sigma}^\dagger f_{i\sigma} = \sum_{n\in\mathfrak{G}} \langle n | f_\sigma^{\mathrm{phys}\dagger} f_\sigma^{\mathrm{phys}} | n \rangle \phi_{in}^\dagger \phi_{in} = \phi_{i\sigma}^\dagger \phi_{i\sigma} + \phi_{i\uparrow\downarrow}^\dagger \phi_{i\uparrow\downarrow}. \tag{3.3}$$

The first constraint condition imposes that each site i should be occupied by one of the bosons. The second constraint condition comes from the equality of the number of electrons. There are two ways of counting the number of electrons of spin σ ($f_{i\sigma}^{\mathrm{phys}\dagger} f_{i\sigma}^{\mathrm{phys}}$ in the original Hamiltonian): one is to count the pseudo fermions $f_{i\sigma}^\dagger f_{i\sigma}$ and the other is to count the slave bosons $\phi_{i\sigma}^\dagger \phi_{i\sigma} + \phi_{i\uparrow\downarrow}^\dagger \phi_{i\uparrow\downarrow}$. The second constraint condition requires that these two ways of counting must be the same. It is easy to prove that all the unphysical states are excluded by these two constraints.

Next we rewrite the original Hamiltonian eq. (1.1) by using the four slave bosons and two pseudo fermions. Let us call the localized part of original Hamiltonian as $\mathcal{H}_{\mathrm{loc}}$, where it is given by,

$$\mathcal{H}_{\mathrm{loc}} = \sum_{i\sigma} (E_f - \mu)\, f_{i\sigma}^{\mathrm{phys}\dagger} f_{i\sigma}^{\mathrm{phys}} + \sum_i U f_{i\uparrow}^{\mathrm{phys}\dagger} f_{i\downarrow}^{\mathrm{phys}\dagger} f_{i\downarrow}^{\mathrm{phys}} f_{i\uparrow}^{\mathrm{phys}}. \tag{3.4}$$

In KRSB, $\mathcal{H}_{\mathrm{loc}}$ is transformed in terms of slave bosons as follows:

$$\mathcal{H}_{\mathrm{loc}}^{\mathrm{SB}} = \sum_{i\sigma} (E_f - \mu)\, \phi_{i\sigma}^\dagger \phi_{i\sigma} + \sum_i (2E_f - 2\mu + U)\, \phi_{i\uparrow\downarrow}^\dagger \phi_{i\uparrow\downarrow}. \tag{3.5}$$

It is easy to check that eq. (3.5) satisfies the relation $\langle n|\mathcal{H}_{\mathrm{loc}}|m\rangle = \langle \underline{n}|\mathcal{H}_{\mathrm{loc}}^{\mathrm{SB}}|\underline{m}\rangle$ when $n, m \in \mathfrak{G}$.

On the other hand, for the transformation of the hybridization terms (the third term of eq. (1.1)), we need to define the "creation" operators $\underline{f}_\sigma^{\mathrm{phys}\dagger}$ (omitting the site index i for simplicity) that acts similarly to the original creation operator $f_\sigma^{\mathrm{phys}\dagger}$ on the enlarged Hilbert space as follows:

$$\underline{f}_\sigma^{\mathrm{phys}\dagger} |\underline{n}\rangle = \sum_{m\in\mathfrak{G}} \langle m | f_\sigma^{\mathrm{phys}\dagger} | n \rangle |\underline{m}\rangle. \tag{3.6}$$

Here, it is to be noted that the choice of $\underline{f}_{\sigma}^{\mathrm{phys}\dagger}$ is not unique. The simplest definition is given by,

$$\underline{f}_{\sigma}^{\mathrm{phys}\dagger} = \left(\phi_{\sigma}^{\dagger}\phi_0 + \phi_{\uparrow\downarrow}^{\dagger}\phi_{\overline{\sigma}}\right) f_{\sigma}^{\dagger}. \tag{3.7}$$

The choice of $\underline{f}_{\sigma}^{\mathrm{phys}\dagger}$ unaffects the results if we solve the slave boson Hamiltonian exactly under the constraint conditions. However, the equivalence among different choices breaks down when some approximations are performed such as saddle point approximation. In the saddle point approximation, all the boson operators are treated as mean-fields. For example, in the case of $U = 0$ at half filling of f-electrons, one can see that all the boson operators becomes $1/2$ due to the constraint conditions in eqs. (3.2) and (3.3) [64]. Then, eq. (3.7) becomes $\underline{f}_{\sigma}^{\mathrm{phys}\dagger} = 1/2 f_{\sigma}^{\dagger}$ which gives apparently inconsistent results for $U = 0$ case.

In order to reproduce the exact results at least for the $U = 0$ case, Kotliar and Ruckenstein proposed the following form of the operator:

$$\begin{aligned}\underline{f}_{\sigma}^{\mathrm{phys}\dagger} &= \Delta_{\sigma}^{-1/2}\left(\phi_{\sigma}^{\dagger}\phi_0 + \phi_{\uparrow\downarrow}^{\dagger}\phi_{\overline{\sigma}}\right)(1-\Delta_{\sigma})^{-1/2} f_{\sigma}^{\dagger} \\ &= z_{\sigma}^{\dagger} f_{\sigma}^{\dagger},\end{aligned} \tag{3.8}$$

where $\Delta_{\sigma} = \phi_{\sigma}^{\dagger}\phi_{\sigma} + \phi_{\uparrow\downarrow}^{\dagger}\phi_{\uparrow\downarrow}$ represents the number of electrons of spin σ. Kotliar and Ruckenstein demonstrated that the saddle point approximation with eq. (3.8) gives exact results for any filling of the f-electrons in the case of $U = 0$ [64]. For example, at half-filling, Δ_{σ} becomes $1/2$ for each spin and eq. (3.8) becomes a reasonable result $\underline{f}_{\sigma}^{\mathrm{phys}\dagger} = f_{\sigma}^{\dagger}$. Using eq. (3.8), the hybridization term $\mathcal{H}_{\mathrm{hyb}}$ is rewritten as,

$$\mathcal{H}_{\mathrm{hyb}} = \sum_{i\sigma} V c_{i\sigma}^{\dagger} f_{i\sigma}^{\mathrm{phys}} + \mathrm{h.c.} \to \sum_{i\sigma} z_{i\sigma} V c_{i\sigma}^{\dagger} f_{i\sigma} + \mathrm{h.c.}. \tag{3.9}$$

Therefore, the total Hamiltonian of eq. (1.1) becomes:

$$\begin{aligned}\mathcal{H} = &\sum_{\boldsymbol{k}\sigma} \xi_{\boldsymbol{k}} c_{\boldsymbol{k}\sigma}^{\dagger} c_{\boldsymbol{k}\sigma} + \sum_{i\sigma} (E_f - \mu)\, \phi_{i\sigma}^{\dagger}\phi_{i\sigma} + \sum_{i} (2E_f - 2\mu + U)\, \phi_{i\uparrow\downarrow}^{\dagger}\phi_{i\uparrow\downarrow} \\ &+ \sum_{i\sigma} z_{i\sigma} V c_{i\sigma}^{\dagger} f_{i\sigma} + \mathrm{h.c.}.\end{aligned} \tag{3.10}$$

In the KRSB formalism, one needs to solve this Hamiltonian (3.10) under the constraint conditions in eqs. (3.2) and (3.3). Frésard and Kopp solved the two site model of this Hamiltonian exactly under the constraint conditions in the case of $U = \infty$ and obtained the same results with that of the original Hamiltonian [75]. In the saddle point approximation, Kotliar and Ruckenstein showed that this formalism reproduces consistent results with the results obtained in the Gutzwiller approximation [76].

However, Li, Wöfle, and Hirschfeld pointed out that the KRSB formalism contains a severe problem when a transverse magnetic field is considered [61]. The effects of the magnetic fields along the z-axis and the x-axis are written in terms of slave operators as,

$$\mathcal{H}_z^{\mathrm{mag}} = -h\phi_{\uparrow}^{\dagger}\phi_{\uparrow} + h\phi_{\downarrow}^{\dagger}\phi_{\downarrow}, \tag{3.11}$$

$$\mathcal{H}_x^{\mathrm{mag}} = -h\phi_{\uparrow}^{\dagger}\phi_{\downarrow} f_{\uparrow}^{\dagger} f_{\downarrow} - h\phi_{\downarrow}^{\dagger}\phi_{\uparrow} f_{\downarrow}^{\dagger} f_{\uparrow}, \tag{3.12}$$

where h represents the magnetic field. It is easy to check that eqs. (3.11) and (3.12) give the same matrix elements with the original Hamiltonian. However, while $\mathcal{H}_z^{\rm mag}$ is written in a quadratic form of the slave bosons, $\mathcal{H}_x^{\rm mag}$ is expressed as a fermion-boson coupling term. This non-equivalent treatment between the transverse and the longitudinal magnetic fields breaks the spin-rotational symmetry under some approximations. In fact, Li, Wöfle, and Hirschfeld studied the saddle point approximation and Gaussian fluctuations of the KRSB formalism and pointed out that this formalism cannot discuss the transverse spin ordered state and the transverse magnetic fluctuations.

In order to recover the spin-rotational symmetry, Li, Wöfle, and Hirschfeld proposed a new slave boson formalism called the spin-rotationally invariant slave boson (SRISB) formalism. While KRSB formalism uses the four boson operators, the SRISB formalism introduces additional slave boson operators which come from the "off-diagonal" part of the single occupied state:

$$\begin{pmatrix} \phi_0 & - & - & - \\ - & \phi_\uparrow & - & - \\ - & - & \phi_\downarrow & - \\ - & - & - & \phi_{\uparrow\downarrow} \end{pmatrix} \to \begin{pmatrix} \phi_{(0,0)} & - & - & - \\ - & \phi_{(\uparrow,\uparrow)} & \phi_{(\uparrow,\downarrow)} & - \\ - & \phi_{(\downarrow,\uparrow)} & \phi_{(\downarrow,\downarrow)} & - \\ - & - & - & \phi_{(\uparrow\downarrow,\uparrow\downarrow)} \end{pmatrix}. \tag{3.13}$$

Then, instead of eq. (3.1), SRISB uses,

$$\begin{aligned} |0\rangle \to |\underline{0}\rangle &= \phi^\dagger_{(0,0)}|{\rm vac}\rangle_b \otimes |{\rm vac}\rangle_f, \\ |\sigma\rangle \to |\underline{\sigma}\rangle &= \frac{1}{\sqrt{2}}\sum_{\sigma'} \phi^\dagger_{(\sigma,\sigma')}|{\rm vac}\rangle_b \otimes f^\dagger_{\sigma'}|{\rm vac}\rangle_f, \\ |\uparrow\downarrow\rangle \to |\underline{\uparrow\downarrow}\rangle &= \phi^\dagger_{(\uparrow\downarrow,\uparrow\downarrow)}|{\rm vac}\rangle_b \otimes f^\dagger_\uparrow f^\dagger_\downarrow|{\rm vac}\rangle_f. \end{aligned} \tag{3.14}$$

By using these slave boson operators, both the longitudinal and the transverse magnetic field are rewritten as,

$$\mathcal{H}_z^{\rm SRISB} = -h\phi^\dagger_{(\uparrow,\uparrow)}\phi_{(\uparrow,\uparrow)} - h\phi^\dagger_{(\uparrow,\downarrow)}\phi_{(\uparrow,\downarrow)} + h\phi^\dagger_{(\downarrow,\uparrow)}\phi_{(\downarrow,\uparrow)} + h\phi^\dagger_{(\downarrow,\downarrow)}\phi_{(\downarrow,\downarrow)}, \tag{3.15}$$

$$\mathcal{H}_x^{\rm SRISB} = -h\phi^\dagger_{(\uparrow,\uparrow)}\phi_{(\downarrow,\uparrow)} - h\phi^\dagger_{(\uparrow,\downarrow)}\phi_{(\downarrow,\downarrow)} - h\phi^\dagger_{(\downarrow,\uparrow)}\phi_{(\uparrow,\uparrow)} - h\phi^\dagger_{(\downarrow,\downarrow)}\phi_{(\uparrow,\downarrow)}. \tag{3.16}$$

In this case, the spin-rotational symmetry obviously recovers, and it is easy to check the validity of eqs. (3.15) and (3.16) by acting on the states in eq. (3.14). Since there are the additional boson operators, the constraint conditions in eqs. (3.2) and (3.3) are modified as,

$$\begin{aligned} 1 =& \phi^\dagger_{i(0,0)}\phi_{i(0,0)} + \phi^\dagger_{i(\uparrow,\uparrow)}\phi_{i(\uparrow,\uparrow)} + \phi^\dagger_{i(\downarrow,\downarrow)}\phi_{i(\downarrow,\downarrow)} \\ &+ \phi^\dagger_{i(\uparrow,\downarrow)}\phi_{i(\uparrow,\downarrow)} + \phi^\dagger_{i(\downarrow,\uparrow)}\phi_{i(\downarrow,\uparrow)} + \phi^\dagger_{i(\uparrow\downarrow,\uparrow\downarrow)}\phi_{i(\uparrow\downarrow,\uparrow\downarrow)}, \end{aligned} \tag{3.17}$$

$$f^\dagger_{i\sigma}f_{i\sigma} = \phi^\dagger_{i(\sigma,\sigma)}\phi_{i(\sigma,\sigma)} + \phi^\dagger_{i(\overline{\sigma},\sigma)}\phi_{i(\overline{\sigma},\sigma)} + \phi^\dagger_{i(\uparrow\downarrow,\uparrow\downarrow)}\phi_{i(\uparrow\downarrow,\uparrow\downarrow)}, \tag{3.18}$$

$$f^\dagger_{i\sigma}f_{i\overline{\sigma}} = \phi^\dagger_{i(\uparrow,\overline{\sigma})}\phi_{i(\uparrow,\sigma)} + \phi^\dagger_{i(\downarrow,\overline{\sigma})}\phi_{i(\downarrow,\sigma)}, \tag{3.19}$$

where $\overline{\sigma}$ indicates the opposite sign of spin σ. Furthermore, the simplest definition of "creation" operator eq. (3.7) is also modified as,

$$\underline{f}^{\rm phys\dagger}_\sigma = \frac{1}{\sqrt{2}}f^\dagger_\sigma\left(\phi^\dagger_{(\sigma,\sigma)}\phi_{(0,0)} + \phi^\dagger_{(\uparrow\downarrow,\uparrow\downarrow)}\phi_{(\overline{\sigma},\overline{\sigma})}\right) + \frac{1}{\sqrt{2}}f^\dagger_{\overline{\sigma}}\left(\phi^\dagger_{(\sigma,\overline{\sigma})}\phi_{(0,0)} - \phi^\dagger_{(\uparrow\downarrow,\uparrow\downarrow)}\phi_{(\overline{\sigma},\sigma)}\right). \tag{3.20}$$

The SRISB formalism enables us to discuss the transverse spin fluctuations and the transverse spin ordered state. We mention that the additional slave boson operators $\phi^\dagger_{(\sigma,\overline{\sigma})}$ do nothing in the case of saddle point approximation when we consider the longitudinal spin ordered state or the states without order parameters. Therefore, as far as in the saddle point approximation, both the KRSB formalism and the SRISB formalism give the same results.

3.2 Kotliar-Ruckenstein slave boson in multi-orbital systems

In this section, we discuss that the KRSB formalism *cannot* be applied to general multi-orbital systems in contrast to the single-orbital system. Let us consider the $N_{\rm orb}$-orbital system where $N_{\rm orb}$ means the number of localized orbitals. All the $2N_{\rm orb}$ orbitals (including "spin" degeneracy) are denoted as ν that belongs to the orbital space $\mathcal{N}$. More explicitly, in chapter 2, we defined two kinds of orbital space $\mathcal{N}$ in the case of $N_{\rm orb} = 3$: one is for the cubic symmetry $\mathcal{N} = \{\Gamma_{+7}, \Gamma_{-7}, \Gamma_{+81}, \Gamma_{-81}, \Gamma_{+82}, \Gamma_{-82}\}$ (see eq. (2.17)) and the other is for the hexagonal symmetry $\mathcal{N} = \{\Gamma_{+7}, \Gamma_{-7}, \Gamma_{+8}, \Gamma_{-8}, \Gamma_{+9}, \Gamma_{-9}\}$ (see eq. (2.28)). Although the following discussions are developed to the general $N_{\rm orb}$-orbital systems, we calculate the two kinds of three-orbital models in this thesis.

In the $N_{\rm orb}$-orbital system, there are $2^{2N_{\rm orb}}$ localized states from the empty state to the fully-occupied state. Hereafter, we will use two kinds of basis set to describe these localized states: one is the set of eigenstates of the localized Hamiltonian $\mathfrak{G}$ and the other is the Fock space $\mathfrak{F}$. In the case of cubic symmetry, one of the Fock states $|n\rangle$ ($n \in \mathfrak{F}$) is written as

$$|n\rangle = |\left(m_{\Gamma_{+7}}, m_{\Gamma_{-7}}\right)_{\Gamma_7} \left(m_{\Gamma_{+81}}, m_{\Gamma_{-81}}\right)_{\Gamma_{81}} \left(m_{\Gamma_{+82}}, m_{\Gamma_{-82}}\right)_{\Gamma_{82}}\rangle = \prod_{\nu\in\mathcal{N}} \left(f^{\rm phys\dagger}_\nu\right)^{m_\nu} |{\rm vac}\rangle, \quad (3.21)$$

where m_ν takes the values 0 or 1. Likewise, in the case of hexagonal symmetry $|n\rangle$ is written as

$$|n\rangle = |\left(m_{\Gamma_{+7}}, m_{\Gamma_{-7}}\right)_{\Gamma_7} \left(m_{\Gamma_{+8}}, m_{\Gamma_{-8}}\right)_{\Gamma_8} \left(m_{\Gamma_{+9}}, m_{\Gamma_{-9}}\right)_{\Gamma_9}\rangle = \prod_{\nu\in\mathcal{N}} \left(f^{\rm phys\dagger}_\nu\right)^{m_\nu} |{\rm vac}\rangle. \quad (3.22)$$

On the other hand, one of the eigenstates $|\Gamma\rangle$ ($\Gamma \in \mathfrak{G}$) satisfies $\mathcal{H}_{\rm loc}|\Gamma\rangle = E_\Gamma|\Gamma\rangle$, where $\mathcal{H}_{\rm loc}$ is derived in eq. (2.4). Although in the single-orbital system, all the eigenstates correspond to the Fock states $\mathfrak{F} = \mathfrak{G}$, this correspondence breaks in the case of general multi-orbital systems. Namely, $|\Gamma\rangle$ is written as the linear combination of Fock states as $|\Gamma\rangle = \sum_{n\in\mathfrak{F}} \langle n|\Gamma\rangle |n\rangle$ where the coefficients $\langle n|\Gamma\rangle$ can be obtained by diagonalizing $\mathcal{H}_{\rm loc}$ in eq. (2.4). For example, Γ_4 singlet state with f^2-configuration in the case of hexagonal symmetry can be written as

$$|\Gamma_4\rangle = \frac{1}{\sqrt{2}} \left(|\left(1,0\right)_{\Gamma_7} \left(1,0\right)_{\Gamma_8} \left(0,0\right)_{\Gamma_9}\rangle - |\left(0,1\right)_{\Gamma_7} \left(0,1\right)_{\Gamma_8} \left(0,0\right)_{\Gamma_9}\rangle \right). \quad (3.23)$$

In order to obtain the slave boson Hamiltonian by using the Fock states $|n\rangle$, we first consider the following transformation similar to the single-orbital system eq. (3.1):

$$|n\rangle \to |\underline{n}\rangle = \phi^\dagger_n |{\rm vac}\rangle_b \otimes |n\rangle_f, \quad (3.24)$$

where the pseudo fermion state $|n\rangle_f$ is represented as $\prod_{\nu\in\mathcal{N}} \left(f^\dagger_\nu\right)^{m_\nu} |{\rm vac}\rangle_f$. Here, all the states $|\underline{n}\rangle$ represent physical states. This is a natural extension of eq. (3.1). In this transformation,

we introduce $2^{2N_{\rm orb}}$ slave bosons and $2N_{\rm orb}$ pseudo fermions and the constraint conditions are given by,

$$1 = \sum_n \phi_n^\dagger \phi_n, \tag{3.25}$$

$$f_\nu^\dagger f_\nu = \sum_n |\langle n|f_\nu^\dagger f_\nu|n\rangle|^2 \phi_n^\dagger \phi_n. \tag{3.26}$$

However, there is a serious problem that the above definition cannot describe non-density-density-type interactions in eq. (2.19) in a quadratic form of boson operators. Here, the non-density-density-type interactions are the off-diagonal matrix elements with $\nu_1 \neq \nu_4$ or $\nu_2 \neq \nu_3$, while the density-density-type interactions are the diagonal matrix elements with $\nu_1 = \nu_4$ and $\nu_2 = \nu_3$. For example, in the case of hexagonal symmetry, one of the density-density-type interactions is the intra-orbital interaction of Γ_7 state $I^{\Gamma_{-7}\Gamma_{+7}}_{\Gamma_{+7}\Gamma_{-7}} f^{\rm phys\dagger}_{\Gamma_{+7}} f^{\rm phys\dagger}_{\Gamma_{-7}} f^{\rm phys}_{\Gamma_{-7}} f^{\rm phys}_{\Gamma_{+7}}$, while one of the non density-density type interactions is the Kramers spin flipping interaction among Γ_7 and Γ_8 state $I^{\Gamma_{-8}\Gamma_{+7}}_{\Gamma_{-7}\Gamma_{+8}} f^{\rm phys\dagger}_{\Gamma_{+7}} f^{\rm phys\dagger}_{\Gamma_{-8}} f^{\rm phys}_{\Gamma_{+8}} f^{\rm phys}_{\Gamma_{-7}}$. These interactions are transformed as,

$$I^{\Gamma_{-7}\Gamma_{+7}}_{\Gamma_{+7}\Gamma_{-7}} f^{\rm phys\dagger}_{\Gamma_{+7}} f^{\rm phys\dagger}_{\Gamma_{-7}} f^{\rm phys}_{\Gamma_{-7}} f^{\rm phys}_{\Gamma_{+7}} \to I^{\Gamma_{-7}\Gamma_{+7}}_{\Gamma_{+7}\Gamma_{-7}} \phi^\dagger_{\Gamma_{+7}\Gamma_{-7}} \phi_{\Gamma_{+7}\Gamma_{-7}}, \tag{3.27}$$

$$I^{\Gamma_{-8}\Gamma_{+7}}_{\Gamma_{-7}\Gamma_{+8}} f^{\rm phys\dagger}_{\Gamma_{+7}} f^{\rm phys\dagger}_{\Gamma_{-8}} f^{\rm phys}_{\Gamma_{+8}} f^{\rm phys}_{\Gamma_{-7}} \to I^{\Gamma_{-8}\Gamma_{+7}}_{\Gamma_{-7}\Gamma_{+8}} \phi^\dagger_{\Gamma_{+7}\Gamma_{-8}} \phi_{\Gamma_{-7}\Gamma_{+8}} f^\dagger_{\Gamma_{+7}} f^\dagger_{\Gamma_{-8}} f_{\Gamma_{+8}} f_{\Gamma_{-7}}. \tag{3.28}$$

As we discussed in the previous section, eq. (3.28) is undesirable from the concept of the slave boson formalism. In other words, we cannot apply the KRSB formalism in the multi-orbital systems which contain non-density-density-type interactions.

In order to obtain the localized slave-boson Hamiltonian in the quadratic form, we use the other boson operator representations in terms of eigenstates Γ which belong to $\mathfrak{G}$:

$$|\Gamma\rangle \to |\underline{\Gamma}\rangle = \sum_{n\in\mathfrak{F}} \langle n|\Gamma\rangle \phi^\dagger_\Gamma |{\rm vac}\rangle_b \otimes |n\rangle_f, \tag{3.29}$$

where the summation takes over the Fock states. (Ikeda and Kusunose used this basis to discuss the Γ_4 ground-state of the f^2-configuration system [40, 41].) Here, all the states $|\underline{\Gamma}\rangle$ represent physical states. By using this basis, the localized Hamiltonian is converted to the quadratic form $\mathcal{H}_{\rm loc} \to \underline{\mathcal{H}}_{\rm loc} = \sum_\Gamma E_\Gamma \phi^\dagger_\Gamma \phi_\Gamma$, where E_Γ is the eigenvalue of the eigenstate $|\Gamma\rangle$. However, this basis raises a new problem that this basis cannot construct proper constraint conditions. The second constraint conditions in eq. (3.3) may be written as,

$$f^\dagger_{i\nu} f_{i\nu} = \sum_{\Gamma\in\mathfrak{G}} |\langle\Gamma|f^{\rm phys\dagger}_\nu f^{\rm phys}_\nu|\Gamma\rangle|^2 \phi^\dagger_{i\Gamma}\phi_{i\Gamma}. \tag{3.30}$$

At first glance, this constraint condition seems to work. However, this equation breaks the operator identity. The operator on the left hand side (lhs) is 0 or 1 when it acts on an arbitrary state. On the other hand, the operator on the right hand side (rhs) becomes some non-integer number due to the coefficient $\langle\Gamma|f^{\rm phys\dagger}_\nu f^{\rm phys}_\nu|\Gamma\rangle$. Obviously, the constraint condition in eq. (3.30) cannot exclude the unphysical states in the enlarged Hilbert space.

Here, it should be noted that the constraint condition seems to work in the saddle point approximation: all the constraint conditions are imposed not on each site i but on the averaged expectation values of slave boson operators. In this case, eq (3.30) seems to work because both

side of eq. (3.30) are some non-integer numbers. However, because the constraint condition is not correct in the exact slave boson Hamiltonian, it has been shown that the saddle point approximation of this Hamiltonian gives unphysical results [40, 41].

So far, We have pointed out why the KRSB formalism cannot be applied to the general multi-orbital systems. The problem of the KRSB formalism is that both the constraint conditions and the quadratic form representations of the localized Hamiltonian cannot be obtained at the same time. When we use the Fock state basis, the constraint conditions are all right but the quadratic form is broken, and when we use the eigenstate basis, the quadratic form is realized but the constraint conditions become non-integer equalities. However, if the unitary transformation for the boson operator

$$\phi_n^\dagger = \sum_{\Gamma\in\mathfrak{G}} \langle\Gamma|n\rangle \phi_\Gamma^\dagger, \tag{3.31}$$

holds, the properties of the Hamiltonian do not depend on its basis, i.e., the quadratic forms for ϕ_Γ are the quadratic forms for ϕ_n after the unitary transformation.

Actually, in the following discussion, we can show that if the unitary transformation (3.31) holds in the KRSB formalism, a contradiction appears. In the original states, the following unitary transformation is obviously satisfied:

$$|n\rangle = \sum_{\Gamma\in\mathfrak{G}} \langle\Gamma|n\rangle |\Gamma\rangle. \tag{3.32}$$

In the KRSB transformation, the right hand side (rhs) of eq. (3.32) becomes,

$$\sum_{\Gamma\in\mathfrak{G}} \langle\Gamma|n\rangle |\Gamma\rangle \to \sum_{\Gamma\in\mathfrak{G}} \langle\Gamma|n\rangle |\underline{\Gamma}\rangle = \sum_{\Gamma\in\mathfrak{G},m\in\mathfrak{F}} \langle\Gamma|n\rangle\langle m|\Gamma\rangle \phi_\Gamma^\dagger |\mathrm{vac}\rangle_b \otimes |m\rangle_f, \tag{3.33}$$

using eq. (3.29). On the other hand, the left hand side (lhs) of eq. (3.32) becomes,

$$|n\rangle \to |\underline{n}\rangle = \sum_{\Gamma\in\mathfrak{G}} \langle\underline{\Gamma}|\underline{n}\rangle |\underline{\Gamma}\rangle = \sum_{\Gamma\in\mathfrak{G}} \sum_{n\in\mathfrak{F}} \left(\langle\Gamma|n\rangle\right)^2 \langle m|\Gamma\rangle \phi_\Gamma^\dagger |\mathrm{vac}\rangle_b \otimes |m\rangle_f, \tag{3.34}$$

where we use eqs. (3.24) and (3.29) and assume that the relation (3.31) holds to derive $\langle\underline{\Gamma}|\underline{n}\rangle = \left(\langle\Gamma|n\rangle\right)^2$. The two eqs. (3.33) and (3.34) means

$$|\underline{n}\rangle \neq \sum_{\Gamma\in\mathfrak{G}} \langle\Gamma|n\rangle |\underline{\Gamma}\rangle. \tag{3.35}$$

However, it is required that $|\underline{n}\rangle = \sum_{\Gamma\in\mathfrak{G}} \langle\Gamma|n\rangle |\underline{\Gamma}\rangle$ should hold according to the unitary transformation on the original state in eq. (3.32), because both $|\underline{n}\rangle$ and $|\underline{\Gamma}\rangle$ are physical states as mentioned before. Hence, we conclude that the unitary transformation for the boson operators (3.31) does not hold in the KRSB formalism.

From the above arguments, we can see that the key for constructing a proper slave boson formalism for the general multi-orbital system is to recover the unitary transformation for the boson operators.

3.3 Rotationally invariant slave boson formalism

In this section, we review the rotationally invariant slave boson (RISB) formalism, which can be applied to the general multi-orbital systems [56]. We will use this formalism throughout in this thesis. We first mention that this formalism is an equivalent transformation between the original Hamiltonian and the slave boson Hamiltonian under several constraint conditions. Although the contribution from superconductivity can be discussed in the RISB formalism [77], we do not consider superconductivity in this thesis.

The concept of the RISB formalism is similar to the SRISB formalism discussed in sec. 3.1; i.e., this formalism takes into account "off-diagonal" slave boson operators ϕ_{AB}, where A and B represent localized states in the original Hilbert space. We introduce slave boson operators when the electron number of $|A\rangle$ state is same as that of $|B\rangle$ state. Namely, we consider,

$$\phi_{AB} = \begin{cases} \phi_{AB} & (N_A = N_B) \\ 0 & (\text{otherwise}) \end{cases} \tag{3.36}$$

where N_A indicates the electron number of the state $|A\rangle$. The first and the second subscripts of ϕ_{AB} are named as physical state and QP state, respectively. We will show later that the RISB formalism does not depend on basis sets in contrast to the KRSB formalism. In this section, we mainly use two kinds of slave boson operators with different basis sets: one is ϕ_{nm} where $n, m \in \mathfrak{F}$, and the other is $\phi_{\Gamma m}$ where $\Gamma \in \mathfrak{G}$ and $m \in \mathfrak{F}$. The RISB formalism introduces these slave boson operators and pseudo fermion operators f_ν for each orbital $\nu \in \mathcal{N}$. In the case of $N_{\rm orb}$-orbital system, the number of the boson and the fermion operators in the RISB formalism are $\sum_{i=0}^{2N_{\rm orb}} \left({}_{2N_{\rm orb}}\mathrm{C}_i\right)^2$ and $2N_{\rm orb}$, respectively.

As we pointed out in the previous section, the key for constructing a proper slave boson formalism for the general multi-orbital system is to recover the unitary transformation of the boson operators. When this unitary transformation holds in the RISB formalism, it is obvious that this formalism does not depend on the basis sets and can satisfy the two conditions in the previous section simultaneously: one is to construct proper constraint conditions and the other is to express the localized Hamiltonian in terms of a quadratic form of boson operators.

Let us assume that one of the original eigenstates $|\Gamma\rangle$ and one of the original Fock states $|n\rangle$ are transformed by means of the RISB formalism as follows:

$$|\Gamma\rangle \to |\underline{\Gamma}\rangle = \frac{1}{\sqrt{D_\Gamma}} \sum_{m\in\mathfrak{F}} \phi^\dagger_{\Gamma m}|\mathrm{vac}\rangle_b \otimes |m\rangle_f, \tag{3.37}$$

$$|n\rangle \to |\underline{n}\rangle = \frac{1}{\sqrt{D_n}} \sum_{m\in\mathfrak{F}} \phi^\dagger_{nm}|\mathrm{vac}\rangle_b \otimes |m\rangle_f, \tag{3.38}$$

where $|n\rangle_f$ is represented by the pseudo fermions as $\prod_\nu f_\nu^{\dagger m_\nu}|\mathrm{vac}\rangle_f$ and D_n (D_Γ) is the normalization factor: $D_n = {}_{2N_{\rm orb}}\mathrm{C}_{N_n}$ ($D_\Gamma = {}_{2N_{\rm orb}}\mathrm{C}_{N_\Gamma}$). Here, all the states of $|\underline{n}\rangle$ (or $|\underline{\Gamma}\rangle$) represent the original states written by the slave boson and the pseudo fermion operators. We call these states $|\underline{n}\rangle$ (or $|\underline{\Gamma}\rangle$) as physically meaningful states and the other states in the enlarged Hilbert space as unphysical states. The validity of the representations (3.37) and (3.38) will be shown later.

First, we show that the unitary transformation for the physical states of the slave boson

operators,

$$\phi^\dagger_{nm} = \sum_{\Gamma\in\mathfrak{G}} \langle\Gamma|n\rangle \phi^\dagger_{\Gamma m}, \tag{3.39}$$

holds in the RISB formalism in contrast to the KRSB formalism discussed in eqs. (3.33) and (3.34). Since all the physically meaningful states should behave as same as the original states, the unitary transformation of the physically meaningful states has the following relation:

$$|\underline{n}\rangle = \sum_{\Gamma\in\mathfrak{G}} \langle\Gamma|n\rangle |\underline{\Gamma}\rangle. \tag{3.40}$$

Using eq. (3.37), the rhs of eq. (3.40) becomes,

$$\begin{aligned}\sum_{\Gamma\in\mathfrak{G}} \langle\Gamma|n\rangle|\underline{\Gamma}\rangle &= \sum_{\Gamma\in\mathfrak{G}} \langle\Gamma|n\rangle \frac{1}{\sqrt{D_\Gamma}} \sum_{m\in\mathfrak{F}} \phi^\dagger_{\Gamma m}|\mathrm{vac}\rangle_b \otimes |m\rangle_f \\ &= \frac{1}{\sqrt{D_\Gamma}} \sum_{m\in\mathfrak{F}} \sum_{\Gamma\in\mathfrak{G}} \langle\Gamma|n\rangle \phi^\dagger_{\Gamma m}|\mathrm{vac}\rangle_b \otimes |m\rangle_f, \end{aligned} \tag{3.41}$$

where $D_\Gamma = D_n$ since $\langle\Gamma|n\rangle$ is finite in the case of $N_\Gamma = N_n$. Comparison this equation with eq. (3.38) (the lhs of eq. (3.40)), The relation (3.39) is obtained. Because eq. (3.39) is satisfied in any basis sets, the RISB formalism does not depend on the basis sets in contrast to the KRSB formalism. In the following discussion, we use the Fock state basis set for both the physical and the QP states ϕ_{nm}, $nm \in \mathfrak{F}$. It is to be noted that the unitary transformation for the QP states is also guaranteed in the case of $\langle\Gamma|n\rangle = \langle n|\Gamma\rangle$ [56].

As a next step, let us discuss the validity of the assumption of eq. (3.38). Namely, we discuss what kind of constraint conditions can uniquely determine the physically meaningful states as eq. (3.38). Since all these states consist of the single boson states, one of the constraint conditions should exclude all the other occupancy states of bosons. Namely, we consider the states which hold the following relation:

$$\mathcal{Q}_0|\underline{A}\rangle' = \left(\sum_{nm\in\mathfrak{F}} \phi^\dagger_{nm}\phi_{nm} - 1\right)|\underline{A}\rangle' = 0, \tag{3.42}$$

where the prime on the states $|\underline{A}\rangle$ indicates that some unphysical states are still included. $|\underline{A}\rangle'$ is written as,

$$\phi^\dagger_{np}|\mathrm{vac}\rangle_b \otimes |q\rangle_f, \tag{3.43}$$

or a linear combination of eq. (3.43).

Let us assume that the linear combination with n represents the original state $|n\rangle$:

$$|n\rangle \to |\underline{n}\rangle' = \sum_{pq\in\mathfrak{F}} W_{pq}\phi^\dagger_{np}|\mathrm{vac}\rangle_b \otimes |q\rangle_f. \tag{3.44}$$

It is to be noted that $|\underline{n}\rangle'$ is not uniquely determined yet due to the arbitrary coefficient W_{pq}; additional constraint conditions are needed to construct the one-to-one correspondence between

$|n\rangle$ and $|\underline{n}\rangle$ as eq. (3.38). Although the proof is a little difficult (see appendix A), the additional constraint conditions are written as,

$$\mathcal{Q}_{\nu\nu'}|\underline{n}\rangle = \left(f_\nu^\dagger f_{\nu'} - \sum_{nml\in\mathfrak{F}} \phi_{nm}^\dagger \phi_{nl} \langle l| f_\nu^\dagger f_{\nu'} |m\rangle_f \right) |\underline{n}\rangle = 0, \tag{3.45}$$

where $|\underline{n}\rangle$ corresponds to eq. (3.38). All the other states included in $|\underline{n}\rangle'$ gives finite value when $\mathcal{Q}_{\nu\nu'}$ is operated. Hence, these states are excluded due to the constraint condition (3.45). From the above consideration, we can conclude that the assumption eq. (3.38) is valid under the constraint conditions eqs. (3.42) and (3.45). It is to be noted that eq. (3.37) is also valid since we have already shown that the RISB formalism guarantees the unitary transformation of boson operators, which is defined in the physically meaningful states.

It is remarkable that all the constraint conditions are written in the quadratic form of the boson or the fermion operators. This makes calculation simple. Moreover, we can easily show that the transformation of the localized Hamiltonian $\underline{\mathcal{H}}_{\rm loc}$ are also written in the simple quadratic form as,

$$\underline{\mathcal{H}}_{\rm loc} = \sum_{nml\in\mathfrak{F}} \langle n|\mathcal{H}_{\rm loc}|m\rangle \phi_{nl}^\dagger \phi_{ml} = \sum_{nml\in\mathfrak{F}} E_{nm} \phi_{nl}^\dagger \phi_{ml}, \tag{3.46}$$

since this Hamiltonian exactly gives the same matrix components of the original Hamiltonian $\langle m|\mathcal{H}_{\rm loc}|n\rangle = \langle \underline{m}|\underline{\mathcal{H}}_{\rm loc}|\underline{n}\rangle$:

$$\begin{aligned}
\langle \underline{m}|\underline{\mathcal{H}}_{\rm loc}|\underline{n}\rangle &= \sum_{n'm'l'} E_{m'n'} \langle \underline{m}|\phi_{m'l'}^\dagger \phi_{n'l'}|\underline{n}\rangle \\
&= \frac{1}{\sqrt{D_n}} \sum_{n'm'l'l} E_{m'n'} \langle \underline{m}|\phi_{m'l'}^\dagger \phi_{n'l'} \phi_{nl}^\dagger |{\rm vac}\rangle_b \otimes |l\rangle_f \\
&= \frac{1}{\sqrt{D_n}} \sum_{m'l} E_{m'n} \langle \underline{m}|\phi_{m'l'}^\dagger |{\rm vac}\rangle_b \otimes |l\rangle_f \\
&= \sum_{m'} E_{m'n} \langle \underline{m}|\underline{m}'\rangle \\
&= E_{mn}.
\end{aligned} \tag{3.47}$$

According to eqs. (3.42), (3.45), and (3.46), we obtain both the proper constraint conditions and the quadratic Hamiltonian by means of the RISB formalism simultaneously. Hence, the serious problems in the KRSB formalism discussed in the previous section are solved in the RISB formalism.

Let us transpose the original Hamiltonian (2.1) by means of the RISB formalism. Since we already derived the localized Hamiltonian (3.46), we focus on the transformation of the hybridization terms (the third term of eq. (2.1)) in the following discussion.

Similarly to the discussion on sec 3.1 (see eqs. (3.7) and (3.8)), we need to define a "creation" operator $\underline{f}_\nu^{\rm phys\dagger}$ that acts as,

$$\underline{f}_\nu^{\rm phys\dagger} |\underline{n}\rangle = \sum_{n'\in\mathfrak{F}} \langle n'| f_\nu^{\rm phys\dagger} |n\rangle |\underline{n}'\rangle. \tag{3.48}$$

It is known that $\underline{f}_\nu^{\rm phys\dagger}$ is not uniquely determined. Hence, we first derive the simplest form of $\underline{f}_\nu^{\rm phys\dagger}$ where we call ${}_{\rm sim}\underline{f}_\nu^{\rm phys\dagger}$. After that, we correct ${}_{\rm sim}\underline{f}_\nu^{\rm phys\dagger}$ to the proper form of $\underline{f}_\nu^{\rm phys\dagger}$ for the saddle point approximation.

The form of ${}_{\rm sim}\underline{f}_\nu^{\rm phys\dagger}$ should be written as,

$$ {}_{\rm sim}\underline{f}_\nu^{\rm phys\dagger} = \sum_{n_1 n_2 m_1 m_2 \in \mathfrak{F}} \langle n_1 | f_\nu^{\rm phys\dagger} | n_2 \rangle \phi^\dagger_{n_1 m_1} \phi_{n_2 m_2} \hat{X}^f_{m_1 m_2}, \tag{3.49} $$

where $\hat{X}^f_{m_1 m_2}$ includes the fermion operators. Because the slave boson operators are introduced as eq. (3.36), the electron number of each Fock state should have the following relations: $N_{n_1} = N_{m_1}$, $N_{n_2} = N_{m_2}$, and $N_{m_1} = N_{m_2} + 1$. The specific form of the fermion operators $\hat{X}^f_{m_1 m_2}$ is a little difficult to derive. Substituting eq. (3.49) into the lhs of eq. (3.48) becomes

$$ \begin{aligned} {}_{\rm sim}\underline{f}_\nu^{\rm phys\dagger} |\underline{n}\rangle &= \sum_{n_1 n_2 m_1 m_2 \in \mathfrak{F}} \langle n_1 | f_\nu^{\rm phys\dagger} | n_2 \rangle \phi^\dagger_{n_1 m_1} \phi_{n_2 m_2} \hat{X}^f_{m_1 m_2} |\underline{n}\rangle \\ &= \sum_{n_1 n_2 m_1 m_2 l \in \mathfrak{F}} \frac{1}{\sqrt{D_n}} \langle n_1 | f_\nu^{\rm phys\dagger} | n_2 \rangle \phi^\dagger_{n_1 m_1} \phi_{n_2 m_2} \phi^\dagger_{n l} |{\rm vac}\rangle_b \otimes \hat{X}^f_{m_1 m_2} |l\rangle_f \\ &= \sum_{n' m_1 l \in \mathfrak{F}} \frac{1}{\sqrt{D_n}} \langle n' | f_\nu^{\rm phys\dagger} | n \rangle \phi^\dagger_{n' m_1} |{\rm vac}\rangle_b \otimes \hat{X}^f_{m_1 l} |l\rangle_f \end{aligned} \tag{3.50} $$

where commutation rule of boson operators $[\phi_{nm}, \phi^\dagger_{lk}] = \delta_{nl}\delta_{mk}$ has been used and the last expression changes the indices: $n_1 \to n'$. Comparison eq. (3.50) with the rhs of eq. (3.48), the following relation should hold:

$$ \sum_{m_1 l \in \mathfrak{F}} \frac{1}{\sqrt{D_n}} \phi^\dagger_{n' m_1} |{\rm vac}\rangle_b \otimes \hat{X}^f_{m_1 l} |l\rangle_f = \frac{1}{\sqrt{D_{n'}}} \sum_{m_1 \in \mathfrak{F}} \phi^\dagger_{n' m_1} |{\rm vac}\rangle_b \otimes |m_1\rangle_f. \tag{3.51} $$

This equation means that

$$ \sum_{l \in \mathfrak{F}} \hat{X}^f_{m_1 l} |l\rangle_f = \sqrt{\frac{D_n}{D_{n'}}} |m_1\rangle = \sqrt{\frac{N_n + 1}{2N_{\rm orb} - N_n}} |m_1\rangle, \tag{3.52} $$

should hold where we use the relation $N_{n'} = N_n + 1$. Since the "creation" operator is originally not unique, any forms of $\hat{X}^f_{m_1 m_2}$ that satisfies eq. (3.52) is allowed. Let us assume that $\hat{X}^f_{m_1 m_2}$ consists of the single fermion operators as,

$$ \hat{X}^f_{m_1 m_2} = \sum_{\nu \in \mathcal{N}} w_\nu^{m_1 m_2} f_\nu^\dagger, \tag{3.53} $$

where $w_\nu^{m_1 m_2}$ is a undetermined coefficient. Then, the lhs of eq. (3.52) becomes,

$$ \sum_{\nu \in \mathcal{N}} \sum_{l \in \mathfrak{F}} w_\nu^{m_1 l} f_\nu^\dagger |l\rangle_f = \sum_{\nu \in \mathcal{N}} \sum_{m' l \in \mathfrak{F}} w_\nu^{m_1 l} {}_f\langle m' | f_\nu^\dagger | l \rangle_f |m'\rangle_f \tag{3.54} $$

Comparison this equation with eq. (3.52), $w_\nu^{m_1 l}$ should act as fixing m' to m_1:

$$ w_\nu^{m_1 l} = w_f \langle m_1 | f_\nu^\dagger | l \rangle_f, \tag{3.55} $$

where w is a constant value. Substituting this equation into eq. (3.54) becomes,

$$\sum_{\nu\in\mathcal{N}}\sum_{m'l\in\mathfrak{F}} w_f\langle m_1|f_\nu^\dagger|l\rangle_f{}_f\langle m'|f_\nu^\dagger|l\rangle_f|m'\rangle_f = \sum_{\nu\in\mathcal{N}}\sum_{l\in\mathfrak{F}} w_f\langle m_1|f_\nu^\dagger|l\rangle_f^2|m_1\rangle_f = N_{m_1}w|m_1\rangle_f. \quad (3.56)$$

Since the rhs of eq. (3.52) and $N_{m_1} = N_n + 1 = N_{m_2} + 1$, w is determined and $\hat{X}_{m_1m_2}$ is written as,

$$\hat{X}^f_{m_1m_2} = \sum_{\nu\in\mathcal{N}} \frac{{}_f\langle m_1|f_\nu^\dagger|m_2\rangle_f}{\sqrt{(N_{m_2}+1)\,(2N_{\rm orb}-N_{m_2})}} f_\nu^\dagger. \quad (3.57)$$

As a result, we can conclude that the simplest form of the "creation" operator should be written as,

$${}_{\rm sim}\underline{f}_\nu^{\rm phys\dagger} = \sum_{n_1n_2m_1m_2\in\mathfrak{F}}\sum_{\nu'\in\mathcal{N}} \frac{\langle n_1|f_\nu^{\rm phys\dagger}|n_2\rangle_f\langle m_1|f_{\nu'}^\dagger|m_2\rangle_f}{\sqrt{(N_{m_2}+1)\,(2N_{\rm orb}-N_{m_2})}}\phi^\dagger_{n_1m_1}\phi_{n_2m_2}f^\dagger_{\nu'}. \quad (3.58)$$

It is to be noted that the localized Hamiltonian (3.46) can be derived by using eq. (3.58) from the original Hamiltonian (2.4) (see appendix B).

Finally, we need a correction to ${}_{\rm sim}\underline{f}_\nu^{\rm phys\dagger}$. Similarly to the KRSB formalism, ${}_{\rm sim}\underline{f}_\nu^{\rm phys\dagger}$ cannot describe the non-interacting system $U = 0$ correctly in the saddle point approximation. Here, we just show the result of the proper "creation" operator for the saddle point approximation (see appendix C for the detail proof). The proper "creation" operator is written as,

$$\underline{f}_\nu^{\rm phys\dagger} = \sum_{n_1n_2m_1m_2\in\mathfrak{F}}\sum_{\nu_1\nu'\in\mathcal{N}} \frac{\langle n_1|f_\nu^{\rm phys\dagger}|n_2\rangle_f\langle m_1|f_{\nu_1}^\dagger|m_2\rangle_f}{\sqrt{N_{m_1}\,(2N_{\rm orb}-N_{m_1}+1)}}\phi^\dagger_{n_1m_1}\hat{M}^{m_1}_{\nu_1\nu'}\phi_{n_2m_2}f^\dagger_{\nu'}, \quad (3.59)$$

$$\hat{M}^{m_1}_{\nu_1\nu'} = \left(\sqrt{(N_{m_2}+1)\,(2N_{\rm orb}-N_{m_2})}\right)^{\mathcal{Q}_0+1}\left[\frac{1}{\sqrt{\hat{1}-\hat{\Delta}^h}}\frac{1}{\sqrt{\hat{1}-\hat{\Delta}^p}}\right]_{\nu_1\nu'}, \quad (3.60)$$

where $\hat{\Delta}^p$ and $\hat{\Delta}^h$ are matrices of the particle and the hole operators whose $\nu\nu'$ component is given by,

$$\left(\hat{\Delta}^p\right)_{\nu\nu'} = \sum_{nml\in\mathfrak{F}}\phi^\dagger_{nm}\phi_{nl}\langle l|f_\nu^{\rm phys\dagger}f_{\nu'}^{\rm phys}|m\rangle, \quad (3.61)$$

$$\left(\hat{\Delta}^h\right)_{\nu\nu'} = \sum_{nml\in\mathfrak{F}}\phi^\dagger_{nm}\phi_{nl}\langle l|f_\nu^{\rm phys}f_{\nu'}^{\rm phys\dagger}|m\rangle. \quad (3.62)$$

It is to be noted that eqs. (3.58) and (3.59) give the same results because the additional part $M^m_{\nu\nu'}$ is an identity operator. Namely, when we act $\underline{f}_\nu^{\rm phys\dagger}$ to the physically meaningful states, all $\phi^\dagger_{ab}\phi_{cd}$ terms in $\hat{M}^{m_1}_{\nu_1\nu'}$ are zero because the annihilation operator $\phi_{n_2m_2}$ in eq. (3.59) makes the boson states of the physically meaningful states vacuum state. While, in the case of saddle point approximation, $M^m_{\nu\nu'}$ gives a finite value since all the slave boson operators are treated as mean values. Hereafter, we call the coefficients of pseudo fermion operators as a subsidiary operator $R^\dagger_{\nu\nu'}$, i.e., $\underline{f}_\nu^{\rm phys\dagger} = R^\dagger_{\nu\nu'}f^\dagger_\nu$. Likewise, we can also show that the proper "annihilation" operator is given by,

$$f_\nu^{\rm phys} = \hat{R}_{\nu\nu'}f_{\nu'}. \quad (3.63)$$

Then, the hybridization terms in the original Hamiltonian can be replaced into a slave boson form by substituting the "creation" and the "annihilation" operators into the original creation and the original annihilation operators, respectively. As a result, the total Hamiltonian eq. (2.1) is transformed as,

$$\mathcal{H} = \sum_{ij}\sum_{\nu\in\mathcal{N}} t_{ij} c^\dagger_{i\nu} c_{j\nu} + \sum_{i}\sum_{\nu\nu'\in\mathcal{N}} \left(V_\nu \hat{R}_{i\nu\nu'} c^\dagger_{i\nu} f_{i\nu'} + \text{h.c.} \right) + \sum_{i}\sum_{nml\in\mathfrak{F}} E_{nm} \phi^\dagger_{inl} \phi_{iml}. \tag{3.64}$$

where i and j indicate the site indices. It is shown that the RISB saddle point approximation by using eq. (3.59) and Gutzwiller approximation give the same results [78].

So far, we discuss how to transpose the original Hamiltonian in the RISB formalism. The RISB formalism succeeds to derive the proper Hamiltonian and the proper constraint conditions. However, in price, the procedure needs enormous number of boson operators; in the case of three-orbital system, the number of slave bosons are $1\times1+6\times6+15\times15+20\times20+15\times15+6\times6+1\times1 = 1324$. However, when we consider the saddle point approximations without any long-range order, the number of boson operators can be reduced, which will be discussed in the next section.

3.4 Saddle point approximation of RISB

In this section, we discuss the saddle point approximation of the slave boson Hamiltonian (3.64) under the constraint conditions in eqs. (3.42) and (3.45). In this approximation, all the slave boson operators are treated as mean values: $\phi_{nm} \to \overline{\phi}_{nm}$ and $\phi^\dagger_{nm} \to \overline{\phi}^*_{nm}$. Since the present model (3.64) does not take into account the inter-orbital hybridizations such as $V_{\Gamma_{+7}\Gamma_{+8}}$ for simplicity, the expectation value of the particle operator (3.61) and the hole operator (3.62) should be diagonalized in the normal state. Likewise, the off-diagonal part of the constraint conditions in eq. (3.45) does not contribute to this system in the case of the saddle point approximation. Hence, we redefine these factors in the following discussion as,

$$R_{i\nu\nu'} \to R_{i\nu}, \tag{3.65}$$

$$\mathcal{Q}_{i\nu\nu'} \to \mathcal{Q}_{i\nu}. \tag{3.66}$$

It is convenient to consider such constraint systems by using path integral techniques because we can introduce the constraint conditions by means of Lagrange multipliers. The partition function $\mathcal{Z}$ with Lagrange multipliers can be obtained by using eqs. (3.42), (3.45), (3.46), and (3.59) as:

$$\begin{aligned}\mathcal{Z} = &\int\cdot\cdot\int \prod_i \prod_{\nu\in\mathcal{N}} \mathcal{D}(f^\dagger_{i\nu} f_{i\nu}) \mathcal{D}(c^\dagger_{i\nu} c_{i\nu}) \prod_{nm\in\mathfrak{F}} \mathcal{D}(\phi^\dagger_{inm}\phi_{inm}) \\ &\exp\left[-\int_0^\beta d\tau \left(\mathcal{L}(\tau) + \sum_{i\nu\in\mathcal{N}} \lambda_{i\nu}\mathcal{Q}_{i\nu} + \sum_i \lambda_{i0}\mathcal{Q}_{i0} + \mu N \right) \right], \end{aligned} \tag{3.67}$$

$$\begin{aligned}\mathcal{L}(\tau) = &\sum_{ij}\sum_{\nu\in\mathcal{N}} c^\dagger_{i\nu} \left(\delta_{i,j}\partial_\tau + t_{ij}\right) c_{i\nu} + \sum_i \sum_{\nu\in\mathcal{N}} f^\dagger_{i\nu}\partial_\tau f_{i\nu} + \sum_i\sum_{\nu\in\mathcal{N}} V_\nu \left(c^\dagger_{i\nu} f_{i\nu} R_{i\nu} + R^\dagger_{i\nu} f^\dagger_{i\nu} c_{i\nu} \right) \\ &+ \sum_i \sum_{n_1 n_2 m\in\mathfrak{F}} \phi^\dagger_{in_1m} \left(\delta_{n_1,n_2}\partial_\tau + E_{n_1n_2}\right) \phi_{in_2m}, \end{aligned} \tag{3.68}$$

where $\lambda_{i\nu}$ and λ_{i0} are the Lagrange multipliers for the constraint conditions eqs. (3.42) and (3.45), respectively. Here, the fermion operators and the boson operators are changed to grassmann numbers and complex numbers, respectively. We omit the imaginary-time dependences of these grassmann numbers and complex numbers in eqs. (3.67) and (3.68), for simplicity.

Although it is significant to be careful for the order of the boson operators included in the subsidiary operators $R_{i\nu}$ owing to the principal rule of the path integral technique, the saddle point approximation does not need to consider this problem because all the boson operators are treated as mean values. In the saddle point approximation, we further restrict ourselves to consider the homogeneous state. Then, the Lagrange multipliers $\lambda_{i\nu}$ and λ_{i0} are regarded as site-independent and written as $\tilde{\lambda}_\nu$ and λ_0. Namely, the present saddle point approximation replaces the complex numbers ϕ_{inm} into both site- and time-independent mean values $\overline{\phi}_{nm}$.

Then, the partition function becomes,

$$\mathcal{Z}_{\mathrm{MF}} = e^{-\beta\mathcal{L}^b_{\mathrm{MF}}} \int\cdot\cdot\int \prod_i \prod_{\nu\in\mathcal{N}} \mathcal{D}(f^\dagger_{i\nu} f_{i\nu}) \mathcal{D}(c^\dagger_{i\nu} c_{i\nu}) \exp\left[-\int_0^\beta d\tau \mathcal{L}^f_{\mathrm{MF}}(\tau) \right], \tag{3.69}$$

$$\mathcal{L}^f_{\mathrm{MF}}(\tau) = \sum_{ij}\sum_{\nu\in\mathcal{N}} c^\dagger_{i\nu}\left(\delta_{i,j}\partial_\tau + t_{ij} - \mu\delta_{i,j}\right) c_{i\nu} + f^\dagger_{i\nu}\left(\partial_\tau + \tilde{\lambda}_\nu\right) f_{i\nu} + \overline{R}_\nu V_\nu \left(c^\dagger_{i\nu} f_{i\nu} + f^\dagger_{i\nu} c_{i\nu} \right), \tag{3.70}$$

$$\mathcal{L}^b_{\mathrm{MF}} = N_L \sum_{n_1 n_2 m\in\mathfrak{F}} \left(E_{n_1 n_2} + \delta_{n_1,n_2} \left(\lambda_0 - \sum_{\nu\in\mathcal{N}} \langle m| f^\dagger_\nu f_\nu |m\rangle \left(\tilde{\lambda}_\nu - \mu \right) \right) \right) \overline{\phi}^*_{n_1 m} \overline{\phi}_{n_2 m} - N_L\lambda_0 + N\mu, \tag{3.71}$$

where N_L describes the number of site i. $\mathcal{L}^b_{\mathrm{MF}}$ includes all the constant terms mainly the mean values of the bosons. According to eq. (3.71), the Lagrange multiplier $\tilde{\lambda}_\nu$ obviously acts as the energy level of the pseudo fermions. Therefore, it is convenient to measure $\tilde{\lambda}_\nu$ from the chemical potential, $\tilde{\lambda}_\nu = \lambda_\nu - \mu$. Then, the chemical potential μ in $\mathcal{L}^b_{\mathrm{MF}}$ cancels with each other.

After performing Fourier transformation and Gaussian integration, the free energy of the present system $\mathcal{F}_{\mathrm{MF}}$ is given by:

$$\mathcal{F}_{\mathrm{MF}} = -\frac{1}{\beta}\ln\mathcal{Z}_{\mathrm{MF}} = \mathcal{F}^{\mathrm{I}}_{\mathrm{MF}} + \mathcal{L}^b_{\mathrm{MF}}, \tag{3.72}$$

$$\mathcal{F}^{\mathrm{I}}_{\mathrm{MF}} = -\frac{1}{\beta}\sum_{\boldsymbol{k}\sigma=\pm}\sum_{\nu\in\mathcal{N}} \ln\left[1 + \exp\left[-\beta(\,\mathcal{E}^\sigma_{\boldsymbol{k}\nu} - \mu\,)\right]\right], \tag{3.73}$$

where $\mathcal{E}^\sigma_{\boldsymbol{k}\nu}$ describes the eigenenergy of the fermions. In the present model, $\mathcal{E}^\sigma_{\boldsymbol{k}\nu}$ can be written as,

$$\mathcal{E}^\pm_{\boldsymbol{k}\nu} = \frac{1}{2}\left(\varepsilon_{\boldsymbol{k}} + \lambda_\nu \pm \sqrt{(\varepsilon_{\boldsymbol{k}} - \lambda_\nu)^2 + 4 z_\nu V_\nu^2} \right). \tag{3.74}$$

Here, $\varepsilon_{\boldsymbol{k}}$ and z_ν represent the energy dispersion and the renormalization factor $z_\nu = \overline{R}^2_\nu$ for the conduction electrons, respectively.

All the mean values of the boson operators, the Lagrange multipliers, and the chemical potential are determined from the saddle point of the free-energy $\mathcal{F}_{\mathrm{MF}}$. Namely, these values

are determined from the following equations,

$$\frac{1}{N_L}\frac{\partial \mathcal{F}_{\rm MF}}{\partial \overline{\lambda}_0} = \sum_{nm\in\mathfrak{F}} \overline{\phi}^*_{nm}\overline{\phi}_{nm} - 1 = 0, \tag{3.75}$$

$$\frac{1}{N_L}\frac{\partial \mathcal{F}_{\rm MF}}{\partial \overline{\lambda}_\nu} = \frac{1}{N_L}\frac{\partial \mathcal{F}^{\rm I}_{\rm MF}}{\partial \overline{\lambda}_\nu} - \sum_{nm\in\mathfrak{F}} \langle m|f^\dagger_\nu f_\nu|m\rangle \overline{\phi}^*_{nm}\overline{\phi}_{nm} = 0, \tag{3.76}$$

$$\frac{1}{N_L}\frac{\partial \mathcal{F}_{\rm MF}}{\partial \overline{\phi}_{nm}} = \frac{1}{N_L}\frac{\partial \mathcal{F}^{\rm I}_{\rm MF}}{\partial \overline{\phi}_{nm}} + \sum_{n'\in\mathfrak{F}} E_{n'n}\overline{\phi}^*_{n'm} = 0, \tag{3.77}$$

$$\frac{1}{N_L}\frac{\partial \mathcal{F}_{\rm MF}}{\partial \overline{\phi}^*_{nm}} = \frac{1}{N_L}\frac{\partial \mathcal{F}^{\rm I}_{\rm MF}}{\partial \overline{\phi}^*_{nm}} + \sum_{n'\in\mathfrak{F}} E_{nn'}\overline{\phi}_{n'm} = 0, \tag{3.78}$$

$$\frac{1}{N_L}\frac{\partial \mathcal{F}_{\rm MF}}{\partial \mu} = \frac{1}{N_L}\frac{\partial \mathcal{F}^{\rm I}_{\rm MF}}{\partial \mu} + N = 0. \tag{3.79}$$

Although these equations can be solved at finite temperature in principle, it is known that the artificial phase transition of Bose-Einstein condensation (BEC) occurs at some finite temperature. Above this transition, the renormalization factor z_ν becomes zero, and we cannot calculate much higher temperature. For this reason, we restrict ourselves to the case of zero temperature. Then, the derivative of $\mathcal{F}^{\rm I}_{\rm MF}$ can be solved analytically by using the constant density-of-state defined in eq. (2.3):

$$\frac{1}{N_L}\frac{\partial \mathcal{F}^{\rm I}_{\rm MF}}{\partial \lambda_\nu} = \sum_{\nu'\sigma} \rho_0 \int_{-D}^{D} d\varepsilon f(\mathcal{E}^\sigma_{\nu'}(\varepsilon)) \frac{\partial \mathcal{E}^\sigma_{\nu'}(\varepsilon)}{\partial \lambda_\nu} = \sum_\sigma C^\lambda_{\nu\sigma}, \tag{3.80}$$

$$C^\lambda_{\nu\sigma} = \begin{cases} \rho_0 z_\nu V_\nu^2 \left(\frac{1}{\lambda_\nu - \min[\mu, \mathcal{E}^\sigma_\nu(D)]} - \frac{1}{\lambda_\nu - \mathcal{E}^\sigma_\nu(-D)} \right) & (\mu \geq \mathcal{E}^\sigma_\nu(-D)) \\ 0 & (\mu < \mathcal{E}^\sigma_\nu(-D)), \end{cases} \tag{3.81}$$

$$\frac{1}{N_L}\frac{\partial \mathcal{F}^{\rm I}_{\rm MF}}{\partial \overline{\phi}_{nm}} = \sum_{\nu\sigma} \frac{\partial z_\nu}{\partial \overline{\phi}_{nm}} \rho_0 \int_{-D}^{D} d\varepsilon f(\mathcal{E}^\sigma_\nu(\varepsilon)) \frac{\partial \mathcal{E}^\sigma_\nu(\varepsilon)}{\partial z_\nu} = \sum_{\nu\sigma} C^\phi_{\nu\sigma}, \tag{3.82}$$

$$C^\phi_{\nu\sigma} = \begin{cases} \rho_0 \frac{\partial z_\nu}{\partial \overline{\phi}_{nm}} V_\nu^2 \ln \left| \frac{\lambda_\nu - \min[\mu, \mathcal{E}^\sigma_\nu(D)]}{\lambda_\nu - \mathcal{E}^\sigma_\nu(-D)} \right| & (\mu \geq \mathcal{E}^\sigma_\nu(-D)) \\ 0 & (\mu < \mathcal{E}^\sigma_\nu(-D)). \end{cases} \tag{3.83}$$

Let us discuss the number of the slave boson operators which we have to treat in the self-consistent equations. As far as we do not consider the ordered state analogous to the discussion of SRISB in sec. 3.1, the number of the boson operators can be reduced in the saddle point approximation. Namely, it is sufficient to consider smaller Hilbert space which is block diagonalized in the local Hamiltonian. Although it obviously breaks down rotationally invariance, the complete rotationally invariance is not so important as far as in the saddle point approximation without long-range order. Furthermore, several mean-field values of boson operators should coincide with each other due to the time reversal symmetry. Then, in the case of the cubic system, we can finally reduce the number of boson states into 126 as shown in Figs. 3.1, 3.2, and 3.3. Likewise, in the case of hexagonal system, the number of boson states can be reduced into 90 shown in Figs. 3.4, 3.5, and 3.6.

In order to obtain the saddle point of this system numerically, we need to solve a system of nonlinear equations $\boldsymbol{F} = 0$, where $\boldsymbol{F}$ is a vector that consists of lhs of eq. (3.79), as a function of

$\boldsymbol{x}$, which involves the Lagrange multiplier, all the mean-field bosons, and the chemical potential. To handle this problem numerically, we use quasi-Newton techniques called Broyden method [79]. This technique first inputs initial values $\boldsymbol{x}_1$, and updates as

$$\boldsymbol{x}_{m+1} = \boldsymbol{x}_m + \boldsymbol{J}_m^{-1}\boldsymbol{F}_m, \tag{3.84}$$

where $\boldsymbol{x}_m$ indicates the m-th updated values. Here, $\boldsymbol{J}$ represents Jacobian defined as:

$$J_{ij} = -\frac{\partial F_i}{\partial x_j}. \tag{3.85}$$

The derivative included in Jacobian is calculated numerically at each step m in this method.

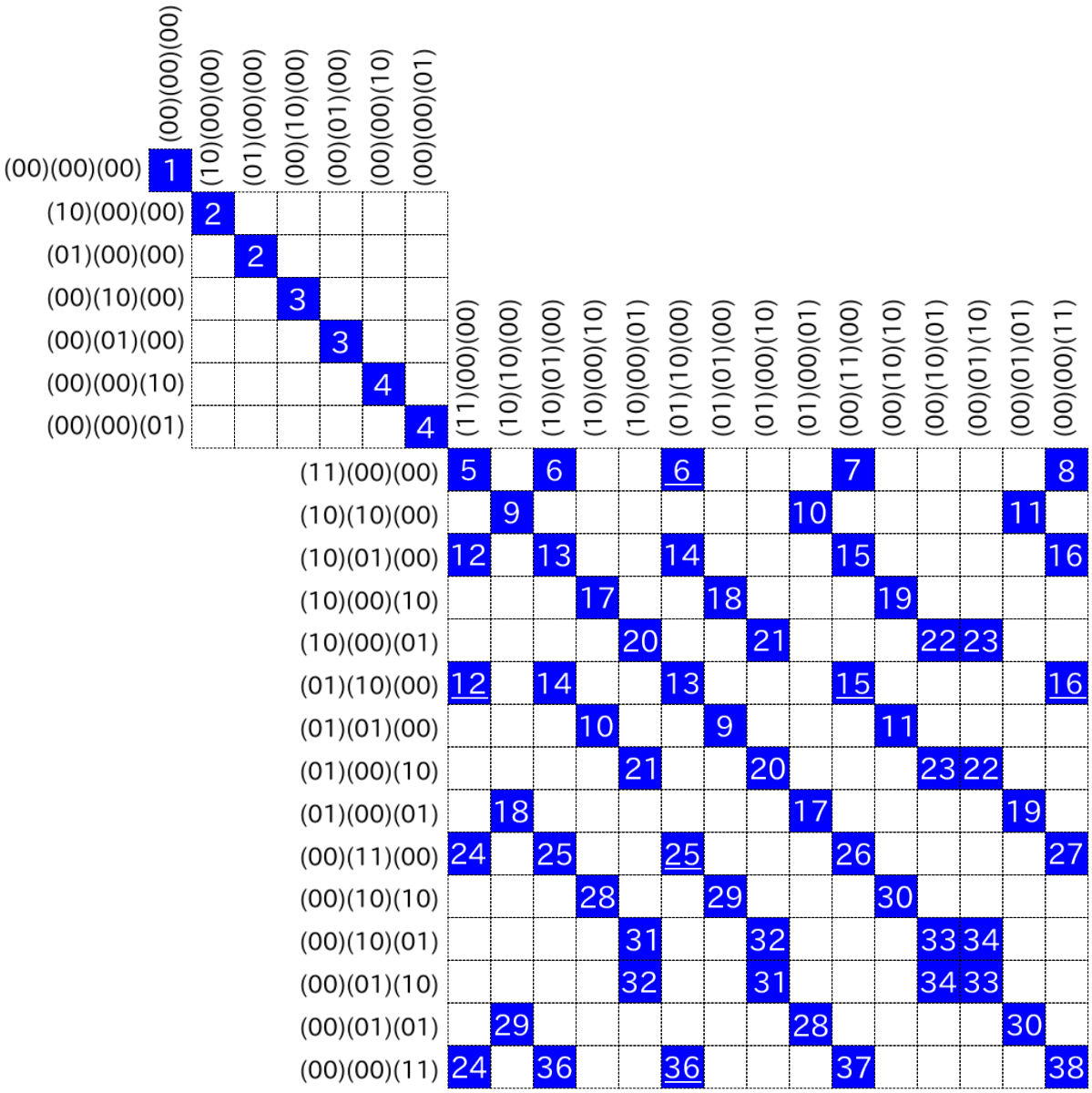

Figure 3.1: Boson operators taken into account in the saddle point approximations in the case of cubic symmetry from f^0-configuration to f^2-configuration. Matrix components of the table filled by blue represent finite slave boson operator ϕ_{nm}. Same number components without underline have the same mean-field value, while that with underline have the inverse sign mean-field value due to the time revearsal symmetry.

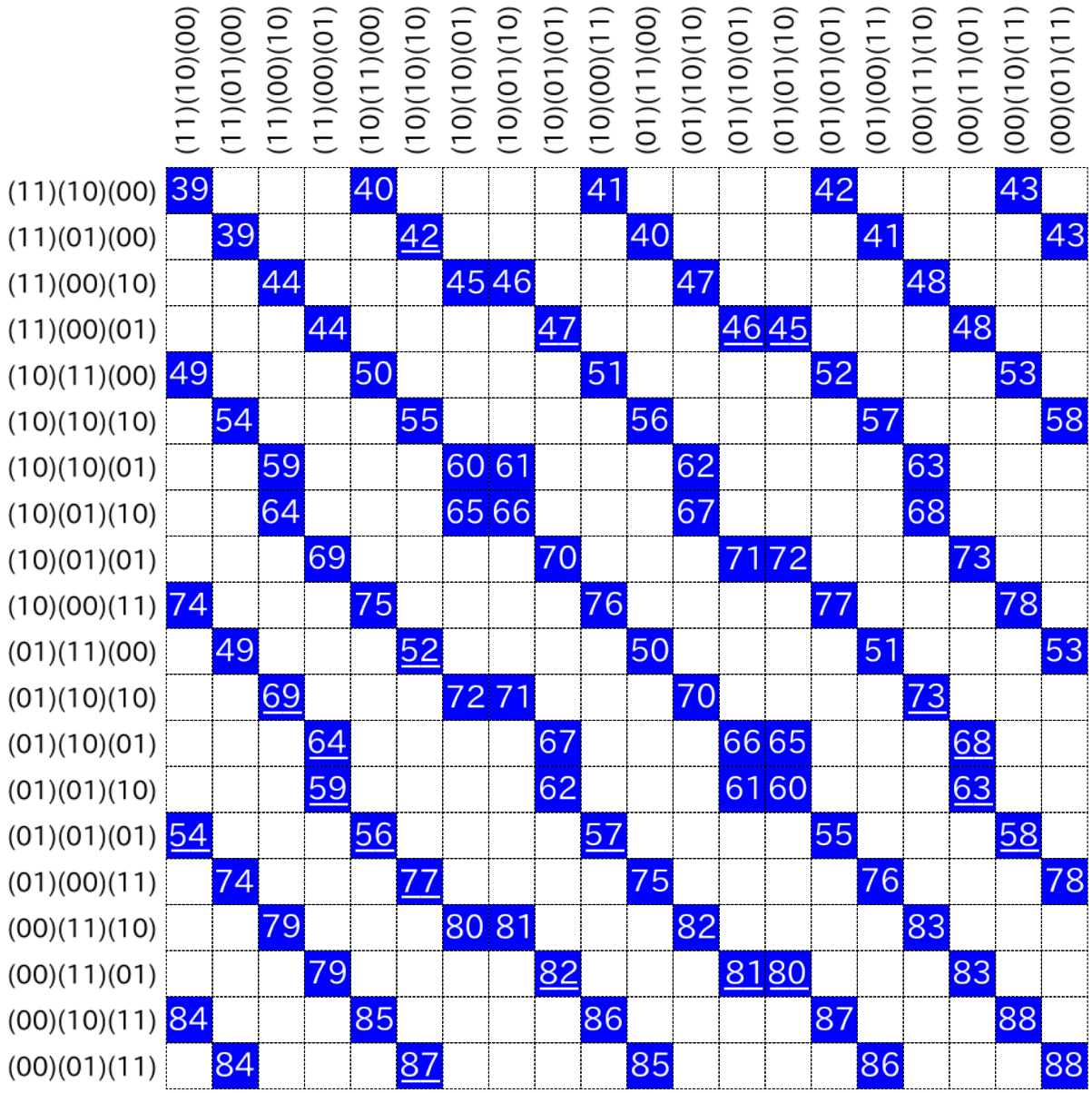

Figure 3.2: Boson operators taken into account in the saddle point approximations in the case of cubic symmetry on f^3-configuration. Matrix components of the table filled by blue represent finite slave boson operator ϕ_{nm}. Same number components without underline have the same mean-field value, while that with underline have the inverse sign mean-field value due to the time revearsal symmetry.

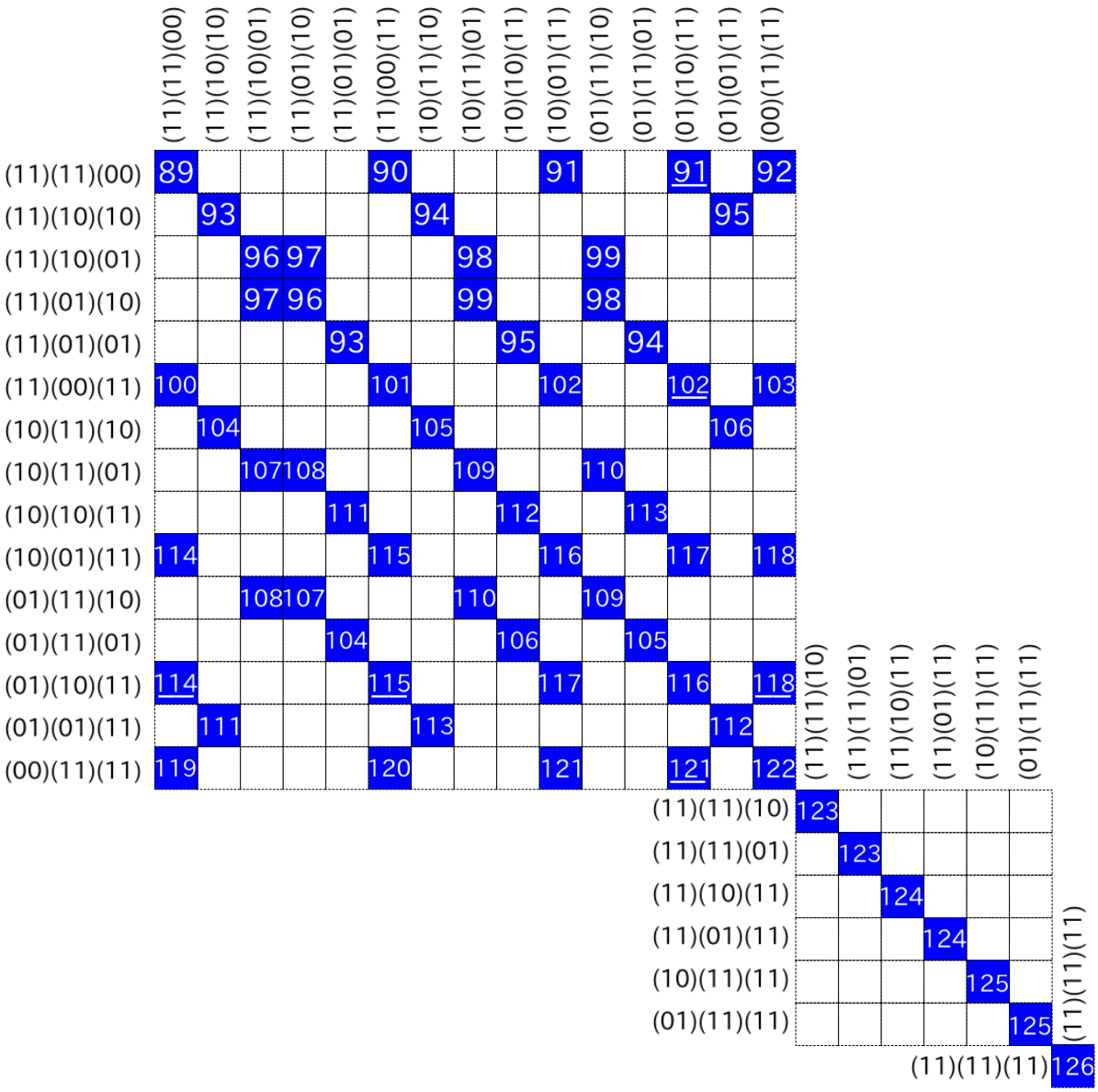

Figure 3.3: Boson operators taken into account in the saddle point approximations in the case of cubic symmetry from f^4-configuration to f^6-configuration. Matrix components of the table filled by blue represent finite slave boson operator ϕ_{nm}. Same number components without underline have the same mean-field value, while that with underline have the inverse sign mean-field value due to the time revearsal symmetry.

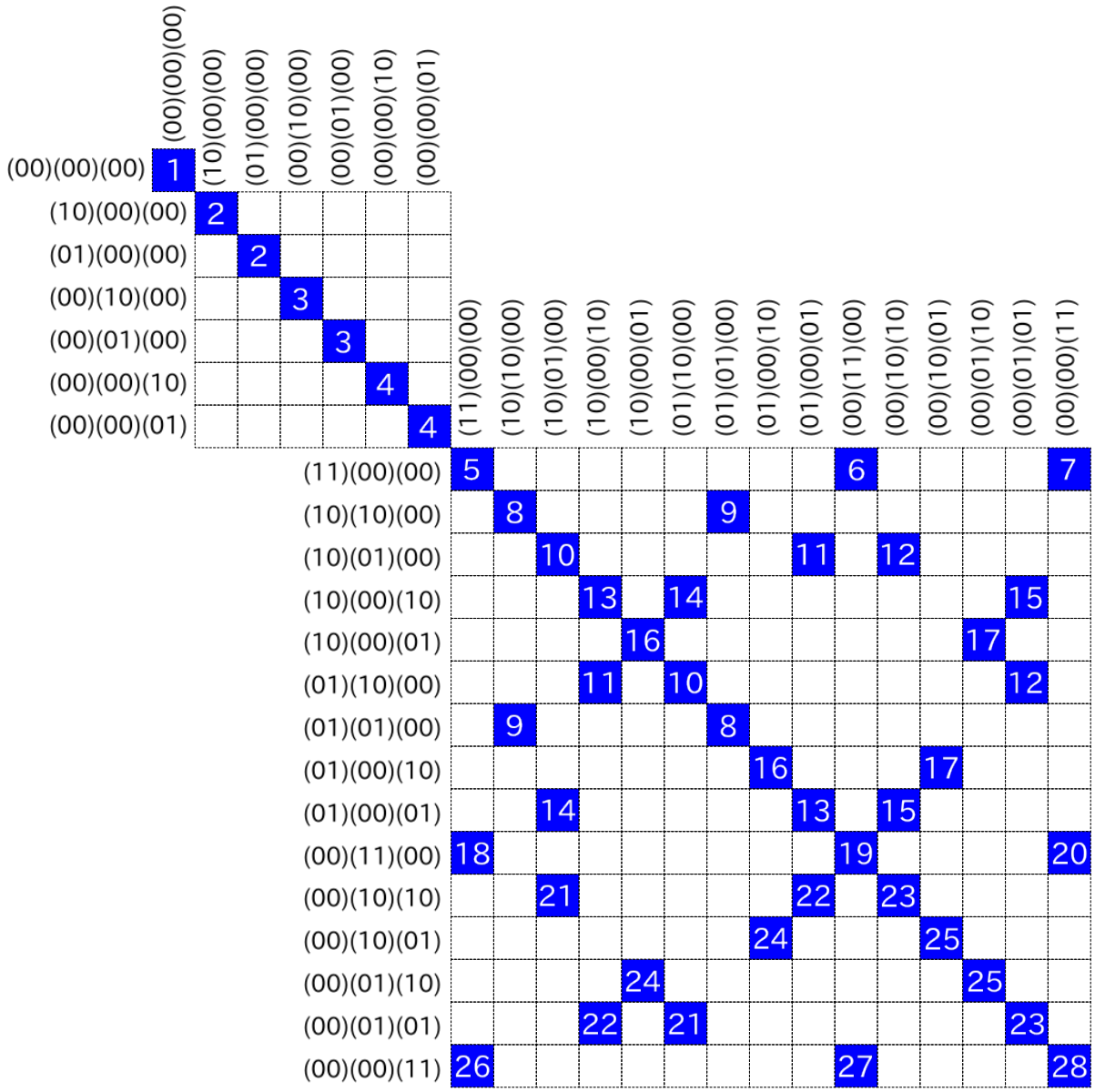

Figure 3.4: Boson operators taken into account in the saddle point approximations in the case of hexagonal symmetry from f^0-configuration to f^2-configuration. Matrix components of the table filled by blue represent finite slave boson operator ϕ_{nm}. Same number components without underline have the same mean-field value, while that with underline have the inverse sign mean-field value due to the time revearsal symmetry.

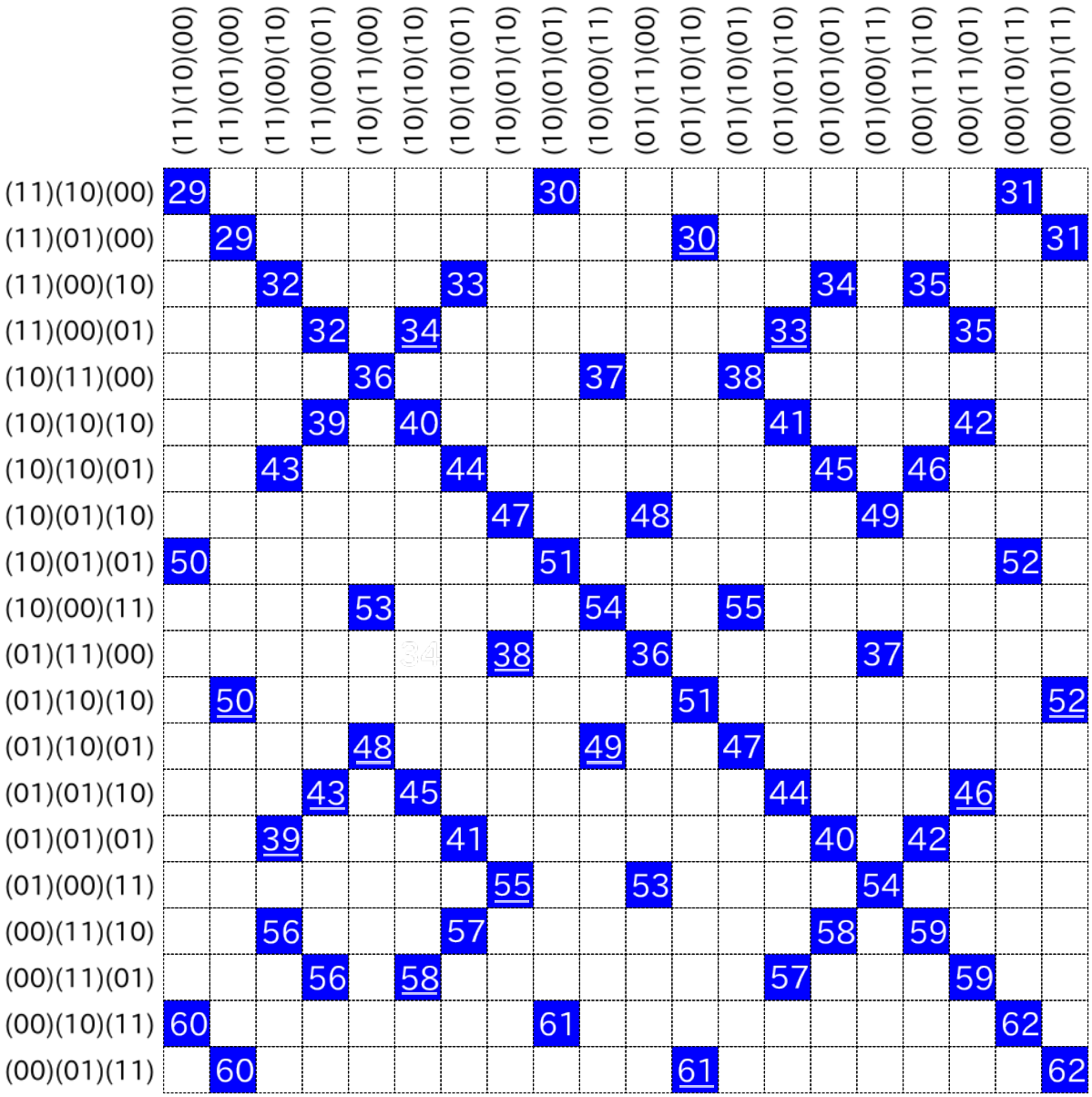

Figure 3.5: Boson operators taken into account in the saddle point approximations in the case of hexagonal symmetry on f^3-configuration. Matrix components of the table filled by blue represent finite slave boson operator ϕ_{nm}. Same number components without underline have the same mean-field value, while that with underline have the inverse sign mean-field value due to the time revearsal symmetry.

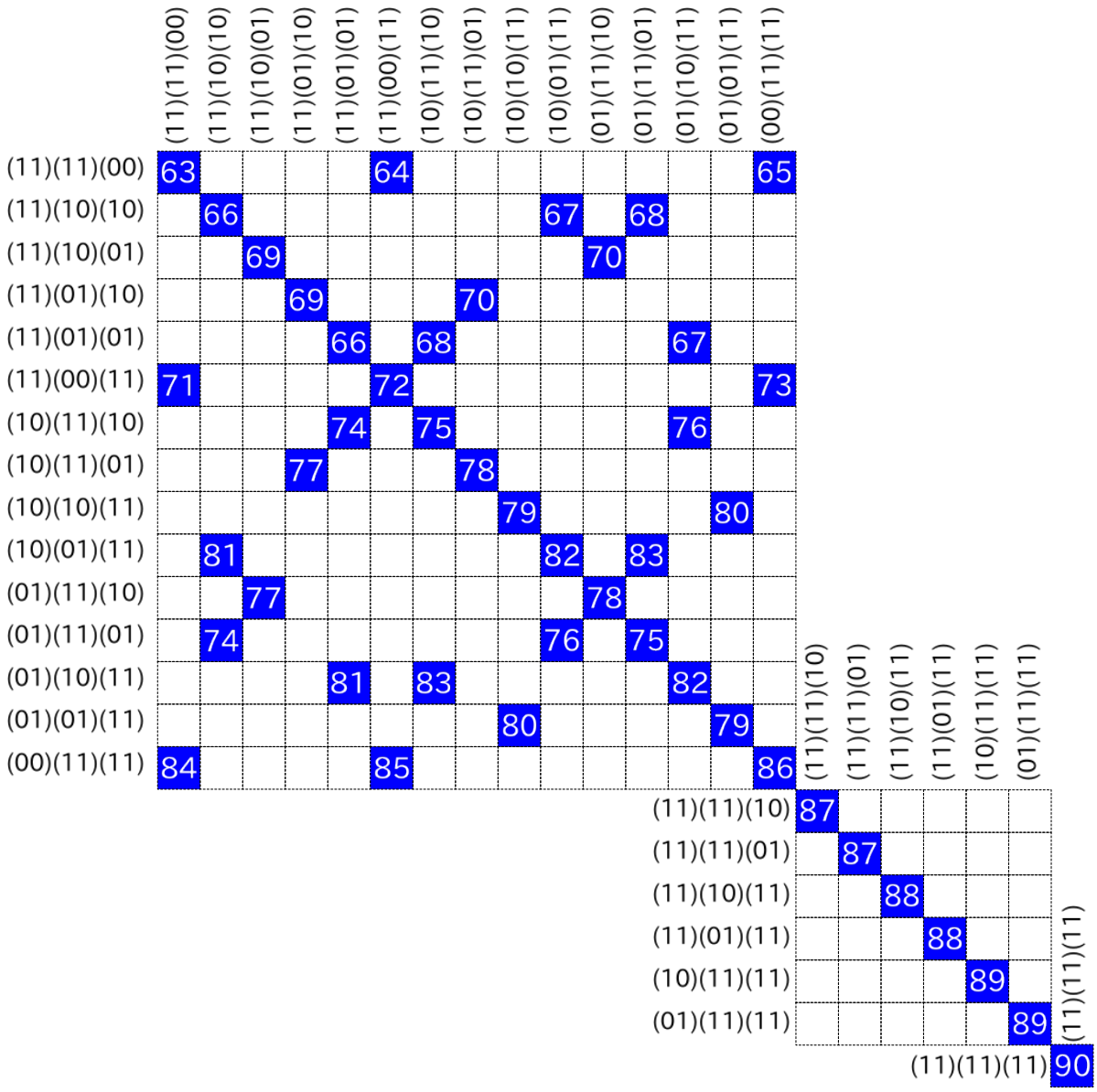

Figure 3.6: Boson operators taken into account in the saddle point approximations in the case of hexagonal symmetry from f^4-configuration to f^6-configuration. Matrix components of the table filled by blue represent finite slave boson operator ϕ_{nm}. Same number components without underline have the same mean-field value, while that with underline have the inverse sign mean-field value due to the time revearsal symmetry.

Chapter 4

Results and Discussion

In this chapter, we show the results of a RISB saddle point approximation with two different ground state systems: a Γ_1 singlet state in cubic symmetry discussed in chapter 2.3, and a Γ_4 singlet state in hexagonal symmetry discussed in chapter 2.4. These systems are candidates of ground states for UBe_{13} and UPt_3, respectively. This chapter is organized as follows. First we show the results of the Γ_1 singlet system in section 4.1. We discuss following two kinds of parameter dependences in this section. In subsection 4.1.1, U and E_f dependence under isotropic V are discussed in order to show the whole behaviors around the f^2-configuration system. This subsection also refers to f^1- and f^3-configuration systems. In subsection 4.1.2, the anisotropic V dependence at the f^2 configuration are discussed to compare the results of the RISB formalism with that of the impurity Anderson model discussed by Nishiyama [80]. In the section 4.2, we discuss the results of Γ_4 singlet system. Following two kinds of parameter dependences are evaluated in this section. One is the U and E_f dependences with an isotropic V in subsection 4.2.1. The other is an anisotropic V dependence around $n_f = 2.5$ in subsection 4.2.2. This is because several works suggest that the n_f of the UPt_3 is an inter-valence.

4.1 Γ_1 non-Kramers singlet state in cubic symmetry

In this section, we focus on the Γ_1 ground state of the f^2 configuration in cubic symmetry. The Γ_1 ground state is one of the candidate systems for UBe_{13}. As we mentioned in chapter 1, there are several scenarios to explain the NFL on UBe_{13}: a two-channel Kondo effect with the Γ_3 ground state, a field-induced QCP, and a competition between a CEF-singlet and a CEF-triplet state (singlet-triplet competition) with the Γ_1 singlet and the Γ_4 triplet state. This chapter focuses on the singlet-triplet competition scenario as following three reasons.

First, the Γ_3 state cannot be a ground state in the case of $\lambda_{ls} \to \infty$ (see Fig. 2.1); the two-channel Kondo effect cannot be discussed by the present model. Second, the RISB saddle point approximation gives unstable results (negative sign of the magnetic susceptibility) under the magnetic field as well as Gutzwiller approximation; it is difficult to evaluate the field-induced QCP. Third, only the singlet-triplet competition scenario succeeds in explaining the behaviors in a series of dilute systems $U_xM_{1-x}Be_{13}$ [10, 80].

The singlet-triplet competition is first suggested in the impurity Anderson model with the several CEF eigenstates in cubic symmetry: the Γ_7 and Γ_8 states of the f^1 configuration and the Γ_1 and Γ_4 states of the f^2-configuration. Nishiyama and Miyake evaluated this model by

using a NRG method and suggested three electron-states: a CEF-singlet state, Kondo-Yosida (KY) singlet state, and CEF-triplet state [80]. They found that a competition between the CEF-singlet and CEF-triplet state drastically suppresses the characteristic energy scale. In the vicinity of this competition region, they proposed that the anomalous Sommerfeld coefficients in the series of dilute systems $U_xM_{1-x}Be_{13}$ can be explained qualitatively.

Although the NRG calculation succeeds in explaining properties of the dilute systems, the following two issues should be resolved. First, it is nontrivial how the rich phenomena are reflected to the lattice system such as UBe_{13}, while theoretical approaches that can tackle the lattice system are limited. Second, it is unclear whether the partially included CEF-eigenstates are enough to describe the system with Γ_1 ground state (Γ_1 system). In fact, the CEF-eigenstates of the f^3 configuration, which are ignored in previous works, are necessary for describing an itinerant nature of f electrons at the f^2 configuration. Taking into account all the CEF eigenstates is necessary to clarify whether the singlet-triplet competition is an artificial phenomenon. Since the NRG method considering all the CEF eigenstates is time consuming, it is preferred to use other theoretical approaches.

Under these circumstances, a RISB formalism sheds light on the physical properties of the Γ_1 system in the lattice model. This is because a RISB saddle point approximation can be applied to a general multi-orbital lattice model and can calculate within a reasonable amount of computational time even when all the CEF eigenstates are taken into account.

In this section, we employ the three-orbital periodic Anderson model derived in chapter 2 (see eqs. (2.1) and (2.3) and evaluate this model by using the RISB saddle point approximation. In cubic symmetry, elements ν of the set $\mathcal{N}$ are listed in chapter 2.3: Γ_{+7}, Γ_{-7}, Γ_{+81}, Γ_{-81}, Γ_{+82}, and Γ_{-82}; we call the element ν as "ν orbital". Meanwhile, the set $\mathfrak{G}$ consists of all the CEF states Γ up to the f^6 configuration composed of $j = 5/2$ in cubic symmetry. This chapter labels each element of $\mathfrak{G}$ as an irreducible representation of a CEF eigenstate, although several CEF eigenstates belong to a same irreducible representation. Hereafter, we call the element Γ in the set $\mathfrak{G}$ as "Γ state". In this thesis, a "Γ state" without any annotations indicates the lowest energy of the Γ state in the f^1 or f^2 configuration. For example, the "Γ_4 state" indicates first excited eigenstate in the f^2 configuration (see Fig. 2.1).

Following parameters in the present model Hamiltonian are fixed throughout in this section: the CEF parameter $B_4^0 = 0.0001D$, the total number of electrons $N = 4.0$, and the temperature $T = 0.0$, where D is a half of the conduction band width. According to Fig. 2.1, the CEF parameter sets the Γ_1 state as a ground state of the f^2 configuration in the case of $U = 2.5D$. We confirmed that this ground state system is also realized even in much smaller U case.

Table 4.1 listed the definitions for several kinds of electron numbers. These values have following relations:

$$N = n_f + n_c, \tag{4.1}$$

$$n_f = \sum_{\nu\in\mathcal{N}} n_\nu, \tag{4.2}$$

$$n_\nu = \sum_{nml\in\mathfrak{F}} \langle l|f_\nu^\dagger f_\nu|m\rangle_f \overline{\phi}_{nm}\overline{\phi}_{nl}, \tag{4.3}$$

$$\Phi_\Gamma = \sum_{n\in\mathfrak{F}} \overline{\phi}_{\Gamma n}^2 = \sum_{nml\in\mathfrak{F}} \langle m|\Gamma\rangle\langle\Gamma|l\rangle\overline{\phi}_{mn}\overline{\phi}_{ln}, \tag{4.4}$$

where n_ν and Φ_Γ are derived from mean values of bosons.

N	number of total electrons (fixed as $N = 4.0$)
n_f	number of total f electrons
n_c	number of total conduction electrons
$n_\nu\,(\nu \in \mathcal{N})$	number of f electrons on ν orbital
$\Phi_\Gamma\,(\Gamma \in \mathfrak{G})$	expectation values of Γ state

Table 4.1: Definitions of electron numbers.

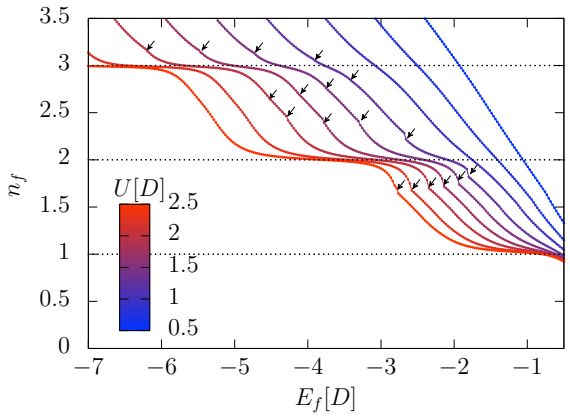

Figure 4.1: Total f-electron number n_f against f-energy level E_f with various values of electron-electron interactions U. Black arrows point a jump (or a kink) of n_f.

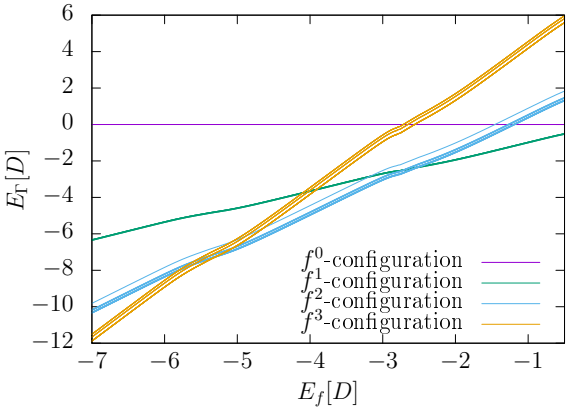

Figure 4.2: All the CEF energy levels measured from the chemical potential up to the f^3-configuration at $U = 2.5D$ and $B_4^0 = 0.0001D$.

Since we do not consider the magnetic field effect, all the typical values for each orbital such as the electron number n_ν, the renormalized energy level λ_ν, and the renormalization factor z_ν, are equivalent within the degenerate orbitals. Hence, following representations are used in this section.

$$\lambda_{\Gamma_{+7}} = \lambda_{\Gamma_{-7}} = \lambda_{\Gamma_7}, \tag{4.5}$$
$$\lambda_{\Gamma_{+81}} = \lambda_{\Gamma_{-81}} = \lambda_{\Gamma_{+82}} = \lambda_{\Gamma_{-82}} = \lambda_{\Gamma_8}, \tag{4.6}$$
$$z_{\Gamma_{+7}} = z_{\Gamma_{-7}} = z_{\Gamma_7}, \tag{4.7}$$
$$z_{\Gamma_{+81}} = z_{\Gamma_{-81}} = z_{\Gamma_{+82}} = z_{\Gamma_{-82}} = z_{\Gamma_8}, \tag{4.8}$$
$$n_{\Gamma_{+7}} + n_{\Gamma_{-7}} = n_{\Gamma_7}, \tag{4.9}$$
$$n_{\Gamma_{+81}} + n_{\Gamma_{-81}} + n_{\Gamma_{+82}} + n_{\Gamma_{-82}} = n_{\Gamma_8}. \tag{4.10}$$

4.1.1 Quasi particle properties around f^2-configuration system

In this subsection, we evaluate the n_f dependence of the QP properties under the isotropic hybridizations $V_{\Gamma_7} = V_{\Gamma_8} = 0.2D$. In $N = 4.0$ case, U, V_ν, and E_f change the f-electron

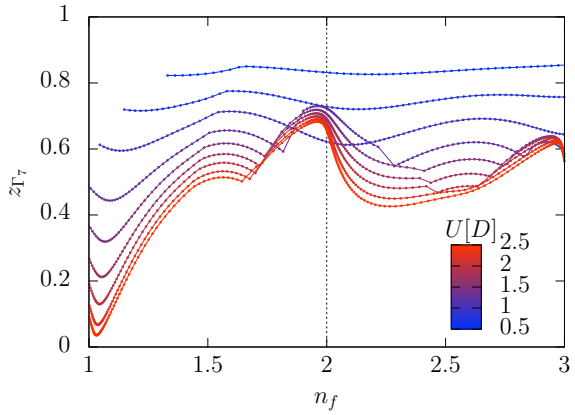

Figure 4.3: Renormalization factor of the Γ_7 orbital as a function of n_f with various values of U.

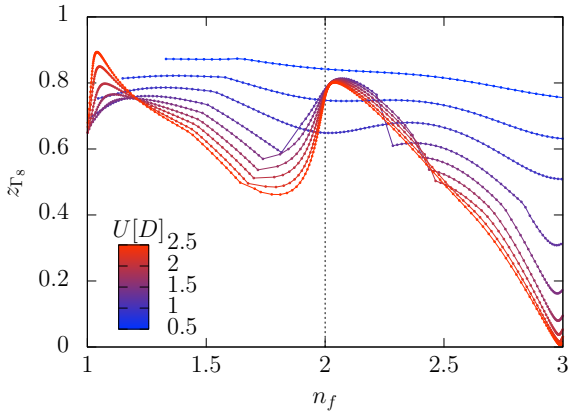

Figure 4.4: Renormalization factor of the Γ_8 orbital as a function of n_f with various values of U.

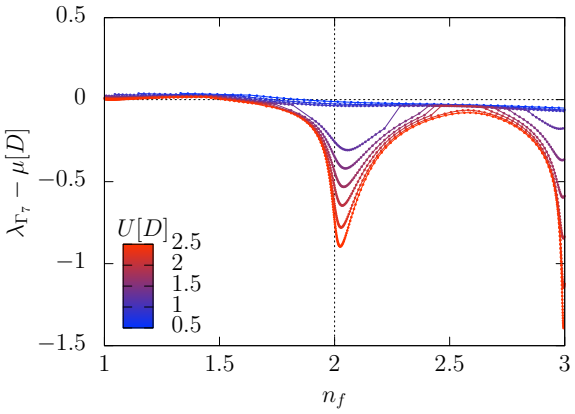

Figure 4.5: Renormalized energy level of the Γ_7 orbital measured from chemical potential as a function of n_f with various values of U.

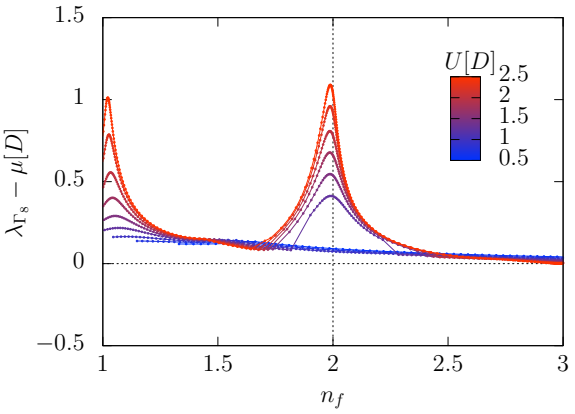

Figure 4.6: Renormalized energy level of the Γ_8 orbital measured from chemical potential as a function of n_f with various values of U.

number n_f up to four. Hence, it is necessary to search for the parameter region realizing the f^2-configuration system: $n_f = 2$.

Figure 4.1 represents the variation of n_f as a function of E_f with various values of U, where $E_f = -1.0D$ corresponds to the lower band edge of the conduction bands. While the small U region monotonically increases n_f with decreasing E_f, the large U region shows a plateau around integer fillings. This behavior indicates that the f electrons tend to be localized at integer fillings due to the strong electron-electron interactions. To reach the plateau at the f^2 configuration, E_f should be lower than $-3D$, which is far below the conduction bands, in the case of $U = 2.5D$ and $V = 0.2D$. The right end of the plateau at each configuration shifts to lower E_f as U increases except for that at the f^1 configuration. In contrast to the f^1 configuration, fine-tuning E_f and U is necessary to obtain the localized behavior at the f^2 configuration.

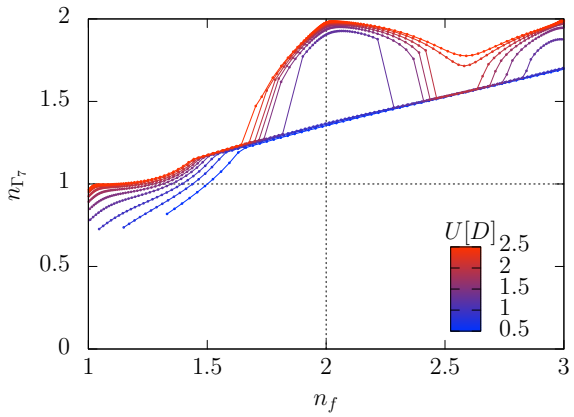

Figure 4.7: Number of f-electrons on the Γ_7 orbital as a function of n_f with various values of U.

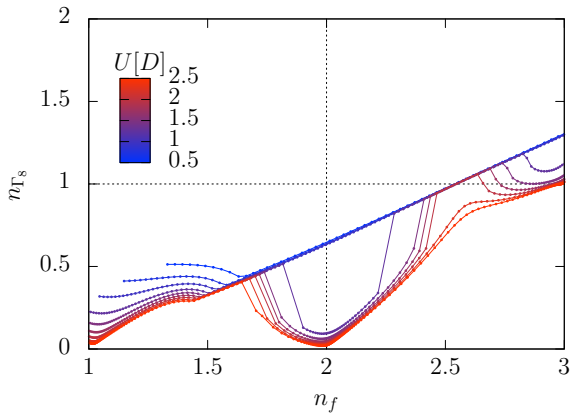

Figure 4.8: Number of f-electrons on the Γ_8 orbital as a function of n_f with various values of U.

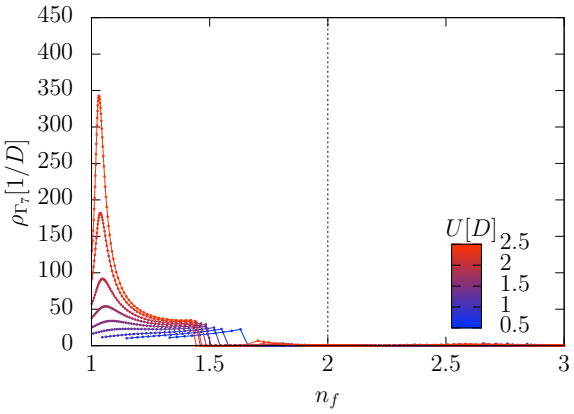

Figure 4.9: Density of state at chemical potential of the Γ_7 orbital as a function of n_f with various values of U.

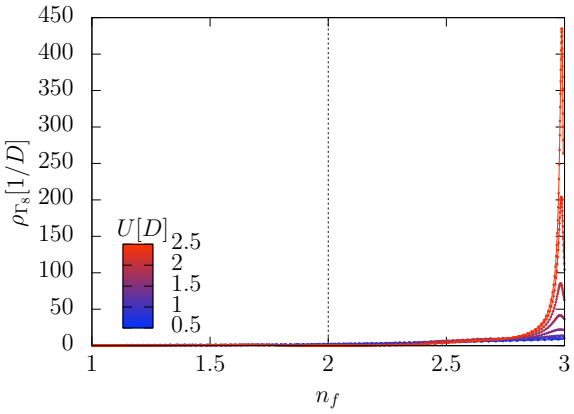

Figure 4.10: Density of state at chemical potential of the Γ_8 orbital as a function of n_f with various values of U.

In addition, nontrivial first-order transitions, which are pointed by black arrows in Fig. 4.1, appear around the f^2 and f^3 configurations. The two transition points in between these configurations are close with each other as U increases and disappear in $U > 2.25D$. This behavior supports that the transitions around the f^2 and f^3 configurations are induced by the same origin. We will discuss the origin of the transition later in this subsection.

All the CEF energy levels measured from μ at $U = 2.5D$ up to the f^3 configuration are shown in figure 4.2. As we mentioned in chapter 2.3, there are 6, 15, and 20 eigenstates belonging to the f^1, f^2, and f^3 configurations, respectively (see figure 2.1). The Γ_1 state, which is the lowest CEF eigenenergy of the f^2 configuration, becomes a ground state in the region of $-5D < E_f < -3D$. Because figure 4.1 shows the plateau behavior in the same region, we can discuss the relation between the itinerant f-electron character and the Γ_1 CEF eigenstate in this region. Likewise, Γ_7 ground state of the f^1 configuration (Γ_8 ground state of the f^3 configuration) realizes in the region of $-2D < E_f < -0.5D$ ($E_f < -6D$).

In the RISB saddle point approximation, the itinerant f electrons are characterized by the renormalization factor z_ν and the renormalized energy level λ_ν. Hereafter, we show the n_f dependence of these characteristic values.

Figures 4.3 and 4.4 display the n_f dependence of z_{Γ_7} and $z_{\Gamma 8}$, respectively. In general, z_ν takes the value among 0 to 1. $z_\nu = 0$ indicates Brinkmann-Rice transition that corresponds to Mott transition in Hubbard model. On the other hand, this quantity should be unity in the uncorrelated system.

There are additional kinks around $n_f \sim 1.5$ even in the small U region, $n_f = 1.65$ with $U = 0.5D$ for instance. These transitions are Lifshitz transition on the Γ_7 orbital that changes Luttinger volume of this system; it becomes clear from ρ_ν behavior, which will be discussed later.

In the small U region, the renomalization factors do not exhibit any strong features. We confirmed that all the renomalization factors become unity at $U = 0$. On the contrary, z_ν shows different behaviors depending on orbitals in the strongly correlated region. The renormalization factor z_{Γ_7} and z_{Γ_8} are strongly suppressed to 0 around the f^1 and the f^3 configurations, respectively. However, at the f^2 configuration, both renormalization factors are enhanced after the first-order transition.

Figures 4.5 and 4.6 show the renormalized energy levels measured from μ as a function of n_f. In the case of $U = 0$, these values correspond to E_ν. At the integer filling, λ_ν approaches μ when z_ν are suppressed to 0 as U increases; otherwise, λ_ν moves away from μ.

The itinerant f-electron behaviors at each integer filling can be understood by the results of z_ν and λ_ν. In the f^1 configuration, the energy dispersion of the Γ_7 orbital $\mathcal{E}^{\pm}_{\boldsymbol{k}\Gamma_7}$ is mostly composed of f electrons at the chemical potential (see eq. (3.74) for the definition of $\mathcal{E}^{\pm}_{\boldsymbol{k}\nu}$). These electrons have a heavy effective mass due to $z_{\Gamma_7} \ll 1$ and $\lambda_{\Gamma_7} \sim \mu$. In contrast, the Γ_8 orbital does nothing to conduction electrons because λ_{Γ_8} moves away from the chemical potential as U increases. These different behaviors are closely related to the CEF energy scheme at the f^1 configuration: Γ_7 eigenstate is the ground state of the present parameter set. The behaviors ensure that the basic property of the f^1-configuration system such as Ce compound can be discussed by a single-orbital Anderson model. Note that the bare energy splitting between the Γ_7 and Γ_8 orbital is $0.036D$ in the present parameter set, much smaller than the hybridization strength $0.2D$. Nevertheless, an effective single-band model is sufficient for the f^1-configuration system due to the many-body effect.

On the contrary, there are no heavy QP behaviors at the f^2 configuration; both the renormalized energy levels, λ_{Γ_7} and λ_{Γ_8}, move away from the chemical potential after the untrivial first-order transition. The quite different behavior from the f^1 configuration is related to the Γ_1 singlet ground state. In the following, we discuss the origin of the transitions from the density of state at the chemical potential ρ_ν and the number of electrons for each orbital n_ν.

Figures 4.9 and 4.10 show the density of state at the chemical potential ρ_ν for each localized orbital. While the density of state enhances at the f^1 configuration on the Γ_7 orbital, no sharp peaks are observed at the f^2-configuration. The sharp peak behavior at the f^1 configuration is caused by formation of the heavy QP on the Γ_7 orbital. In figure 4.9, the jump toward zero around $n_f \sim 1.5$ indicates that the chemical potential positions in between the energy dispersions of the Γ_7 orbital $\mathcal{E}^{\pm}_{\boldsymbol{k}\Gamma_7}$. Hence, the transition is concluded as Lifshitz transition. This transition depends on the form of an energy dispersion of conduction bands. Since present model assumes the unrealistic energy dispersions for simplicity, we do not focus on the Lifshitz transition in this thesis.

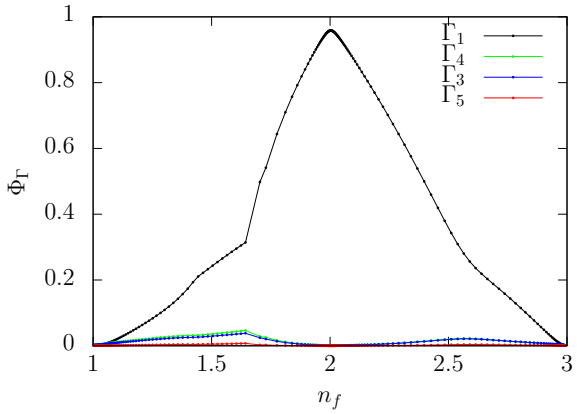

Figure 4.11: Expectation values for occupations Φ_Γ with the CEF eigen states Γ in the f^2 configuration at $U = 2.5D$.

Figures 4.7 and 4.8 show n_ν as a function of n_f. While both n_{Γ_7} and n_{Γ_8} monotonically increase in the small U region, they drastically change its quantities at the vicinity of the f^2- and f^3-configurations in the large U region. At the integer filling of n_f, n_{Γ_7} becomes a half filling, full filling, and full filling at the f^1, f^2, and f^3 configurations, respectively. On the other hand, n_{Γ_8} becomes an empty, empty, and half-filling at the f^1-, f^2-, and f^3-configurations, respectively.

In the vicinity of the f^2-configuration, the first-order transition changes the values of n_{Γ_7} and n_{Γ_8} drastically. Therefore, we conclude that this is a kind of charge transfer transitions among f orbitals. On the analogy of a valence transition discussed by Watanabe, the charge transfer transition is valid for the present model because of the existence of inter-orbital interactions between the Γ_7 and Γ_8 orbital. Watanabe discussed the valence transition in the single-orbital Anderson model with an inter-orbital interaction between conduction and localized electrons U_{fc}. They suggested that the first-order phase transition appears in the case of finite U_{fc}. In the present model, the inter-orbital interactions between the Γ_7 and Γ_8 orbital play a similar role of U_{fc} that realizes the charge transfer transition.

It is interesting to point out that both the heavy QP behavior and the charge transfer transition arise around the f^3 configuration. While the Γ_8 orbital exhibits the heavy QP behavior, the Γ_7 orbital induces the charge transfer transition from an intermediate filling to a full filling.

Let us discuss the relation between the results at the f^2 configuration and the Γ_1 singlet ground state. Figure 4.11 shows several expectation values for occupations Φ_Γ at the CEF eigenstates Γ in the f^2 configuration. Other CEF eigenstates omitted in Fig. 4.11 takes smaller values than listed eigenstates. After the charge-transfer transition, only the Φ_{Γ_1} increases toward 1 at the f^2 configuration. Therefore, we call this electron state as "CEF singlet state", which is one of the localized f-electron states.

In the case of $U = 2.5D$, the eigenstate of Γ_1 singlet is written as:

$$|\Gamma_1\rangle = \alpha|\,(11)_{\Gamma_7}\,(00)_{\Gamma_{81}}\,(00)_{\Gamma_{82}}\rangle + \beta|\,(00)_{\Gamma_7}\,(11)_{\Gamma_{81}}\,(00)_{\Gamma_{82}}\rangle + \gamma|\,(00)_{\Gamma_7}\,(00)_{\Gamma_{81}}\,(11)_{\Gamma_{82}}\rangle, \quad (4.11)$$

where $\alpha = -0.85$ and $\beta = \gamma = 0.37$. One might think that n_ν should reflect the ratio of the coefficients α, β, and γ: $n_{\Gamma_7}/n_{\Gamma_8} = \alpha^2/2\beta^2$. Since the RISB saddle point approximation treats

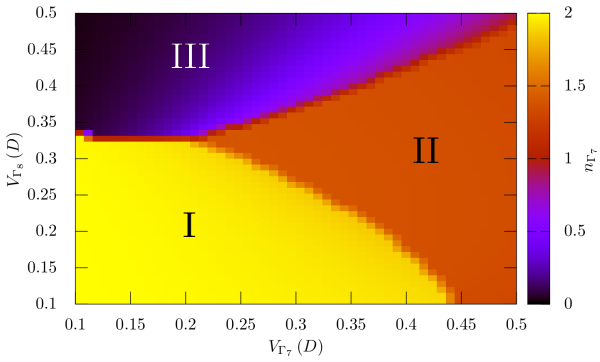

Figure 4.12: Number of electrons on Γ_7 orbital against V_{Γ_7} and V_{Γ_8}. Three phases are denoted as phase I, II, and III.

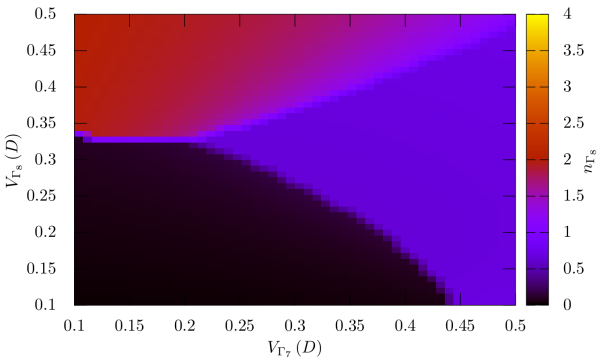

Figure 4.13: Number of electrons on Γ_8 orbital against V_{Γ_7} and V_{Γ_8}.

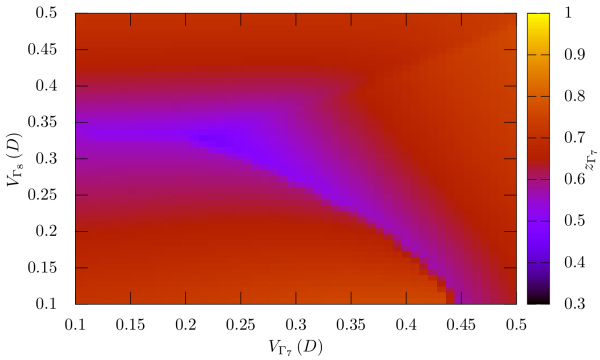

Figure 4.14: Renormalization factor of Γ_7 orbital against V_{Γ_7} and V_{Γ_8}.

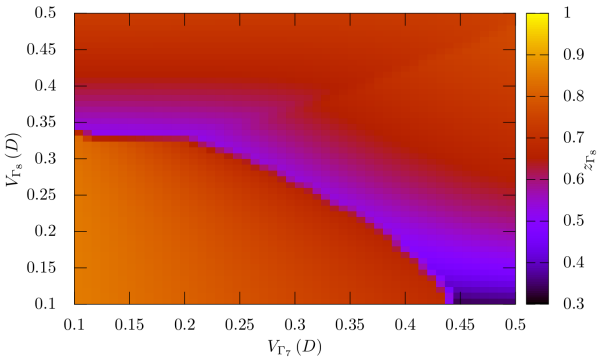

Figure 4.15: Renormalization factor of Γ_8 orbital against V_{Γ_7} and V_{Γ_8}.

all the localized CEF eigenstates as mean values, the above assumption does not hold in the present approximation. The present approximation considers only the coherent part describing an itinerant behavior of the f electron. In addition, there are no constraint conditions that the number of electrons at the coherent part should coincide with those at the incoherent part describing the localized behavior of the f electrons. Hence, the mismatch of the electron number from the Γ_1 eigenstate is an artificial phenomenon due to the RISB saddle point approximation. Other calculations that can consider both the coherent and incoherent part may recover the mismatch. However, the fact that realizing "CEF singlet state" at the f^2 configuration never changes even in the other approximations.

4.1.2 Anisotropic hybridization effect around f^2-configuration

This subsection evaluates an anisotropic hybridization effect at the f^2 configuration and compares with the results of the impurity Anderson model [80]. In the following discussion, we fix $E_f = -3.3D$ and $U = 2.0D$ and change V_{Γ_7} and V_{Γ_8} from $0.1D$ to $0.5D$. Note that n_f varies from 1.9 to 2.1 in this parameter range.

Figures 4.12 and 4.13 show the number of electrons on each orbital as a function of V_{Γ_7} and V_{Γ_8}. These figures indicate three phases: phase I, phase II, and phase III (see Fig. 4.12).

Phase I corresponds to the CEF-singlet state, which appears in the previous section with strong U cases. In this phase, the Γ_7 orbital is full filling, while the Γ_8 orbitals is empty. Because energy levels of both orbitals are positioned far from the chemical potential, this state can regard as a localized f-electron state.

Phase II is an itinerant state because all the n_ν values take intermediate fillings, i.e., $n_{\Gamma_7} \approx 1.5$ and $n_{\Gamma_8} \approx 0.5$. Figures 4.14 and 4.15 show the renormalization factor z_ν. These figures indicate that all the renormalization factors are not suppressed in phase II. These two phases correspond to the CEF-singlet and the Kondo-Yosida singlet states observed in the impurity Anderson model.

On the contrary, phase III behaves different from the CEF-triplet state in the impurity Anderson model. While the CEF-triplet state is a localized f-electron state, this phase exhibits an itinerant f-electron behavior on the Γ_8 orbital. Since the Γ_8 orbital has a four-fold-degeneracy, phase III indicates that the Γ_8-orbital is a half-filling. We note that the origin of the transition between phase III and other phases are not a charge transfer transition but a level crossing of the two effective energy levels: λ_{Γ_7} and λ_{Γ_8}. This transition is also a first-order transition.

The different properties at phase III from the previous works indicate that the CEF states taking into account the previous works are insufficient. Hence, the CEF triplet state suggested in the NRG calculation is considered to be an artificial phase.

Note that the present model ignores inter-orbital hybridizations, while those for Γ_8 orbitals are essential according to a group theory. Hence, it is possible that phase III shows different behavior due to taking into account the inter-orbital hybridizations. However, we do not consider this problem because UBe_{13} is assumed to be located at the boundary between phase I and II nearby phase III.

At $V_{\Gamma_7} = 0.2D$ and $V_{\Gamma_8} = 0.33D$, we find a critical point where three phases compete with each other. Since phase transitions may be overestimated because of the saddle point approximation, it is possible that a NFL arises around the critical point. Further approaches beyond the saddle point approximations are necessary to discuss the NFL.

4.2 Γ_4 non-Kramers singlet state in hexagonal symmetry

In this section, we show the result of the Γ_4 singlet ground state system. As we mentioned in chapter 1, UPt_3 is expected as the f^2-configuration system with this ground state. This compound attracts much attention owing to a spin-triplet SC. Both experimental and theoretical works have been carried out in order to reveal the origin of this SC.

While phenomenological studies have been carried out intensively to determine a gap symmetry of the SC, few theoretical studies based on a microscopic model have been carried out. This is because of the absence of appropriate theoretical approaches that can estimate a SC gap symmetry under the renormalized heavy f-electrons.

Several theoretical studies have evaluated a SC gap symmetry based on microscopic model Hamiltonian [81, 82], while these studies do not consider the renormalization of f-electrons. Nomoto *et al.* evaluated the electronic structure of UPt_3 based on the first-principles theoretical approach and evaluated the SC gap symmetry by means of second-order perturbation theory. Two SC gap symmetry, E_{1u} and E_{2u}, are realized in their results. In addition, they confirmed that both of the SC gap states are consistent with several experimental results [30, 83]. Since the Fermi surface structure evaluated by a de Haas-van Alphen (dHvA) effect is in good agreement with that calculated by first-principles theoretical approaches [84, 85, 86, 87, 88, 82, 89, 90, 91, 92, 83], their results shed new lights on the SC of UPt_3.

Meanwhile, the effect of heavy f-electrons to the SC state is yet unclear. UPt_3 is one of the heavy electron systems, which have itinerant f-electrons with enhanced effective mass at the Fermi energy [93]. It is obvious that first-principle calculations cannot evaluate such an enhanced effective mass. In addition, the large jump of a specific heat at the transition temperature indicates the heavy electron superconductivity [94]. Therefore, the heavy electrons of UPt_3 strongly contribute to the SC of UPt_3.

In this sense, it is crucial to identify f-orbitals providing heavy electrons in UPt_3. In chapter 2.4, we list three orbitals in hexagonal symmetry: Γ_7, Γ_8, and Γ_9. Several theoretical studies pointed out that an effective mass of the Γ_9 orbital is not enhanced in the case of Γ_4 singlet ground state systems by means of a KRSB saddle point approximation[40, 41]. As we remarked in chapter 3, however, the KRSB formalism cannot be applied to general multi-orbital systems in principle. Therefore, evaluating QP states based on the periodic Anderson model by using the RISB formalism is important to identify which orbitals affect the SC.

The model Hamiltonian for this system is derived in eqs. (2.1), (2.4), and (2.28). Throughout in this section, we set total number of electrons $N = 4$, spin-orbit coupling $\lambda_{ls} = 0.5D$, and CEF parameters $B_{20} = 0.003D$, $B_{40} = -0.0002D$, $B_{60} = 0.00005D$, and $B_{66} = -0.002D$. The local energy scheme with these parameters are shown in chapter 2.4 (see Figs. 2.2 and 2.4. According to the parameter set, the energy gap between Γ_4 ground state and Γ_3 first-excited state on f^2-configuration is $0.0276D$.

In this section, we employ the three-orbital periodic Anderson model derived in chapter 2 (see eqs. (2.1) and (2.3) and evaluate this model by using a RISB saddle point approximation. In hexagonal symmetry, elements ν of the set $\mathcal{N}$ are listed in chapter 2.4: Γ_{+7}, Γ_{-7}, Γ_{+8}, Γ_{-8}, Γ_{+9}, and Γ_{-9}. Following representations are used in this chapter.

$$\lambda_{\Gamma_{+i}} = \lambda_{\Gamma_{-i}} = \lambda_{\Gamma_i}, \tag{4.12}$$

$$z_{\Gamma_{+i}} = z_{\Gamma_{-i}} = z_{\Gamma_i}, \tag{4.13}$$

$$n_{\Gamma_{+i}} + n_{\Gamma_{-i}} = n_{\Gamma_i}, \tag{4.14}$$

where i takes 7, 8, and 9.

4.2.1 Quasi particle properties around f^2-configuration system

In this subsection, we first discuss E_f dependence of this system with various values of U under isotropic hybridizations, $V_{\Gamma_7} = V_{\Gamma_8} = V_{\Gamma_9} = 0.2D$. Figure 4.16 shows number of total f-electrons n_f against E_f. Since present calculations fix the total number of electrons as $N = 4$, Figure 4.16 exhibits a similar behavior to the case of cubic symmetry except for the vicinity of f^2 and f^3 configurations: numerical calculation does not converge in this region. We will

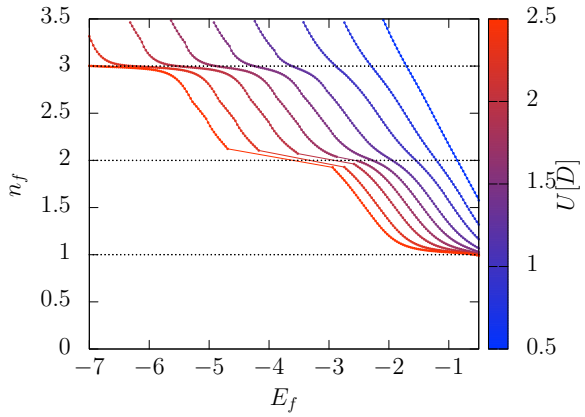

Figure 4.16: Number of total f-electrons n_f against E_f with various values of U.

discuss the different behavior in the following discussion. Note that the first-order transitions occur only around the f^3-configuration different from the case of Γ_1.

Hereafter, we discuss the number of electrons n_ν, the renormalization factor z_ν, the QP energy level measured from the chemical potential $\lambda_\nu - \mu$, and density of state ρ_ν against n_f (instead of E_f) with various values of U. Each results are shown in Figs. 4.17, 4.18, 4.19, and 4.20, respectively.

In the vicinity of the f^1-configuration, the Γ_7 orbital exhibits heavy electrons in strong U region. The rest of two orbitals, Γ_8 and Γ_9, appear far away from the chemical potential. This behaviors indicate that a single-orbital periodic Anderson model is valid as an effective model Hamiltonian at the f^1-configuration.

Jumps around $n_f \sim 1.5$ and $n_f \sim 2.3$ indicate a Lifshitz transition that changes the Luttinger volume of this system because ρ_{Γ_7} becomes 0 after the jump. Namely, lower Γ_7 band $\mathcal{E}^-_{\boldsymbol{k}\Gamma_{\pm 7}}$ which is defined in eq. (3.74) does not affect Fermi surface; i.e., $\mathcal{E}^-_{\boldsymbol{k}\Gamma_{\pm 7}} < \mu$. This jump obviously depends on the structure of the present model Hamiltonian. Hence, we do not focus on the Lifshitz transition in this thesis.

In the vicinity of the f^2-configuration, both the Γ_7 and Γ_8 orbitals form heavy electrons with increasing U, while the Γ_9 orbital appears far away from the chemical potential.

The numerical calculation does not converge in the vicinity of $n_f = 2$ in the range of $U > 1.5D$, as mentioned with regards Fig. 4.16. The similar behaviors have been reported from the study of a multi-orbital Hubbard model by means of the RISB saddle point approximation [56]. The calculation suggests a first-order Mott transition, in which z_ν becomes zero. A Mott insulating state should not appear in the present Anderson model due to existing conduction bands, we call this transition as a first-order Brinkmann-Rice transition in this thesis.

The mass enhancement at the f^2-configuration is smaller than the that at the f^1-configuration in the present model for the reason that the first-order Brinkmann-Rice transition prevent the mass enhancement.

However, we note that further mass enhancement at the f^2-configuration can be obtained by considering other model Hamiltonians: such as a single conduction band model with three f-orbitals. Miyake and Kohno discussed the single conduction band model [95]. They pointed out there are two origins for the mass enhancement at the f^2-configuration: a suppression of renormalization factor and a flat dispersion sandwiched with λ_{Γ_7} and λ_{Γ_8}. Since the present

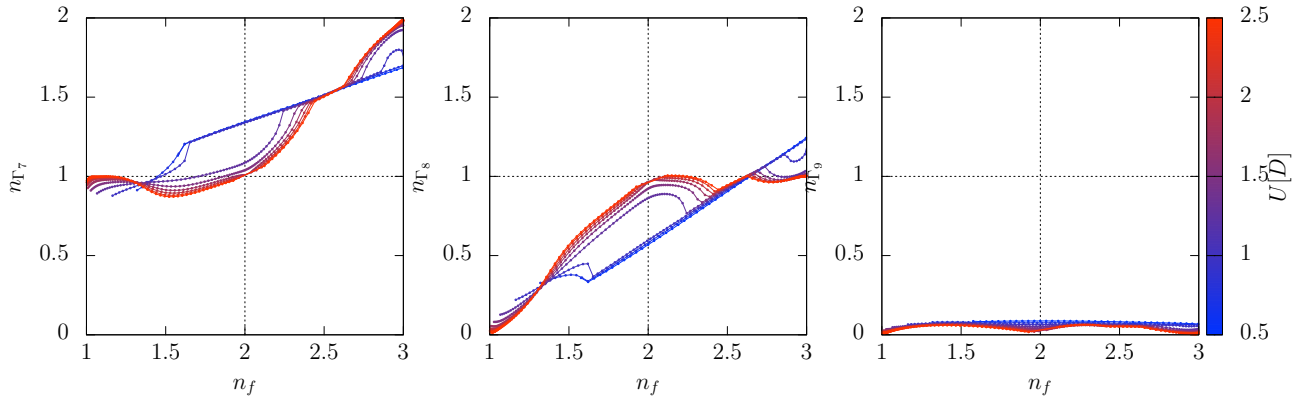

Figure 4.17: Number of electrons against n_f with various values of U for the case of Γ_7 (a), Γ_8 (b), and Γ_9 (c).

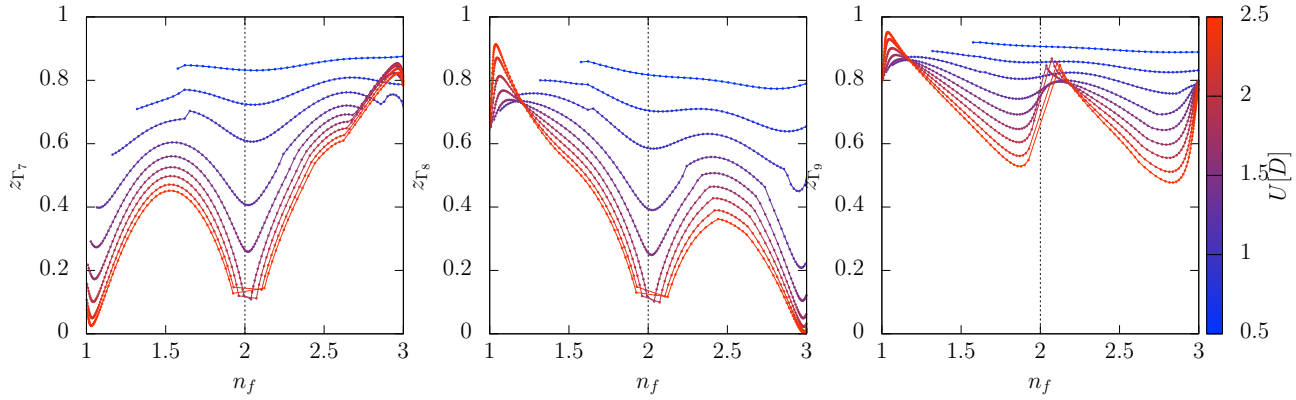

Figure 4.18: Renormalization factor against n_f with various values of U for the case of Γ_7 (a), Γ_8 (b), and Γ_9 (c).

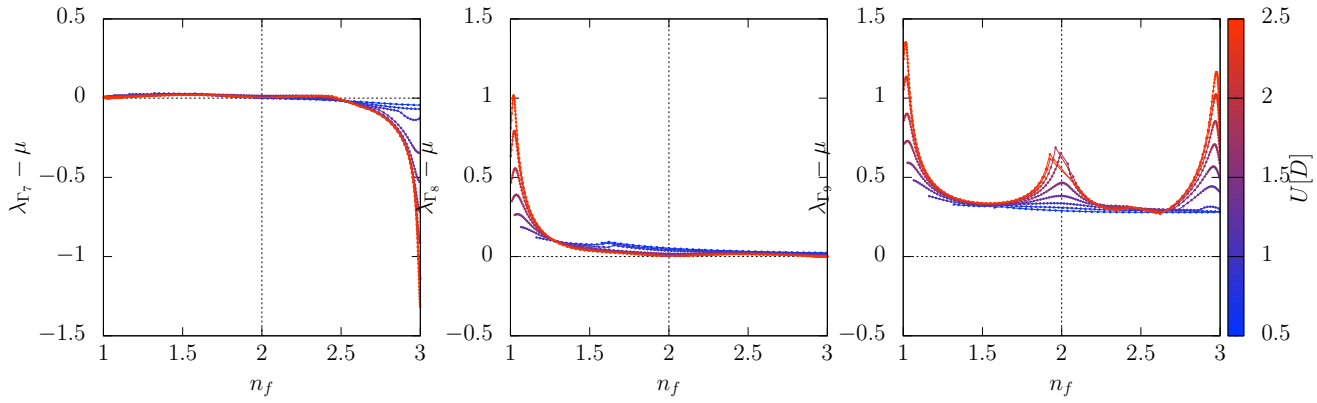

Figure 4.19: QP energy levels measured from the chemical potential against n_f with various values of U for the case of Γ_7 (a), Γ_8 (b), and Γ_9 (c).

model Hamiltonian cannot evaluate the latter, we expect that a mass enhancement in a realistic model is larger than that in the present model.

There are another transitions around $n_f \sim 2.6$. This transitions indicate is a kind of the

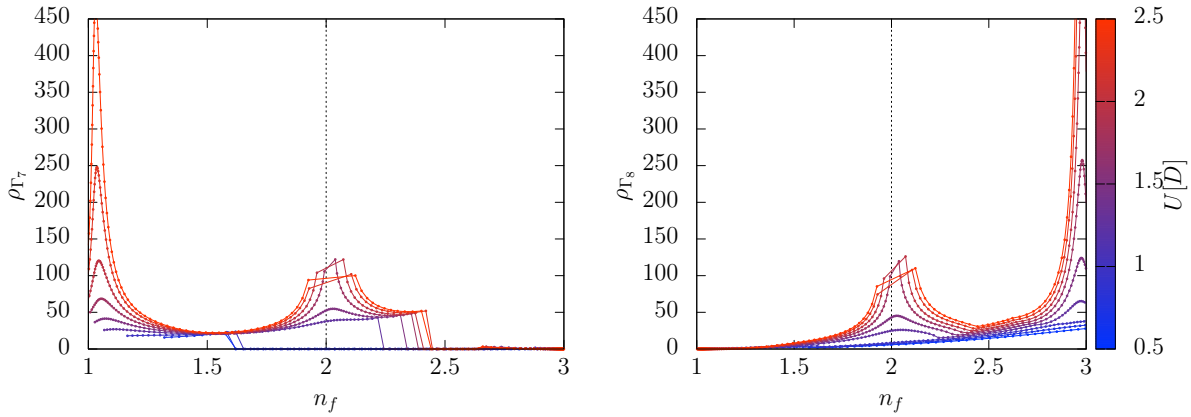

Figure 4.20: Density of states at the chemical potential with various values of U for the case of Γ_7 (a), Γ_8 (b). We omit the DOS of the Γ_9 orbital because this orbital does not shows clear enhancement.

charge transfer transition as mentioned in the case of cubic symmetry, because n_{Γ_7} approaches to fully occupied state after the transition. Such transitions are allowed because of the existence of the inter-orbital interactions analogous to the valence-transition system [96].

Let us discuss why totally different behaviors are obtained in the Γ_4 singlet ground state system in comparison with the Γ_1 singlet ground state. As we mentioned in the previous section, Eigenstate of the Γ_1 is written in eq. (4.11), while that of the Γ_4 state is written as,

$$|\Gamma_4\rangle = \frac{1}{\sqrt{2}}\left(|\,(10)_{\Gamma_7}\,(10)_{\Gamma_8}\,(00)_{\Gamma_9}\rangle - |\,(01)_{\Gamma_7}\,(01)_{\Gamma_8}\,(00)_{\Gamma_9}\rangle\right). \tag{4.15}$$

Here, the Γ_4 state consists of a linear combination of the half-filling orbitals. The half-filling state indicates that the renormalized energy levels are close to the chemical potential; i.e., forming heavy QP states.

On the other hand, the Γ_1 state consists of a linear combination of the full filled orbitals. The full filled orbital indicates that the renormalized energy level is far below the chemical potential and do nothing to the Fermi surface.

As a result, we find that totally different behavior arises from the configuration of the eigenstate: one produces heavy QP states and first-order transition due to the Brinkmann-Rice transition, and the other produces the charge transfer transition.

4.2.2 Quasi particle properties of mixed valence state

In the previous subsection, we discussed the E_f dependence of this system with several values of U under the condition $V_{\Gamma_7} = V_{\Gamma_8} = V_{\Gamma_9} = 0.2D$ and pointed out that heavy electrons arise in the case of integer fillings. However, the f-electron valency in UPt_3 is assumed as a mixed-valence in between the f^2 and f^3-configurations [87, 82]. Hence, the above discussion cannot be applied to UPt_3 directly.

In order to evaluate the heavy electrons in a mixed-valence region, let us discuss the effect of anisotropic hybridizations in this subsection. We fix $U = 2.5D$ and $E_f = -5.115D$ to adjust $n_f = 2.5$ in the case of $V_{\Gamma_7} = V_{\Gamma_8} = V_{\Gamma_9} = 0.2D$. Figures 4.21 shows the n_ν, z_ν, and $\lambda_\nu - \mu$ dependence as a function of V_{Γ_9} with several sets of V_{Γ_7} and V_{Γ_8}: (i) $V_{\Gamma_7} = V_{\Gamma_8} = 0.2D$, (ii)

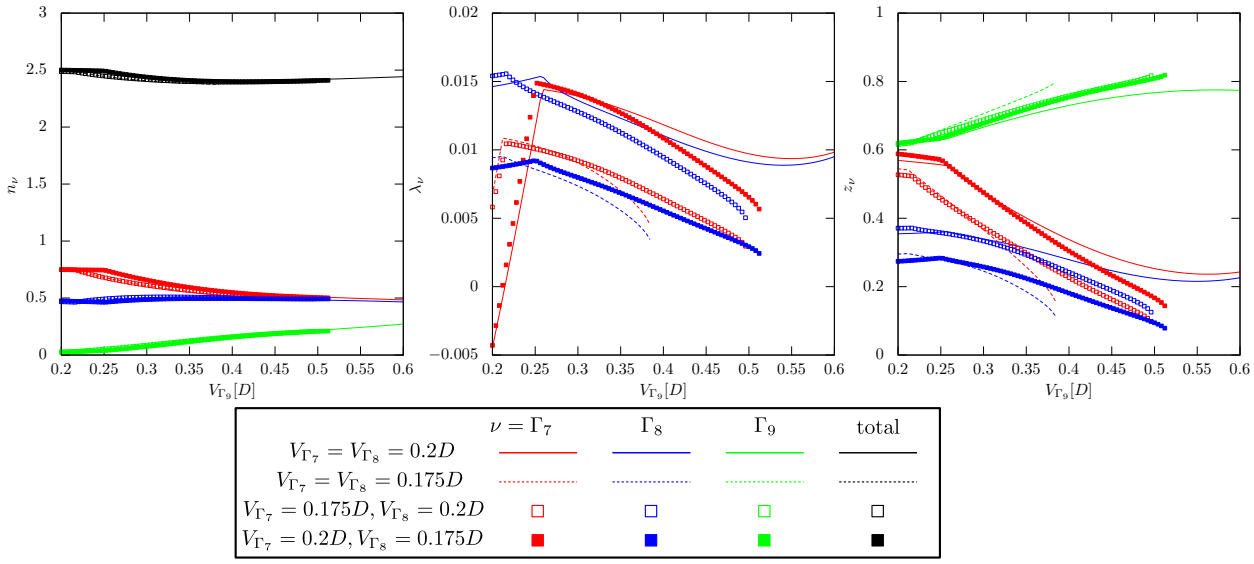

Figure 4.21: Number of electrons (left), QP energy level (center), and renormalization factor (right) against V_{Γ_9} with several values of V_{Γ_7} and V_{Γ_8}.

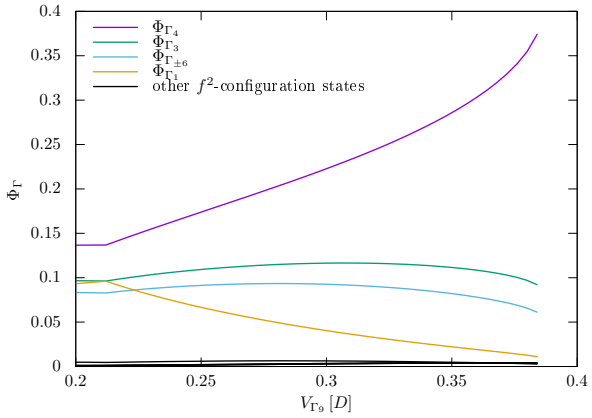

Figure 4.22: Expectation value of the occupation of each localized state in the f^2-configuration against V_{Γ_9} in the case of $V_{\Gamma_7} = V_{\Gamma_8} = 0.175D$.

$V_{\Gamma_7} = V_{\Gamma_8} = 0.175D$, (iii) $V_{\Gamma_7} = 0.175D, V_{\Gamma_8} = 0.2D$, and (iv) $V_{\Gamma_7} = 0.2D, V_{\Gamma_8} = 0.175D$. Here, we do not plot the $\lambda_{\Gamma_9} - \mu$ because this value is far away the rest of two energy levels. A black line in Fig. 4.21 indicates that n_f holds around 2.5 in this calculation.

In the case of (i), solid lines, a kink at $V_{\Gamma_9} \sim 0.25D$ is a Lifshitz transition for the Γ_7 orbital. After the transition, the Γ_7 and Γ_8 orbitals develop heavy electrons toward $V_{\Gamma_9} = 0.55D$. This behavior can be explained as follows. In the case of the isotropic hybridizations, f-electron occupations reflect the energy level E_ν: f-electrons prefer to occupy the Γ_7 and Γ_8 states than the Γ_9 state. As V_{Γ_9} increases, an electron occupation of the Γ_9 orbital increases because of a energy gain of a kinetic energy. Then, number of electrons at the Γ_7 and Γ_8 orbitals approaches to integer fillings. As a result, both the Γ_7 and Γ_8 states tend to exhibit heavy electrons. Note that case (i) does not show 1st-order Brinkmann-Rice transition since the large Γ_9 hybridization effectively increases the rest of two hybridizations.

Case (ii), broken lines, considers smaller hybridizations of V_{Γ_7} and V_{Γ_8} than those of case (i). In this case, 1st-order Brinkmann-Rice transition occurs at $V_{\Gamma_9} = 0.38D$. The upturn behavior similar to the case (i) should also exist in large V_{Γ_9} region, however, we do not plot in this thesis.

Cases (iii), open square, and (iv), filled square, consider anisotropic hybridizations of V_{Γ_7} and V_{Γ_8}. Since both the 1st-order transitions occur at the same points, $V_{\Gamma_9} \sim 0.52D$, the difference between V_{Γ_7} and V_{Γ_8} is insensitive to form heavy electrons in mixed-valence region.

According to case (i) to (iv), we conclude that the Γ_7 and Γ_8 orbitals produce heavy electrons in the case of large V_{Γ_9} and that the Γ_9 orbital cannot be a heavy electron in the case of the Γ_4 singlet ground state.

Let us verify that the heavy electrons in the mixed-valence region strongly relate to the Γ_4 ground state of the f^2-configuration. Figure 4.22 exhibits Φ_Γ for several CEF states of the f^2-configuration in case (ii). Other states that do not list in Fig. 4.22 takes small values comparing with these five states. As V_{Γ_9} increases, it is obvious that only the occupation of the Γ_4 ground state increases. Therefore, even in the mixed-valence region, the heavy electrons strongly relates to the Γ_4 ground state.

As a result, we conclude that the mass enhancement of UPt_3 is given by both the Γ_7 and Γ_8 orbitals (if Γ_4 singlet ground state is realized). Although the Γ_9 orbital also appears at the Fermi surface, this orbital cannot form heavy electrons.

At the end of this section, let us consider the origin of the SC in UPt_3. First-principles calculation suggested that small Fermi surface mainly composed of $j = 3/2$ namely a Γ_9 orbital induces a ferromagnetic spin susceptibility [82]. The ferromagnetic spin susceptibility considered as a driving force of a spin-triplet SC in UPt_3 [81, 82].

However, the present calculation revealed that electrons on the Γ_9 orbital cannot be heavy. Since electrons on the Γ_9 orbital are not strongly renormalized, these electrons may not contribute to the SC in the sense of heavy electron systems.

Thus far, we expect two scenarios for the origin of the SC: one is owing to the ferromagnetic spin susceptibility with light electrons, namely electrons on the Γ_9 orbital, and the another is owing to some other instability on heavy electrons, namely those on the Γ_7 and Γ_8.

In the heavy electron system, it is expected that heavy electrons play an significant role for the SC. In this sense, the SC gap on the Γ_9 orbital is expected to be small in comparison with that on the Γ_7 and Γ_8 orbitals. This is because the gap on the Γ_9 orbital opens indirectly through to the hybridization effect.

In order to identify the origin, it is necessary to evaluate the renormalized electron-electron interactions. Introducing Gaussian fluctuations from the saddle point enables us to discuss the effect of interactions. Further studies based on the RISB formalism may shed light on the origin of the SC in UPt_3.

Chapter 5

Conclusion

In this thesis, we discussed the heavy Fermi liquid state on the f^2-configuration with the two singlet ground states: the Γ_1 singlet ground state and the Γ_4 singlet ground state. We constructed effective Hamiltonians for these models. In particular, we proposed the effective three-orbital Hamiltonian with finite spin-orbit coupling in hexagonal symmetry.

We suggested the RISB foramslism, which mainly used in Hubbard model, can shed light on the f^2-configration systems, and analyzed these Hamiltonians by means of the RISB saddle point approximation.

As a result, it is revealed that these two systems show totally different behaviors. In the case of the Γ_1 singlet ground state, there are three possible phases competing at the f^2-configuration: phase I, CEF singlet state; phase II, itinerant state (Kondo-Yosida singlet state); and phase III, new itinerant state composed of Γ_8 orbital. In the case of the Γ_1 singlet ground state, We pointed out that phase III shows totally different properties from the previous studies suggesting the CEF triplet state. The CEF triplet state may be an artificial state since previous studies omit CEF eigenstates.

On the other hand, the Γ_4 singlet ground state exhibits a first-order Brinkmann-Rice transition. We confirmed that these different behaviors depend on a configuration of these singlet ground state. Namely, Γ_1 singlet state consists of a linear combination of the fully-occupied orbitals, while Γ_4 singlet state consists of a linear combination of the two half-filled orbitals.

We also discussed heavy electron behaviors in the mixed-valence region in hexagonal symmetry. This result suggests that electrons on the Γ_7 and Γ_8 orbitals can be heavy in the case of $V_{\Gamma_7} \approx V_{\Gamma_8} < V_{\Gamma 9}$, while electrons on the Γ_9 orbital cannot be heavy in any region when the ground state at the f^2-configuration is the Γ_4 state. This result indicates that the career of the SC in UPt_3 are electrons on the Γ_7 and Γ_8 orbitals.

This thesis focus on the RISB saddle point approximation, although further approaches that can go beyond the saddle point approximation are necessary to discuss (i)the NFL nearby the critiical point in cubic symmetry and (ii) the SC in hexagonal symmetry. We expect that introducing Gaussian fluctuations from the saddle point values is significant for disucssing above behaviors. That being said, present thesis shed new light on the long-standing problems of UBe_{13} and UPt_3.

Acknowledgement

I would like to express my sincere gratitude to Prof. Kazumasa Miyake, Prof. Masao Ogata for their invaluable advice and continual encouragement throughout the course of this work. I am grateful to Dr. Atsushi Tsuruta and Prof. Seiji Miyashita for a lot of helpful advice and discussions. I would like to appreciate all colleagues of Miyake laboratory, Ogata laboratory, and Miyashita laboratory. Finally, I thank my family for their great supports and encouragements.

Appendix A

Validity of constraint conditions

In this appendix, we discuss the validity of constraint conditions eqs. (3.42) and (3.45). Eq. (3.42) excludes all the states except for the single boson states written as,

$$|\underline{C}\rangle = \sum_{pq\in\mathfrak{F}} W_{pq}\phi^\dagger_{Cp}|\mathrm{vac}\rangle_b \otimes |q\rangle_f, \tag{A.1}$$

in the enlarged Hilbert space. Here, C represents one of the states in the original Hilbert space. Since W_{pq} is not determined, there are an arbitrariness to describe the original state $|C\rangle$ in the enlarged Hilbert space. According to eqs. (3.37) or (3.38), eq. (A.1) should be uniquely determined as $W_{pq} = w\delta_{pq}$ where w is a normalization factor.

Let us show that the constraint condition (3.45),

$$f^\dagger_\nu f_{\nu'} = \sum_{nml\in\mathfrak{F}} {}_f\langle l|f^\dagger_\nu f_{\nu'}|m\rangle_f \phi^\dagger_{nm}\phi_{nl}, \tag{A.2}$$

does give the relation $W_{pq} = w\delta_{pq}$. Performing the left hand side (lhs) of the constraint eq. (A.2) to eq. (A.1) gives,

$$\begin{aligned} f^\dagger_\nu f_{\nu'}|\underline{C}\rangle &= \sum_{pq\in\mathfrak{F}} W_{pq}\phi^\dagger_{Cp}|\mathrm{vac}\rangle \otimes f^\dagger_\nu f_{\nu'}|q\rangle_f \\ &= \sum_{pqm\in\mathfrak{F}} {}_f\langle m|f^\dagger_\nu f_{\nu'}|q\rangle_f W_{pq}\phi^\dagger_{Cp}|\mathrm{vac}\rangle \otimes |m\rangle_f. \end{aligned} \tag{A.3}$$

On the other hand, the right hand side of the constraint eq. (A.2) changes eq. (A.1) as,

$$\begin{aligned} \sum_{nml\in\mathfrak{F}} {}_f\langle l|f^\dagger_\nu f_{\nu'}|m\rangle_f \phi^\dagger_{nm}\phi_{nl}|\underline{C}\rangle &= \sum_{nmlpq\in\mathfrak{F}} {}_f\langle l|f^\dagger_\nu f_{\nu'}|m\rangle_f W_{pq}\phi^\dagger_{nm}\phi_{nl}\phi^\dagger_{Cp}|\mathrm{vac}\rangle \otimes |q\rangle_f \\ &= \sum_{mpq\in\mathfrak{F}} {}_f\langle p|f^\dagger_\nu f_{\nu'}|m\rangle_f W_{pq}\phi^\dagger_{Cm}|\mathrm{vac}\rangle \otimes |q\rangle_f \\ &= \sum_{pqm\in\mathfrak{F}} {}_f\langle q|f^\dagger_\nu f_{\nu'}|p\rangle_f W_{qm}\phi^\dagger_{Cp}|\mathrm{vac}\rangle \otimes |m\rangle_f, \end{aligned} \tag{A.4}$$

where the last expression changes the indices: $m \to p$, $p \to q$, and $q \to m$. Because eqs. (A.3) and (A.4) should be equivalent to each state $\phi^\dagger_{Cp}|\mathrm{vac}\rangle \otimes |m\rangle_f$, the constraint (A.2) provides the

following relation:

$$\sum_q {}_f\langle m|f_\nu^\dagger f_{\nu'}|q\rangle_f W_{pq} = \sum_q {}_f\langle q|f_\nu^\dagger f_{\nu'}|p\rangle_f W_{qm}. \tag{A.5}$$

This relation should be held in all the combination of the orbital indices ν and ν'. In the case of $\nu = \nu'$, eq. (A.5) becomes

$${}_f\langle m|f_\nu^\dagger f_\nu|m\rangle_f W_{pm} = {}_f\langle p|f_\nu^\dagger f_\nu|p\rangle_f W_{pm}. \tag{A.6}$$

In order to satisfy this relation, $W_{pm} = 0$ unless,

$${}_f\langle m|f_\nu^\dagger f_\nu|m\rangle_f = {}_f\langle p|f_\nu^\dagger f_\nu|p\rangle_f. \tag{A.7}$$

Since, this relation should be held in all the orbital indices ν, it is obvious that only the case $|m\rangle_f = |p\rangle_f$ can produce finite W_{pm}:

$$W_{pm} = w_p^C \delta_{pm}, \tag{A.8}$$

where w_p^C is a coefficient of the $\phi_{Cp}^\dagger|\text{vac}\rangle_b \otimes |p\rangle_f$ state in $|\underline{C}\rangle$:

Substituting eq. (A.8) into eq. (A.5), we obtain the following relation:

$$w_{pf}\langle m|f_\nu^\dagger f_{\nu'}|p\rangle_f = w_{mf}\langle m|f_\nu^\dagger f_{\nu'}|p\rangle_f. \tag{A.9}$$

This relation ensures that all the states in the same electron configurations should give same coefficient w. In order to normalize the state $|\underline{C}\rangle$, eq. (A.10) is uniquely determined as,

$$|\underline{C}\rangle = \frac{1}{\sqrt{D_C}} \sum_p \phi_{Cp}^\dagger|\text{vac}\rangle \otimes |p\rangle_f, \tag{A.10}$$

where D_C is a normalization factor from the coefficient w.

As a result, by using constraint conditions eqs. (3.42) and (3.45), all the excess states are excluded and only the physical states eqs. (3.37) or (3.37) remains.

Appendix B

derivation of local energy

In this appendix, we show that the definition of the "creation" operator on eq. (3.58) can derive the localized Hamiltonian (3.46) in the RISB formalism from the original localized Hamiltonian:

$$\mathcal{H}_{\rm loc} = \sum_{\nu\in\mathcal{N}} E_\nu f_\nu^{\rm phys\dagger} f_\nu^{\rm phys} + \sum_{\nu_1\nu_2\nu_3\nu_4\in\mathcal{N}} I_{\nu_1\nu_2}^{\nu_3\nu_4} f_{\nu_4}^{\rm phys\dagger} f_{\nu_3}^{\rm phys\dagger} f_{\nu_2}^{\rm phys} f_{\nu_1}^{\rm phys}. \tag{B.1}$$

Namely, we can obtain eq. (3.46) by substituting the "creation" ("annihilation") operators ${}_{\rm sim}\underline{f}_\nu^{\rm phys\dagger}$ (${}_{\rm sim}\underline{f}_\nu^{\rm phys}$) into original creation (annihilation) operators $f_\nu^{\rm phys\dagger}$ ($f_\nu^{\rm phys}$).

First, we show the following relation:

$${}_{\rm sim}\underline{f}_\nu^{\rm phys\dagger}\,{}_{\rm sim}\underline{f}_{\nu'}^{\rm phys}|\underline{A}\rangle = \sum_{n_1 n_1' m_1\in\mathfrak{F}} \langle n_1|f_\nu^{\rm phys\dagger} f_{\nu'}^{\rm phys}|n_1'\rangle \phi_{n_1 m_1}^\dagger \phi_{n_1' m_1}|\underline{A}\rangle. \tag{B.2}$$

where $|\underline{A}\rangle$ is a physically meaningful states. Hereafter, we omit to describe $|\underline{A}\rangle$ explicitly. However, it is to be mention that several transformations in the following discussion are allowed only when we perform to the physically meaningful states.

Substituting eq. (3.58) into the lhs of eq. (B.2) becomes

$${}_{\rm sim}\underline{f}_\nu^{\rm phys\dagger}\,{}_{\rm sim}\underline{f}_{\nu'}^{\rm phys} = \sum_{n_1 n_2 m_1 m_2\in\mathfrak{F}} \sum_{n_1' n_2' m_1' m_2'\in\mathfrak{F}} \sum_{\nu_1\nu_2\in\mathcal{N}} C_{n_1 m_1}^{n_2 m_2}(\nu\nu_1)\, C_{n_1' m_1'}^{n_2' m_2'\dagger}(\nu'\nu_2)\, \phi_{n_1 m_1}^\dagger \phi_{n_2 m_2} \phi_{n_1' m_1'}^\dagger \phi_{n_2' m_2'} f_{\nu_1}^\dagger f_{\nu_2},$$

where,

$$C_{n_1 m_1}^{n_2 m_2}(\nu\nu_1) = \frac{\langle n_1|f_\nu^{\rm phys\dagger}|n_2\rangle_f \langle m_1|f_{\nu_1}^\dagger|m_2\rangle_f}{\sqrt{N_{n_1}\left(2N_{\rm orb} - N_{n_1} + 1\right)}}, \tag{B.3}$$

$$C_{n_1' m_1'}^{n_2' m_2'\dagger}(\nu'\nu_2) = \frac{\langle n_1'|f_{\nu'}^{\rm phys}|n_2'\rangle_f \langle m_1'|f_{\nu_2}|m_2'\rangle_f}{\sqrt{N_{n_2'}\left(2N_{\rm orb} - N_{n_2'} + 1\right)}}. \tag{B.4}$$

Using the commutation relation of the bosons and recall all the physically meaningful states are the single boson states; plural annihilation boson operators become zero. Eq. (B.3) is

transformed as,

$$
\begin{aligned}
{}_{\rm sim}\underline{f}^{\rm phys\dagger}_{\nu}\,{}_{\rm sim}\underline{f}^{\rm phys}_{\nu'} &= \sum_{n_1n_2m_1m_2\in\mathfrak{F}}\sum_{n_2'm_2'\in\mathfrak{F}}\sum_{\nu_1\nu_2\in\mathcal{N}} C^{n_2m_2}_{n_1m_1}\left(\nu\nu_1\right) C^{n_2'm_2'\dagger}_{n_2m_2}\left(\nu'\nu_2\right)\phi^\dagger_{n_1m_1}\phi_{n_2'm_2'}f^\dagger_{\nu_1}f_{\nu_2} \\
&= \sum_{n_1m_1\in\mathfrak{F}}\sum_{n_2'm_2'\in\mathfrak{F}}\sum_{\nu_1\nu_2\in\mathcal{N}} \frac{\langle n_1|f^{\rm phys\dagger}_{\nu}f^{\rm phys}_{\nu'}|n_2'\rangle_f\langle m_1|f^\dagger_{\nu_1}f_{\nu_2}|m_2'\rangle_f}{N_{n_1}\left(2N_{\rm orb}-N_{n_1}+1\right)}\phi^\dagger_{n_1m_1}\phi_{n_2'm_2'}f^\dagger_{\nu_1}f_{\nu_2}.
\end{aligned}
\tag{B.5}
$$

Here, we use the relation $N_{n_1} = N_{n_2'}$. Since the Hamiltonian is considered to perform to the physically meaningful states, the quadratic pseudo fermion terms can be transformed into quadratic boson terms through the constraint condition (3.45):

$$
\begin{aligned}
&\sum_{n_1m_1\in\mathfrak{F}}\sum_{n_3ll'\in\mathfrak{F}}\sum_{n_2'm_2'\in\mathfrak{F}}\sum_{\nu_1\nu_2\in\mathcal{N}} \frac{\langle n_1|f^{\rm phys\dagger}_{\nu}f^{\rm phys}_{\nu'}|n_2'\rangle_f\langle m_1|f^\dagger_{\nu_1}f_{\nu_2}|m_2'\rangle_f}{N_{n_1}\left(2N_{\rm orb}-N_{n_1}+1\right)}\langle l'|f^\dagger_{\nu_1}f^\dagger_{\nu_2}|l\rangle\phi^\dagger_{n_1m_1}\phi_{n_2'm_2'}\phi^\dagger_{n_3l}\phi_{n_3l'} \\
&= \sum_{n_1m_1\in\mathfrak{F}}\sum_{l'\in\mathfrak{F}}\sum_{n_2'm_2'\in\mathfrak{F}}\sum_{\nu_1\nu_2\in\mathcal{N}} \frac{\langle n_1|f^{\rm phys\dagger}_{\nu}f^{\rm phys}_{\nu'}|n_2'\rangle_f\langle m_1|f^\dagger_{\nu_1}f_{\nu_2}|m_2'\rangle_f}{N_{n_1}\left(2N_{\rm orb}-N_{n_1}+1\right)}\langle l'|f^\dagger_{\nu_1}f^\dagger_{\nu_2}|m_2'\rangle\phi^\dagger_{n_1m_1}\phi_{n_2'l'} \\
&= \sum_{n_1m_1\in\mathfrak{F}}\sum_{n_2'm_2'\in\mathfrak{F}}\sum_{\nu_1\nu_2\in\mathcal{N}} \frac{\langle n_1|f^{\rm phys\dagger}_{\nu}f^{\rm phys}_{\nu'}|n_2'\rangle\left({}_f\langle m_1|f^\dagger_{\nu_1}f_{\nu_2}|m_2'\rangle_f\right)^2}{N_{n_1}\left(2N_{\rm orb}-N_{n_1}+1\right)}\phi^\dagger_{n_1m_1}\phi_{n_2'm_1} \\
&= \sum_{n_1m_1\in\mathfrak{F}}\sum_{n_1'\in\mathfrak{F}}\langle n_1|f^{\rm phys\dagger}_{\nu}f^{\rm phys}_{\nu'}|n_1'\rangle\phi^\dagger_{n_1m_1}\phi_{n_1'm_1},
\end{aligned}
\tag{B.6}
$$

where we use the following relations:

$$
\sum_{m_2'\in\mathfrak{F}}\sum_{\nu_1\nu_2\in\mathcal{N}}\left(\langle m_1|f^\dagger_{\nu_1}f_{\nu_2}|m_2'\rangle\right)^2 = N_{m_1}\left(2N_{\rm orb}-N_{m_1}+1\right), \tag{B.7}
$$

$$
N_{m_1} = N_{n_1}. \tag{B.8}
$$

In the last line of eq. (B.6), we change $n_2' \to n_1'$. This equation corresponds to the lhs of the eq. (B.2). Likewise, the following relation also holds in this system:

$$
\begin{aligned}
{}_{\rm sim}\underline{f}^{\rm phys}_{\nu}\,{}_{\rm sim}\underline{f}^{\rm phys\dagger}_{\nu'} &= \sum_{n_1m_1\in\mathfrak{F}}\sum_{n_1'\in\mathfrak{F}}\langle n_1|f^{\rm phys}_{\nu}f^{\rm phys\dagger}_{\nu'}|n_1'\rangle\phi^\dagger_{n_1m_1}\phi_{n_1'm_1}, \\
&= \delta_{\nu\nu'} - {}_{\rm sim}\underline{f}^{\rm phys\dagger}_{\nu'}\,{}_{\rm sim}\underline{f}^{\rm phys}_{\nu}.
\end{aligned}
\tag{B.9}
$$

Namely, the "creation" and the "annihilation" operator hold the anti-commutation relation.

Second, let us transform eq. (B.1) into slave boson formalism. By using eq. (B.2), the first term of eq. (B.1) becomes,

$$
\sum_{n_1n_1'm_1\in\mathfrak{F}}\sum_{\nu\in\mathcal{N}}\langle n_1|f^{\rm phys\dagger}_{\nu}f^{\rm phys}_{\nu}|n_1'\rangle E_\nu\phi^\dagger_{n_1m_1}\phi_{n_1'm_1}. \tag{B.10}
$$

While, the second term is written as,

$$\begin{aligned}
&\sum_{\nu_1\nu_2\nu_3\nu_4\in\mathcal{N}} I^{\nu_3\nu_4}_{\nu_1\nu_2}\left(\delta_{\nu_2,\nu_3} f^{\text{phys}\dagger}_{\nu_4} f^{\text{phys}}_{\nu_1} - f^{\text{phys}\dagger}_{\nu_4} f^{\text{phys}}_{\nu_2} f^{\text{phys}\dagger}_{\nu_3} f^{\text{phys}}_{\nu_1}\right)\\
&\to \sum_{\nu_1\nu_2\nu_3\nu_4\in\mathcal{N}} \sum_{n_1 n_1' m_1\in\mathfrak{F}} I^{\nu_3\nu_4}_{\nu_1\nu_2}\Bigg[\delta_{\nu_2,\nu_3}\langle n_1| f^{\text{phys}\dagger}_{\nu_1} f^{\text{phys}}_{\nu_4}|n_1'\rangle \phi^\dagger_{n_1 m_1}\phi_{n_1' m_1}\\
&- \sum_{n_2 n_2' m_2\in\mathfrak{F}} \langle n_1| f^{\text{phys}\dagger}_{\nu_4} f^{\text{phys}}_{\nu_2}|n_1'\rangle\langle n_2| f^{\text{phys}\dagger}_{\nu_3} f^{\text{phys}}_{\nu_1}|n_2'\rangle \phi^\dagger_{n_1 m_1}\phi_{n_1' m_1}\phi^\dagger_{n_2 m_2}\phi_{n_2' m_2}\Bigg]\\
&= \sum_{\nu_1\nu_2\nu_3\nu_4\in\mathcal{N}} \sum_{n_1 m_1 n_1'\in\mathfrak{F}} I^{\nu_3\nu_4}_{\nu_1\nu_2}\langle n_1| f^{\text{phys}\dagger}_{\nu_4} f^{\text{phys}\dagger}_{\nu_3} f^{\text{phys}}_{\nu_2} f^{\text{phys}}_{\nu_1}|n_1'\rangle \phi^\dagger_{n_1 m_1}\phi_{n_1' m_1}. \qquad \text{(B.11)}
\end{aligned}$$

As a result, we obtain

$$\mathcal{H}_{\text{loc}} \to \underline{\mathcal{H}}_{\text{loc}} = \sum_{n_1 n_1' m_1\in\mathfrak{F}} E_{n_1 n_1'}\phi^\dagger_{n_1 m_1}\phi_{n_1' m_1}, \qquad \text{(B.12)}$$

where,

$$E_{n_1 n_1'} = \sum_{\nu\in\mathcal{N}}\langle n_1| f^{\text{phys}\dagger}_{\nu} f^{\text{phys}}_{\nu}|n_1'\rangle E_\nu + \sum_{\nu_1\nu_2\nu_3\nu_4\in\mathcal{N}}\langle n_1| f^{\text{phys}\dagger}_{\nu_4} f^{\text{phys}\dagger}_{\nu_3} f^{\text{phys}}_{\nu_2} f^{\text{phys}}_{\nu_1}|n_1'\rangle I^{\nu_3\nu_4}_{\nu_1\nu_2}. \qquad \text{(B.13)}$$

Appendix C

Construction of creation operators

In the saddle point approximation for the RISB formalism by using the simple expression eq. (3.58), unrealistic results are obtained in the case of uncorrelated system ($U = 0$) similer to one-orbital system in KRSB formalism. In the one-orbital system, Kotliar and Ruckenstein proposed the expression eq. (3.8) for $\underline{f}_{\nu}^{\dagger \mathrm{phys}}$ and pointed out the results of saddle point approximation by using eq. (3.8) correspond to Gutzwiller approximation. Lechermann and coworkers suggested that similar expressions from eq. (3.8) in the RISB is possible to obtain the same results of Gutzwiller approximation even in the multi-orbital system.

They first prepared the "natural orbital" (NO) basis that diagonalizes the particle density operator $\hat{\Delta}^p$ and hole oprator $\hat{\Delta}^h$ in the saddle point approximation. We denote the NO eigenvalue and eigenstate as ξ_ζ and $|\zeta\rangle$ which are defined as follows:

$$\hat{\Delta}^p_{\nu\nu'} = \sum_{\zeta} \xi_\zeta \langle \nu|\zeta\rangle\langle\zeta|\nu'\rangle,$$
$$|\zeta\rangle = \sum_{\nu} \langle\zeta|\nu\rangle|\nu\rangle. \tag{C.1}$$

where ξ_ζ is classical value in the case of the saddle point approximation.

By using this basis, quasiparticle fermion operator $f_\zeta^\dagger$ are also transformed as,

$$f_\zeta^\dagger = \sum_{\nu} \langle\zeta|\nu\rangle f_\nu^\dagger, \tag{C.2}$$
$$\langle f_\zeta^\dagger f_{\zeta'}\rangle = \xi_\zeta \delta_{\zeta\zeta'} \tag{C.3}$$

The set of quasi particle operator in NO basis $\boldsymbol{f}^{\dagger\zeta} = \left\{ f_{\zeta_1}^\dagger, f_{\zeta_2}^\dagger \dots \right\}$ and that in original basis $\boldsymbol{f}^{\dagger\nu} = \left\{ f_{\nu_1}^\dagger, f_{\nu_2}^\dagger \dots \right\}$ are related by the rotation matrix $\hat{U}^{\zeta\nu}$ as $\boldsymbol{f}^{\dagger\zeta} = \hat{U}^{\zeta\nu}\boldsymbol{f}^{\dagger\nu}$.

By using operators in NO basis, the physical f-electron "creation" operator $\underline{f}_{\nu}^{\dagger \mathrm{phys}}$ According to the KRSB formalism, the saddle point approximation should gives the same result of Gutzwiller approximation when the "creation" operator is the following form:

$$\underline{f}_{\nu}^{\dagger \mathrm{phys}} = \sum_{\zeta AB\tilde{n}\tilde{m}} \frac{\langle A|f_\nu^{\dagger\mathrm{phys}}|B\rangle\langle\tilde{n}|f_\zeta^\dagger|\tilde{m}\rangle_f}{\sqrt{\xi_\zeta^{\mathrm{B}}\left(1-\xi_\zeta^{\mathrm{B}}\right)}} \phi_{A\tilde{n}}^\dagger \phi_{B\tilde{m}} f_\zeta^\dagger. \tag{C.4}$$

We now rotate back the eq. (C.4) to the original basis.

$$\begin{aligned}\underline{f}_{\nu}^{\dagger\mathrm{phys}} =& \sum_{\zeta AB\tilde{n}\tilde{m}} \sum_{nm\nu'\nu''} \langle\nu'|\zeta\rangle\langle\nu''|\zeta\rangle\langle n|\tilde{n}\rangle_f\langle\tilde{m}|m\rangle_f \frac{\langle A|f_{\nu}^{\dagger\mathrm{phys}}|B\rangle\langle\tilde{n}|f_{\nu'}^{\dagger}|\tilde{m}\rangle_f}{\sqrt{\xi_{\zeta}^{\mathrm{B}}\left(1-\xi_{\zeta}^{\mathrm{B}}\right)}}\phi_{An}^{\dagger}\phi_{Bm}f_{\nu''}^{\dagger} \\ =& \sum_{AB} \sum_{nm\nu'\nu''} \langle A|f_{\nu}^{\dagger\mathrm{phys}}|B\rangle\langle n|f_{\nu'}^{\dagger}|m\rangle_f\langle\nu'|\left(\hat{\Delta}^p\hat{\Delta}^h\right)^{-1/2}|\nu''\rangle\phi_{An}^{\dagger}\phi_{Bm}f_{\nu''}^{\dagger}. \end{aligned} \tag{C.5}$$

It is to be noted that the above equation is in the case of the saddle point approximation.

Now, let us discuss what kind of the "creation" operator gives eq. (C.5) in the saddle point approximation. There are another condition that should be equivalent with eq. (3.58) under the physically meaningful states. We can simply obtain this form by using the fact that all $\phi_{nm}^{\dagger}\phi_{lk}$ terms returns zero when performing to $\phi_{AB}|\underline{C}\rangle$ state, where $|\underline{C}\rangle$ indicates physically meaningful state. This is because all the physically meaningful states consist of single boson state. As a result, eq. (3.59) can be obtained.

Appendix D

derivative of subsidiary operator

In this appendix, we discuss how to obtain the derivative of $\overline{R}^*_{\nu\nu^p rime}$ by boson operators $\overline{\phi_{nm}}$. Here, $\overline{R}^*_{\nu\nu^p rime}$ is written as,

$$\overline{R}^*_{\nu\nu'} = \sum_{AB}\sum_{nm\nu''} \langle A|f^{\dagger \mathrm{phys}}_{\nu}|B\rangle\langle n|f^{\dagger}_{\nu''}|m\rangle_f \hat{K}_{\nu''\nu'}\overline{\phi}_{An}\overline{\phi}_{Bm}, \tag{D.1}$$

$$\hat{K}_{\nu''\nu'} = \langle\nu''|\langle(\hat{\underline{\Delta}}^p\hat{\underline{\Delta}}^h\rangle)^{-1/2}|\nu'\rangle, \tag{D.2}$$

$$\hat{\underline{\Delta}}^p_{\nu\nu'} = \sum_{Anm}\langle m|f^{\dagger}_{\nu}f_{\nu'}|n\rangle\overline{\phi}_{An}\overline{\phi}_{Am}. \tag{D.3}$$

Then, the derivative of $\overline{R}^*_{\nu\nu'}$ by $\overline{\phi}_{Cl}$ is given by,

$$\begin{aligned}\frac{\partial\overline{R}^*_{\nu\nu'}}{\partial\overline{\phi}_{Cl}} =& \sum_{A}\sum_{n\nu''}\langle A|f^{\dagger \mathrm{phys}}_{\nu}|C\rangle\langle n|f^{\dagger}_{\nu''}|l\rangle_f\hat{K}_{\nu''\nu'}\overline{\phi}_{An}\\ &+\sum_{B}\sum_{m\nu''}\langle C|f^{\dagger \mathrm{phys}}_{\nu}|B\rangle\langle l|f^{\dagger}_{\nu''}|m\rangle_f\hat{K}_{\nu''\nu'}\overline{\phi}_{Bm}\\ &+\sum_{AB}\sum_{nm\nu''}\langle A|f^{\dagger \mathrm{phys}}_{\nu}|B\rangle\langle n|f^{\dagger}_{\nu''}|m\rangle_f\frac{\partial\hat{K}_{\nu''\nu'}}{\partial\overline{\phi}_{Cl}}\overline{\phi}_{An}\overline{\phi}_{Bm}.\end{aligned} \tag{D.4}$$

Let us discuss how to compute the derivative of matrix $\hat{K}$. We can simply calculate the derivative of $\hat{X} = \hat{\Delta}^p\hat{\Delta}^h$ as follows:

$$\frac{\partial\hat{X}}{\partial\overline{\phi}_{Cl}} = \frac{\partial\hat{\Delta}^p}{\partial\overline{\phi}_{Cl}}\hat{\Delta^h} + \hat{\Delta^p}\frac{\partial\hat{\Delta}^h}{\partial\overline{\phi}_{Cl}}. \tag{D.5}$$

Here, the derivative of $\hat{\Delta}^p$ and that of $\hat{\Delta}^h$ can be derived analytically from eqs. (3.61) and (3.62). The derivative of matrix $\hat{K}$ is derived by using the following relation:

$$\begin{aligned}\hat{X}^{-1} &= \hat{X}^{-1/2}\hat{X}^{-1/2},\\ \partial_\phi\hat{X}^{-1} &= \partial_\phi\hat{X}^{-1/2}\hat{X}^{-1/2} + \hat{X}^{-1/2}\partial_\phi\hat{X}^{-1/2}.\end{aligned} \tag{D.6}$$

By rotating to NO basis, $\hat{X}^{-1/2}$ becomes a diagonalized matrix with eigenvalue L_i and, Then, eq. (D.6) is transformed as:

$$\begin{aligned} \partial_\phi \tilde{X}_{ij}^{-1} &= \partial_\phi \tilde{X}_{ij}^{-1/2} L_j + L_i \partial_\phi \tilde{X}_{ij}^{-1/2}. \\ \partial_\phi \tilde{X}_{ij}^{-1/2} &= \frac{\partial_\phi \tilde{X}_{ij}^{-1}}{L_j + L_i}, \end{aligned} \tag{D.7}$$

where $\tilde{X}$ denotes the matrix $\hat{X}$ in NO basis. Thus, we obtain the derivative of matrix $\hat{K}$ after rotating back from NO basis if we obtain the $\partial_\phi \tilde{X}_{ij}^{-1}$. This derivative is straightforwardly derived from $\partial_\phi \hat{X}$ in eq. (D.5) by following relation:

$$\begin{aligned} \hat{X}\hat{X}^{-1} &= \hat{I} \\ \partial_\phi \hat{X}\hat{X}^{-1} + \hat{X}\partial_\phi \hat{X}^{-1} &= \hat{0} \\ \partial_\phi \hat{X}\hat{X}^{-1} + \hat{X}\partial_\phi \hat{X}^{-1} &= \hat{0} \\ \partial_\phi \hat{X}^{-1} &= \hat{X}^{-1}\partial_\phi \hat{X}\hat{X}^{-1}. \end{aligned} \tag{D.8}$$

Bibliography

[1] G. R. Stewart: Rev. Mod. Phys. **56** (1984) 755.

[2] S. Doniach: Phys. B+C **91** (1977) 231.

[3] C. Varma: Phys. Rev. Lett. **55** (1985) 2723.

[4] Y. Yanase and H. Harima: *Kotai Butsuri* **543** (2011) 229.

[5] H. R. Ott, H. Rudigier, Z. Fisk, and J. L. Smith: Phys. Rev. Lett. **50** (1983) 1595.

[6] H. R. Ott: Phys. B Condens. Matter **378-380** (2006) 1.

[7] P. Gegenwart, C. Langhammer, R. Helfrich, N. Oeschler, M. Lang, J. Kim, G. Stewart, and F. Steglich: Phys. C Supercond. **408-410** (2004) 157.

[8] Y. Shimizu, A. Pourret, G. Knebel, A. Palacio-Morales, and D. Aoki: Phys. Rev. B **92** (2015) 241101.

[9] M. McElfresh, M. B. Maple, J. O. Willis, D. Schiferl, J. L. Smith, Z. Fisk, and D. L. Cox: Phys. Rev. B **48** (1993) 10395.

[10] J. S. Kim, B. Andraka, C. S. Jee, S. B. Roy, and G. R. Stewart: Phys. Rev. B **41** (1990) 11073.

[11] D. Cox: Phys. Rev. Lett. **59** (1987) 1240.

[12] D. L. Cox and M. Jarrell: J. Phys. Condens. Matter **8** (1996) 9825.

[13] K. Hattori and K. Miyake: J. Phys. Soc. Japan **74** (2005) 2193.

[14] S. Nishiyama, H. Matsuura, and K. Miyake: J. Phys. Soc. Japan **79** (2010) 104711.

[15] S. Nishiyama and K. Miyake: J. Phys. Soc. Japan **80** (2011) 124706.

[16] G. Schmiedeshoff and J. Smith: Philos. Mag. **89** (2009) 1839.

[17] G. R. Stewart, Z. Fisk, J. O. Willis, and J. L. Smith: Phys. Rev. Lett. **52** (1984) 679.

[18] S. M. Hayden, L. Taillefer, C. Vettier, and J. Flouquet: Phys. Rev. B **46** (1992) 8675.

[19] A. Grauel, A. Böhm, H. Fischer, C. Geibel, R. Köhler, R. Modler, C. Schank, F. Steglich, G. Weber, T. Komatsubara, and N. Sato: Phys. Rev. B **46** (1992) 5818.

[20] A. De Visser, A. Menovsky, and J. J. M. Franse: Phys. B+C **147** (1987) 81.

[21] A. Krimmel, A. Loidl, R. Eccleston, C. Geibel, and F. Steglich: J. Phys. Condens. Matter **8** (1996) 1677.

[22] S. Adenwalla, S. Lin, Q. Ran, Z. Zhao, J. Ketterson, J. Sauls, L. Taillefer, D. Hinks, M. Levy, and B. Sarma: Phys. Rev. Lett. **65** (1990) 2298.

[23] K. Hasselbach, L. Taillefer, and J. Flouquet: Phys. Rev. Lett. **63** (1989) 93.

[24] R. Fisher, S. Kim, B. Woodfield, N. Phillips, L. Taillefer, K. Hasselbach, J. Flouquet, A. Giorgi, and J. Smith: Phys. Rev. Lett. **62** (1989) 1411.

[25] M. Sigrist and K. Ueda: Rev. Mod. Phys. **63** (1991) 239.

[26] B. Shivaram, Y. Jeong, T. Rosenbaum, and D. Hinks: Phys. Rev. Lett. **56** (1986) 1078.

[27] Y. Kohori, T. Kohara, H. Shibai, Y. Oda, Y. Kitaoka, and K. Asayama: J. Phys. Soc. Japan **57** (1988) 395.

[28] J. P. Brison, N. Keller, P. Lejay, J. L. Tholence, A. Huxley, N. Bernhoeft, A. I. Buzdin, B. Fk, J. Flouquet, L. Schmidt, A. Stepanov, R. A. Fisher, N. Phillips, and C. Vettier: J. Low Temp. Phys. **95** (1994) 145.

[29] H. Suderow, J. P. Brison, A. Huxley, and J. Flouquet: J. Low Temp. Phys. **108** (1997) 11.

[30] K. Izawa, Y. Machida, A. Itoh, Y. So, K. Ota, Y. Haga, E. Yamamoto, N. Kimura, Y. Onuki, Y. Tsutsumi, and K. Machida: J. Phys. Soc. Japan **83** (2014) 061013.

[31] H. Tou, Y. Kitaoka, K. Ishida, K. Asayama, N. Kimura, Y. Ohnuki, E. Yamamoto, Y. Haga, and K. Maezawa: Phys. Rev. Lett. **80** (1998) 3129.

[32] Y. Kitaoka, H. Tou, K. Ishida, N. Kimura, Y. Ohnuki, E. Yamamoto, Y. Haga, and K. Maezawa: Phys. B **281** (2000) 878.

[33] H. Tou, K. Ishida, and Y. Kitaoka: Phys. C Supercond. **408** (2004) 305.

[34] K. Miyake: in*Theory of Heavy Fermions and Valence Fluctuations*, ed. T.Kasuya and T. Saso (Springer, 1985).

[35] K. Ishida, H. Mukuda, Y. Kitaoka, K. Asayama, Z. Q. Mao, Y. Mori, and Y. Maeno: Nature **396** (1998) 658.

[36] Y. Yanase and M. Ogata: J. Phys. Soc. Japan **72** (2003) 673.

[37] Y. Yanase, S. Takamatsu, and M. Udagawa: J. Phys. Soc. Japan **83** (2014) 061019.

[38] K. K. Ng and M. Sigrist: Europhys. Lett. **49** (2000) 473.

[39] H. Tou, Y. Kitaoka, K. Asayama, N. Kimura, Y. Onuki, E. Yamamoto, and K. Maezawa: Phys. Rev. Lett. **77** (1996) 1374.

[40] H. Ikeda and K. Miyake: J. Phys. Soc. Japan **66** (1997) 3714.

[41] H. Kusunose and H. Ikeda: J. Phys. Soc. Japan **74** (2005) 405.

[42] S. Yotsuhashi, K. Miyake, and H. Kusunose: J. Phys. Soc. Japan **85** (2016) 034719.

[43] O. Sakai, Y. Shimizu, and T. Kasuya: J. Phys. Soc. Japan **58** (1989) 3666.

[44] Y. Yanase and K. Yamada: J. Phys. Soc. Japan **66** (1997) 3551.

[45] M. Koga, W. Liu, M. Dolg, and P. Fulde: Phys. Rev. B **57** (1998) 10648.

[46] S. Yotsuhashi, H. Kusunose, and K. Miyake: J. Phys. Soc. Japan **70** (2001) 186.

[47] K. G. Wilson: Rev. Mod. Phys. **47** (1975) 773.

[48] J. Otsuki, H. Kusunose, and Y. Kuramoto: J. Phys. Soc. Japan **74** (2005) 200.

[49] Y. Shimizu and O. Sakai: J. Phys. Soc. Japan **74** (2005) 27.

[50] M. Koga and M. Matsumoto: J. Phys. Soc. Japan **76** (2007) 074714.

[51] S. Yotsuhashi, K. Miyake, and H. Kusunose: J. Phys. Soc. Japan **71** (2002) 389.

[52] S. Hoshino, J. Otsuki, and Y. Kuramoto: J. Phys. Soc. Japan **79** (2010) 074720.

[53] S. Hoshino and Y. Kuramoto: Phys. Rev. Lett. **112** (2014) 167204.

[54] G. Kotliar, S. Y. Savrasov, K. Haule, V. S. Oudovenko, O. Parcollet, and C. A. Marianetti: Rev. Mod. Phys. **78** (2006) 865.

[55] A. Tsuruta and K. Miyake: J. Phys. Soc. Japan **84** (2015) 114714.

[56] F. Lechermann, A. Georges, G. Kotliar, and O. Parcollet: Phys. Rev. B **76** (2007) 155102.

[57] H. Ikeda, M.-T. Suzuki, R. Arita, T. Takimoto, T. Shibauchi, and Y. Matsuda: Nat. Phys. **8** (2012) 528.

[58] T. Nomoto and H. Ikeda: Phys. Rev. B **90** (2014) 125147.

[59] W. F. Brinkman and T. M. Rice: Phys. Rev. B **2** (1970) 4302.

[60] M. Lavagna: Phys. Rev. B **41** (1990) 142.

[61] T. Li, P. Wölfle, and P. J. Hirschfeld: Phys. Rev. B **40** (1989) 6817.

[62] T. Li: Phys. Rev. B **48** (1993) 4991.

[63] N. Read and D. M. Newns: J. Phys. C Solid State Phys. **16** (1983) L1055.

[64] G. Kotliar and A. Ruckenstein: Phys. Rev. Lett. **57** (1986) 1362.

[65] T. Jolicoeur and J. C. Le Guillou: Phys. Rev. B **44** (1991) 2403.

[66] E. Arrigoni and G. Strinati: Phys. Rev. Lett. **71** (1993) 3178.

[67] E. Arrigoni, C. Castellani, R. Raimondi, and G. C. Strinati: Phys. Rev. B **50** (1994) 2700.

[68] E. Arrigoni and G. C. Strinati: Phys. Rev. B **52** (1995) 2428.

[69] J. Bünemann: Phys. status solidi **248** (2011) 203.

[70] M. Hutchings: Solid State Phys. **16** (1964) 227.

[71] J. C. Slater: Phys. Rev. **34** (1929) 1293.

[72] E. U. Condon and G. H. Shortley: Phys. Rev. **37** (1931) 1025.

[73] G. Racah: Phys. Rev. **62** (1942) 438.

[74] T. Hotta and H. Harima: Phys. Soc. Japan **74** (2006) 124711.

[75] R. Frésard and T. Kopp: Ann. Phys. **524** (2012) 175.

[76] T. M. Rice and K. Ueda: Phys. Rev. B **34** (1986) 6420.

[77] A. Isidori and M. Capone: Phys. Rev. B **80** (2009) 115120.

[78] J. Bünemann and F. Gebhard: Phys. Rev. B **76** (2007) 193104.

[79] C. G. Broyden: Math. Comput. **19** (1965) 577.

[80] S. Nishiyama: *Numerical Renormalization Group Study on Multiorbital Impurity Anderson Model* (phD. thesis, Osaka University, 2013).

[81] S. Shinkai and K. Yamada: J. Phys. Soc. Japan **74** (2005) 1811.

[82] T. Nomoto and H. Ikeda: Phys. Rev. Lett. **117** (2016) 217002.

[83] Y. Ohnuki, R. Settai, Y. Haga, Y. Machida, K. Izawa, F. Honda, and D. Aoki: Comptes Rendus Phys. **15** (2014) 616.

[84] T. Oguchi and A. Freeman: J. Magn. Magn. Mater. **52** (1985) 174.

[85] C. S. Wang, M. R. Norman, R. C. Albers, A. M. Boring, W. E. Pickett, H. Krakauer, and N. E. Christensen: Phys. Rev. B **35** (1987) 7260.

[86] M. Norman, R. Albers, A. Boring, and N. Christensen: Solid State Commun. **68** (1988) 245.

[87] G. Zwicknagl, A. N. Yaresko, and P. Fulde: Phys. Rev. B **65** (2002) 081103.

[88] G. J. McMullan, P. M. C. Rourke, M. R. Norman, A. D. Huxley, N. Doiron-Leyraud, J. Flouquet, G. G. Lonzarich, A. McCollam, and S. R. Julian: New J. Phys. **10** (2008) 053029.

[89] N. Kimura, R. Settai, Y. Onuki, H. Toshima, E. Yamamoto, K. Maezawa, H. Aoki, and H. Harima: J. Phys. Soc. Japan **64** (1995) 3881.

[90] N. Kimura, R. Settai, Y. Ohnuki, K. Maezawa, H. Aoki, and H. Harima: Phys. B Condens. Matter **216** (1996) 313.

[91] N. Kimura, T. Komatsubara, D. Aoki, Y. Ohnuki, Y. Haga, E. Yamamoto, H. Aoki, and H. Harima: J. Phys. Soc. Japan **67** (1998) 2185.

[92] L. Taillefer and G. G. Lonzarich: Phys. Rev. Lett. **60** (1988) 1570.

[93] T. Ito, H. Kumigashira, H.-D. Kim, T. Takahashi, N. Kimura, Y. Haga, E. Yamamoto, Y. nuki, and H. Harima: Phys. Rev. B **59** (1999) 8923.

[94] K. Hasselbach, L. Taillefer, and J. Flouquet: Phys. Rev. Lett. **63** (1989) 93.

[95] K. Miyake and H. Kohno: J. Phys. Soc. Japan **74** (2005) 254.

[96] Y. Onishi and K. Miyake: J. Phys. Soc. Japan **69** (2000) 3955.